



MONASH UNIVERSITY

**THE ROLE OF CIRCULATING CERAMIDE
IN INSULIN RESISTANCE &
INFLAMMATION**

James Boon

B.Sc. (Biomed, Hons)
Department of Physiology
School of Biomedical Sciences, Faculty of Medicine, Nursing
and Health Sciences
Monash University
Melbourne, Victoria Australia

Submitted to Monash University in accordance with the
the requirements for the degree of
Doctorate of Philosophy
May 2012

Copyright Notices

Notice 1

Under the Copyright Act 1968, this thesis must be used only under the normal conditions of scholarly fair dealing. In particular no results or conclusions should be extracted from it, nor should it be copied or closely paraphrased in whole or in part without the written consent of the author. Proper written acknowledgement should be made for any assistance obtained from this thesis.

Notice 2

I certify that I have made all reasonable efforts to secure copyright permissions for third-party content included in this thesis and have not knowingly added copyright content to my work without the owner's permission.

Table of Contents

Abstract	I
General declaration	II
Acknowledgements	III
Abbreviations	IV
Index of Figures and Tables	VII

Chapter 1: Literature review

1.1 Introduction	2
1.2 Type 2 diabetes and the insulin resistant state	3
1.2.1 Type 2 Diabetes and obesity	3
1.2.2 Glucose clearance and homeostasis	3
1.2.3 Insulin action and mechanism	5
1.2.4 Lipid-induced insulin resistance: Lipidtoxicity	6
1.3 Ceramides and its intracellular synthesis.	7
1.3.1 Ceramides	7
1.3.2 Sphingomyelinase pathway	8
1.3.3 De novo pathway	8
1.3.4 Salvage/recycle pathway	9
1.3.5 Variable acyl-chain ceramides	11
1.4 Observations implicating ceramide to insulin resistance.	11
1.4.1 <i>In vitro</i> observations implicating ceramide to insulin resistance.	11
1.4.2 <i>In vivo</i> accumulation of ceramide decreases insulin sensitivity.....	12
1.5 Mechanism of ceramide induced insulin resistance.	13
1.5.1 Ceramide mediated PP2A activation leads to AKT deactivation.....	13
1.5.2 Ceramide activated aPKC λ/ξ associates with AKT and causes repression.	14
1.5.3 Caveolae influences aPKC λ/ξ and PPA2 activation.....	14
1.6 Observations implicating ceramide to inflammation	17
1.6.1 Inflammation and insulin resistance.	17
1.6.2 Ceramide activates pro-inflammatory NF- κ B pathway and JNK	17
1.6.3 Ceramide activates c/EBP and COX-2 pathway	19
1.6.4 Ceramide activated protein kinase the link between MAPK inflammatory signalling and ceramide.....	19
1.6.5 Toll-like receptor-4 signalling mediates ceramide accrual during lipid loading.	21
1.7 Ceramide in systematic circulation	23

1.7.1 Plasma ceramide	23
1.7.2 Sub-species of ceramide in plasma.....	23
1.7.3 Lipoproteins are transporters of plasma ceramide.....	23
1.7.4 Lipoproteins.....	24
1.7.5 Low-density lipoprotein clearance in plasma.....	25
1.7.6 Modified LDL potential in eliciting pathological states.....	26
1.8 Summary and research aims.....	27

Chapter 2: Elevated lipoprotein-ceramides in plasma is associated to type 2 diabetes in humans

2.1 Introduction.....	29
2.2 Aims	30
2.3 Materials and methods	30
2.3.1 Subjects and experimental pProcedures.....	30
2.3.2 Blood sampling and analysis.....	31
2.3.3 FPLC isolation of lipoproteins.....	31
2.3.4 Ceramide quantification.....	32
2.3.5 Statistical analysis.....	32
2.4 Results.....	33
2.4.1 Type 2 diabetic patients and lean patients' characteristics	33
2.4.2 Majority of circulating ceramides are localized to lipoproteins.....	33
2.4.3 Circulating ceramides are elevated in obese type 2 diabetic patients.....	35
2.4.4 Circulating ceramides correlate with plasma insulin and whole body insulin sensitivity	36
2.5 Discussion.....	37

Chapter 3: Design and constuction of reconstituted LDL-ceramide preparation

3.1 Introduction.....	41
3.2 Aims	42
3.3 Materials and methods	42
3.3.1 Associating exogenous long chain ceramide with human LDL.....	42
3.3.2 Quantification of LDL-ceramide via DAG-K assay.....	44
3.3.3 Bicinchoninic acid (BCA) protein assay.....	45
3.3.4 Western blotting	45
3.3.5 Transmission electron microscopy	47

3.3.6 Analysis of lipid composition of LDL-ceramide by mass spectrometry.	47
3.3.7 Analysis of LDL-ceramide oxidation status.....	47
3.4 Results	48
3.4.1 Amount of exogenous ceramide associated with LDL.	48
3.4.2 ApoB-100 is present in LDL-ceramide preparation.	48
3.4.3 Ceramide content in the LDL-ceramide preparation is dependent on the initial amount of exogenous ceramide, but not LDL amount.	49
3.4.4 LDL-ceramide preparation is similar in shape to LDL.....	51
3.4.5 LDL is not oxidized during LDL -ceramide preparation.....	51
3.4.6 Lipid composition of LDL -ceramide preparation.....	52
3.5 Discussion	53

Chapter 4: LDL-ceramide decreases insulin action in cultured myotubes & skeletal muscle

4.1 Introduction	59
4.2 Aims	60
4.3 Materials and methods	60
4.3.1 Cell culture.....	60
4.3.1.1 Standard L6 & L6 Glut4-myc skeletal myoblast cell culture.....	61
4.3.1.2 Primary mouse hepatocyte cell culture.....	61
4.3.1.3 HepG2 hepatocyte cell culture.....	62
4.3.1.4 CRL 1439 hepatocyte cell culture.....	62
4.3.1.5 3T3-L1 adipocyte cell culture.....	62
4.3.2 Insulin stimulated 2-deoxy-D-1[³ H] glucose uptake assay.....	63
4.3.3 Glut-4 translocation assay.....	64
4.3.4 Bicinchoninic acid (BCA) protein assay.....	65
4.3.5 Western blotting.....	65
4.3.6 Mass spectrometric analysis.....	65
4.3.7 Caspase-3 assay.....	66
4.3.8 Glucose oxidase assay.....	66
4.3.9 Statistical analyses.....	67
4.4.0 LDL-ceramide infusion in to mice.....	67
4.4.1 Plasma membrane fractionation.....	68
4.4 Results	69
4.4.1 Testing basal glucose uptake in standard L6 Glut4-myc myotubes in response to insulin.....	69
4.4.2 Increasing insulin concentration does not lead to increase glucose uptake in L6 Glut4-myc myotubes.....	69
4.4.3 LDL treatment does not affect insulin stimulated glucose uptake in L6 Glut4-myc myotubes.....	70

4.4.4	LDL ceramide effects decreases insulin stimulated glucose uptake in L6 Glut4-myc myotubes.....	71
4.4.5	LDL-ceramide decrease AKT phosphorylation in L6 Glut4-myc myotubes	72
4.4.6	Testing viability of L6 Glut4-myc myotubes for use in insulin stimulated Glut4 translocation assay.	72
4.4.7	LDL-ceramide reduces insulin stimulated Glut4 translocation in L6 Glut4-myc myotubes.....	73
4.4.8	LDL-ceramide does not influence JNK or NFκB signalling in myotubes... ..	74
4.4.9	LDL-Ceramide treatment does not induce apoptosis via caspase-3.	75
4.4.10	LDL-Ceramide treatment induces intracellular ceramide accrual in L6 Glut4-myc myotubes.....	75
4.4.11	Myriocin does not prevent ceramide accrual in LDL-ceramide treated L6 Glut4-myc myotubes.....	76
4.4.12	Anti LDL-receptor antibody does not prevent ceramide accrual in LDL-ceramide treated in L6 Glut4-myc myotubes.	77
4.4.13	Testing insulin responsiveness of HEPG2 and CRL 1439 hepatocyte cell line in suppressing glucose output.....	78
4.4.14	Testing insulin responsiveness of mouse primary hepatocytes in suppressing glucose output.....	79
4.4.15	LDL-ceramide does not cause insulin resistance in mouse hepatocytes. ...	80
4.4.16	LDL does not reduce insulin stimulated glucose uptake in 3T3-L1 adipocytes.....	81
4.4.17	LDL-ceramide infusion into lean mice cause insulin resistance.	81
4.4.18	LDL-ceramide infusion cause inflammation in lean mice.....	84
4.5	Discussion.....	87

Chapter 5: Inflammatory effects of LDL-ceramide in macrophages

5.1	Introduction.....	96
5.2	Aims	97
5.3	Materials and methods	97
5.3.1	Cell culture	97
5.3.1.1	Raw 264.7 macrophage cell culture.....	98
5.3.1.2	MyD88 ^{-/-} / TRIF ^{-/-} macrophage cell culture	98
5.3.2	Isolation of mRNA	98
5.3.3	cDNA synthesis	99
5.3.4	Quantitative real time polymerase chain reaction (qRT-PCR)	99
5.3.5	Enzyme-linked immunosorbent assay (ELISA).....	100
5.3.6	Bicinchoninic acid (BCA) protein assay.....	100
5.3.7	Western blotting	100
5.3.8	Mass spectrometry analysis.....	100
5.4	Results.....	101

5.4.1 LDL-ceramide treatment upregulate M1 inflammatory genes and down-regulate M2 anti-inflammatory genes in RAW 264.7 macrophages.	101
5.4.2 Western Analysis of TNF- α protein in RAW 264.7 cells following LDL-ceramide treatment.....	101
5.4.3 ELISA analysis of secreted inflammatory cytokines in LDL-ceramide stimulated RAW 264.7 cell culture medium.	102
5.4.4 LDL-ceramide induces JNK activation in a time dependent manner in RAW 264.7 macrophages	103
5.4.5 LDL-ceramide reduces I κ B α levels in RAW 264.7 macrophage in a sustained manner.	105
5.4.6 LDL-Ceramide treatment induces intracellular ceramide accrual in RAW 264.7 macrophages	107
5.4.7 LDL-ceramide induces JNK activation in a time dependent manner in macrophages deficient in MyD88 (MyD88 ^{-/-}) and TRIF (Ticam ^{-/-})	108
5.4.8 LDL-ceramide does not reduce I κ B α in macrophages deficient in MyD88 (MyD88 ^{-/-}) and TRIF (Ticam ^{-/-}).....	110
5.4.9 LDL-ceramide activated RAW 264.7 macrophage conditioned medium reduce insulin stimulated glucose uptake in L6 Glut4-myc myotubes.....	112
5.5 Discussion.....	113
<hr/>	
6. General discussion	119
<hr/>	
References	127
<hr/>	

Abstract

Dysregulated lipid metabolism and inflammation are linked to the development of insulin resistance in type 2 diabetes. Plasma ceramide levels are associated with insulin resistance in type 2 diabetes, although their exact role and function have not been elucidated.

This thesis has defined the role of circulating ceramide on the pathogenesis of insulin resistance and inflammation using a multi-level approach consisting of several components, namely a human study examining patients with type 2 diabetes, construction of reconstituted LDL-ceramide for use in mechanistic studies, and investigation of the insulin desensitizing and inflammatory effects of LDL-ceramide in *in vitro* and *in vivo* models.

This thesis found that ceramide transported in low density lipoproteins (LDL) is elevated in the plasma of obese, type 2 diabetes patients and correlated with insulin resistance, but not body mass index (BMI). Treating cultured myotubes with LDL containing ceramide promoted ceramide uptake by cells in association with reduced insulin stimulated glucose uptake, Akt phosphorylation and GLUT4 translocation compared with LDL deficient in ceramide. LDL-ceramide induced a pro-inflammatory response in cultured macrophages via toll-like receptor-dependent and –independent mechanisms. Finally, infusing LDL-ceramide into lean mice reduced insulin stimulated glucose uptake and this was due to impaired insulin action, specifically in skeletal muscle.

What this thesis achieved is to serve as a prospectus that clarifies the poorly investigated role of circulating ceramide in the development of insulin resistance and to show that circulating ceramides is part of the constellation of provocateurs that contribute to the pathophysiology of the disorder which is a feature in type 2 diabetes.

General Declaration

Monash Research Graduate School, declaration for thesis partially based on jointly published or unpublished work

In accordance with Monash University Doctorate Regulation 17 / Doctor of Philosophy and Master of Philosophy (MPhil) regulations the following declarations are made: I hereby declare that this thesis contains no material which has been accepted for the award of any other degree or diploma at any university or equivalent institution and that, to the best of my knowledge and belief, this thesis contains no material previously published or written by another person, except where due reference is made in the text of the thesis. I certify that I have made all reasonable efforts to secure copyright permissions for third-party content included in this thesis and have not knowingly added copyright content to my work without the owner's permission.

Signed: 

28 April 2012

Date:

Copyright Notice

Under the Copyright Act 1968, this thesis must be used only under the normal conditions of scholarly fair dealing. In particular no results or conclusions should be extracted from it, nor should it be copied or closely paraphrased in whole or in part without the written consent of the author. Proper written acknowledgment should be made for any assistance obtained from this thesis.

Acknowledgments

The inclusion of persons in this thesis reflects the fact that the work came from active collaboration between researchers and acknowledges input into team-based research. In particular, the following should be noted:

Experimental direction, supporting ideas, manuscript and thesis direction & revision were provided by:

A/Prof Matthew Watt.

Thesis revision, direction and supporting ideas provided by:

Prof Helena Parkington

Technical assistance

A/Prof Matthew Watt (*Multiple technical ideals and assistance*), Dr Romana Stark (*Plasma membrane fractionation, 3T3 L1 cell work, Technical ideas*), Dr Clinton Bruce & A/Prof. Peter Meikle (*Mass-spectrometry*), Alaina Natoli (*oxLDL analysis*), A/Prof Bronwyn Kingwell and Dr Darren Hentsridge (*Human sample procurement*), Dr Russell Brown (*Animal surgery*), Dr Andrew Hoy (*Mice tissue harvesting*), Joanne Pagnon (*Technical ideas and miscellaneous assistance during my work injury*) and Alex Morris (*Primary Hepocyte extraction*).

General ideals & knowledge

Researchers and clinicians I met throughout the years as a volunteer and lab technician from the fields of embryonic stem cells, diabetes, genomics, liver and lung development who primed me with the knowledge & technical skills that aided me in completing this undertaking.

Abbreviations

aPKC λ/ξ	Atypical protein kinase C λ/ξ
APS	Ammonium Persulfate
ATP	Adenosine triphosphate
AS160	Akt substrate of 160 kDA
ANOVA	Analysis of variance
BSA	Bovine serum albumin
CAP-K	Ceramide activated protein kinase
CerSs	Ceramide synthases
CO ₂	Carbon dioxide
COX-2	Cyclooxygenase-2
DAG	Diacylglycerol
DAG-K	Diacylglycerol kinase.
ECL	Enhanced chemiluminescence
ERK	Extracellular signal regulated kinases
ESI-MS/MS	Electrospray tandem mass spectrometry
FACS	Fluorescence activated cell sorting
FBS	Fetal bovine serum
FCS	Fetal calf serum
FPLC	Fast protein liquid chromatography
GC-MS	Gas chromatography mass spectrometry
Glut4	Glucose transporter type 4
h	Hour
H ₂ SO ₄	Sulphuric acid
HBSS	Hank's buffered salt solution
HCL	Hydrochloric acid
HDL	High density lipoprotein
HPLC	High-performance liquid chromatography
HPLC-MS	High-performance liquid chromatography mass spectrometry
HRP	Horse radish peroxidase
IDL	Intermediate density lipoprotein
I κ B α	Nuclear factor of kappa light polypeptide enhancer in B cell inhibitor α

IL	Interleukin
IMTG	Intramuscular triacylglycerol
IRS-1/2	Insulin receptor substrate-1/2
JNK	C-jun N-terminal kinases
KSR	Kinase suppressor of Ras
LASSs	Longevity-assurance homologues
LCFAs	Long chain fatty acids.
LDL	Low density lipoprotein
mAB	Monoclonal antibody
MAPK	Mitogen-activated protein kinase
Mcp-1	Monocyte chemo-attractant protein-1
Min	Minute
NEFAs	Non-esterified fatty acids
NF- κ B	Nuclear factor-kappa- β
OPD	O- phenylenediamine dihydrochloride
ox-LDL	Oxidised low density lipoprotein
PBS +	Phosphate buffer saline containing magnesium and calcium
PBS -	Phosphate buffer saline without magnesium and calcium
PDK1	3-phosphoinositide-depedent protein kinase 1
PDK2	Phosphoinositide-dependent protein kinase 2
PFA	Paraformaldehyde
PGHS-2	Prostaglandin-endoperoxide synthase 2
PGE ₂	Prostaglandin E ₂
PIP ₃	Phosphatidylinositol 4,5-biphospate
PIP ₃	Phosphatidylinositol (3-4-5)-triphosphate
PI-3K	Phosphatidy-linositol 3-kinase
PKB	Protein kinase B
PP2A	Protein phosphatase 2A
RT	Room temperature
SAPKs	Stress activated protein kinases
SDS	Sodium Dodecyl Sulphate
SDS-PAGE	Sodium Dodecyl Sulphate Polyacrylamide Gel Electrophoresis
SFAs	Saturated fatty acids
SPT	Serine palmitoyl-CoA acyltransferase

TBS	Tris buffered saline
TBST	Tris buffered saline + 0.1% Tween 20
TEMED	Tetramethylethylenediamine
TLC	Thin layer chromatography
TLR4	Toll-like receptor-4
TNF- α	Tumour necrosis factor- α
V/V	Volume/volume
VLDL	Very low-density lipoprotein
WAT	White adipose tissue
W/W	Weight/weight

Index of figures and tables

Chapter 1: Literature Review

Fig.1-1.	Regulation of blood glucose levels by liver and skeletal muscle in the presence of insulin during changes in homeostatic glucose level	4
Fig.1-2.	Insulin signalling transduction in skeletal muscle	6
Fig. 1-3.	Ceramide synthesis and its derivatives	10
Fig.1-4.	Mechanism of PKB (AKT) repression via α PKC λ/ξ complex formation	16
Fig.1-5.	Inflammatory pathways documented in literature known to be induced by ceramide and short-chain ceramides	21
Fig.1-6.	Structure of low density lipoprotein (LDL)	24
Table.1-1.	Characteristic of major plasma lipoproteins in humans	25
Table 1-2.	Percentage of whole-body clearance rate of plasma LDL in hamster	26

Chapter 2: Elevated lipoprotein-ceramides in plasma is associated to type 2 diabetes in humans

Table.2-1.	Patient characteristics	33
Fig 2-1.	Validation of FPLC separation	34
Fig 2-2.	Distribution of ceramides in lipoprotein fractions of plasma	34
Fig 2-3.	Total plasma ceramide content in lean patients and obese patients with type 2 diabetes	35
Fig 2-4.	Plasma ceramide content in lipoproteins fraction of lean patients and obese patients with type 2 diabetes	35
Fig 2-5.	Plasma ceramide correlation to (A) HOMA IR, (B) plasma glucose, (C) plasma insulin and (D) LDL-Ceramide	36

Chapter 3: Design and construction of reconstituted LDL-ceramide preparation.

Table 3.1.	Solutions and buffers used in Western blotting	46
Fig 3-1.	ApoB-100 is present in LDL-ceramide preparation	49
Fig 3-2.	Increasing the amount of exogenous ceramide as starting material leads to increase association with LDL	50

Fig 3-3.	Increasing amount of LDL as starting material does not lead to increase association with LDL	50
Fig 3-3.	Transmission electron microscopic image of LDL-ceramide preparation	51
Fig 3-4.	Thiobarbituric acid reactive substances (TBARS) in LDL-ceramide, normal LDL, and oxLDL	52
Table 3.4-1	Lipid composition in LDL-ceramide preparation and depleted LDL analysed by mass spectrometry	52

Chapter 4: LDL-ceramide decreases insulin action in cultured myotubes & skeletal muscle

Fig 4-1.	2-deoxy-D-1[³ H] glucose uptake in L6 Glut4-myc myotubes following 10nM insulin stimulation	69
Fig 4-2.	2-deoxy-D-1[³ H] glucose uptake in L6 Glut4-myc myotubes following 10nM and 100nM insulin stimulation	70
Fig 4-3.	LDL administration does not influence insulin-stimulated 2-deoxy-D-1[³ H] glucose uptake compared with untreated L6 Glut4-myc myotubes	70
Fig 4-4.	6h LDL-C24:0 and C16:0 ceramide treatment does not decrease 2-deoxy-D-1[³ H] glucose uptake in L6 Glut4-myc myotubes	71
Fig 4-5.	24h LDL-C24:0 and C16:0 ceramide treatment decreases 2-deoxy-D-1[³ H] glucose uptake in L6 Glut4-myc myotubes	71
Fig 4-6.	AKT phosphorylation (Ser ⁴⁷³ and Thr ³⁰⁸) is reduced in LDL-ceramide treated L6 Glut4-myc myotubes following 24 h treatment	72
Fig 4-7.	Glut4-myc protein detected at cell surface of L6 Glut4-myc myotubes following 10nM insulin stimulation	73
Fig 4-8.	Glut4-myc protein detected at cell surface of 24 h LDL-ceramide treated L6 Glut4-myc myotubes following 10nM insulin stimulation	74
Fig 4-9.	LDL-ceramide has no effect on ERK, JNK and Iκβ	74
Fig 4-10.	LDL-ceramide treatment does not increase caspase-3 activity	75
Fig 4-11.	L6 Glut4-myc myotubes treated for 24 h with LDL-ceramide leads to an increase in intracellular ceramide of the corresponding ceramide sub-species	76

Fig 4-12.	Sphingomyelin content in L6 Glut4-myc myotubes is not decreased by LDL-ceramide treatment	76
Fig 4-13.	Myriocin does not prevent C24:0 ceramide accrual in LDL-C24:0 ceramide treated L6 Glut4-myc skeletal myotubes	77
Fig 4-14.	Anti LDL-receptor antibody does not prevent C24:0 ceramide accrual in LDL-C24:0 ceramide treated myotubes	78
Fig 4-15.	Glucose output in HEPG2 following 4 h and 8 h insulin stimulation	79
Fig 4-16.	Glucose output in CRL 1439 following 4 h and 8 h insulin stimulation	79
Fig 4-17.	Glucose output in primary mouse hepatocytes following insulin stimulation	80
Fig 4-18.	LDL-ceramide does not cause insulin resistance in primary mouse hepatocytes	80
Fig 4-19.	24h LDL-C16:0/C24:0 ceramide treatment does not reduce 2-deoxy-D-1[³ H] glucose uptake in insulin stimulated 3T3-L1 adipocytes	81
Fig 4-20.	Rates of insulin stimulated 3H 2-deoxyglucose disappearance from blood of lean mice infused with LDL (white bar) or LDL-24:0 ceramide (black bar)	82
Fig 4-21.	Rates of insulin stimulated ³ H-2-deoxyglucose clearance into mixed quadriceps and mixed gastrocnemius skeletal muscle in lean mice infused with LDL (white bar) or LDL-24:0 ceramide (black bar)	82
Fig 4-22.	AKT (Ser ⁴⁷³) phosphorylation is decreased in vastus lateralis muscle of LDL-C24:0 ceramide infused mice	83
Fig 4-23.	Ceramide content in mixed vastus lateralis muscle analysed by mass spectrometry	83
Fig 4-24.	Ceramide content in plasma membrane enriched fraction of mixed vastus lateralis muscle measured by mass spectrometry	84
Fig 4-25.	LDL-ceramide does not induce insulin resistance in adipose tissue, heart and liver	84
Fig 4-26.	Quantification of immunoblots analysis of phosphorylated JNK (Thr ¹⁸³ /Tyr ¹⁸⁵)/JNK and IκBα/α-actin in lysates of skeletal muscle obtain immediately after iv insulin injection	85

Fig 4-27.	Transcript levels of pro-inflammatory cytokines in mixed vastus lateralis skeletal muscle	85
Fig 4-28.	Plasma pro-inflammatory cytokine in lean mice infused with LDL or LDL-C24:0 ceramide for 4h and intravenous insulin tolerance tests preformed 24h later	86

Chapter 5: Inflammatory effects of LDL-ceramide on macrophages

Fig 5-1	LDL-ceramide upregulates M1 inflammatory genes and downregulate M2 anti-inflammatory genes	101
Fig 5-2	Western blot analysis of TNF- α in RAW 264.7 macrophage treated with LDL-ceramide for 4 h, 8 h, 24 h	102
Fig 5-3.	RAW 264.7 macrophage increase TNF- α and IL-6 secretion into culture medium following 24h LDL-ceramide treatment	103
Fig 5-4.	LDL-ceramide induces JNK activation in RAW 264.7 macrophage in a time dependent manner	104
Fig 5-5.	LDL-ceramide reduces I κ B α levels in RAW 264.7 macrophage in a sustained but less acute manner compared to palmitate and LPS treatment	106
Fig 5-6.	RAW 264.7 macrophage treated for 24 h with LDL-ceramide leads to increase in intracellular ceramide of the corresponding ceramide sub-species	107
Fig 5-7.	LDL-ceramide is able to activate JNK in MYD88/TRIF double knockout macrophages	109
Fig 5-8.	LDL-ceramide does not reduce I κ B α levels in MYD88/TRIF double knockout macrophages	111
Fig 5.9.	Conditioned medium from LDL-ceramide activated RAW 264.7 cells reduces insulin stimulated glucose uptake in L6 Glut4-myc myotubes.(A) LDL activated RAW 264.7 condition medium, (B) LDL-C16:0 ceramide activated RAW 264.7 condition medium, (C) LDL-C24:0 ceramide activated RAW 264.7 condition medium	112

Chapter 6: General Discussion

Fig. 6-1.	General schematic of LDL-ceramide interaction among tissue	126
------------------	------------------------------------------------------------------	-----

CHAPTER 1

Literature Review

1.1 Introduction

Insulin is required for proper postprandial uptake and storage of glucose. When non adipose tissues, such as skeletal muscle and liver accumulate lipids because of excessive supply, they become insulin resistant, a state of impaired insulin action that requires higher insulin levels to maintain euglycemia. Insulin resistance and inflammation are hallmarks of type 2 diabetes and ample evidence exists which unequivocally link lipids as a causality of this pathological state ¹.

The sphingoid lipid, ceramide has been strongly implicated in the aetiology of insulin resistance and inflammation. Intracellular ceramide accumulation has been associated with insulin resistance ²⁻⁶ and cell culture models using ceramide analogues have implicated its role in repressing key molecules of insulin signal transduction^{3, 7-9}. In addition, ceramide has been well documented to trigger various pro-inflammatory pathways¹⁰⁻²⁷, which produce cytokines that are antagonizing to insulin signalling.

However, unlike most studies which use water soluble ceramide analogues, natural ceramides are hydrophobic and do not exist by itself in the systematic circulation, which is a highly aqueous environment, yet their existence has been verified in plasma^{28, 29}. Additionally, plasma ceramide levels are elevated in insulin resistant type 2 diabetic patients ³⁰ and circulating ceramides are transported via carrier proteins. What is unknown, however, is the roles of these circulating ceramides in eliciting inflammation and insulin resistance.

This literature review discusses the role of ceramides in insulin de-sensitization and the nature of ceramide transport in the circulation and in so doing, how ceramide is the basis through which hyperlipidemia and inflammation converge to elicit insulin resistance is highlighted.

1.2 Type 2 diabetes and the insulin resistant state

1.2.1 Type 2 Diabetes and obesity

Type 2 diabetes mellitus (T2DM) is a metabolic disorder that is characterized by high blood glucose in the context of insulin resistance and relative insulin deficiency³¹. It is well established that the development of T2DM is due to a combination of genetic background and environmental factors³². Whilst this disease has a strong genetic component, lifestyle factors such as obesity, high blood pressure, diet and lack of physical activity can greatly exacerbate the development of this disease. Chronically high blood glucose levels in T2DM can lead to deleterious and serious medical conditions, with retinopathies related to microvascular disease among the most common, in addition to an increased risk of heart attacks, kidney failure, strokes, cognitive dysfunction and loss of hearing.

A feature of T2DM patients is that almost all are obese and the risk of developing T2DM increases greatly beyond a BMI of 25kg/m^2 , depending on the distribution of adiposity, ethnicity and gender^{33, 34, 35, 36}. However, not all obese patients have T2DM.

Two major theories in obesity-related T2DM development are the concepts of lipotoxicity and inflammation. Lipotoxicity is the pathogenic link which is proposed to tie obesity and T2DM. Briefly, lipotoxicity refers to the deleterious cellular consequence of exposure to chronically high concentrations of fatty acids and excessive lipid deposition into non-adipose tissue. The concept of inflammation refers to the low-grade inflammatory state which is characteristic of obesity and the increased production of pro-inflammatory cytokines by macrophages contained in expanding adipose depots which play a role in insulin sensitivity. Both of these concepts will be further expanded in the course of this review.

1.2.2 Glucose clearance and homeostasis

The brain, which does not need insulin to utilize glucose, accounts for approximately 50% of all glucose uptake under basal conditions³⁷. Liver and gastrointestinal tissues, which also do not require insulin for glucose uptake, make up 25% of glucose disposal under basal conditions, and the remaining 25% of glucose clearance, occurs

in the insulin-dependent tissues such as muscle and adipose tissue in their post absorptive phase ³⁸. During an insulin stimulation (e.g after feeding) however, skeletal muscle accounts for the majority of total glucose disposal (75-90%) ³⁹, while adipose tissue accounts for approximately 10% ⁴⁰.

In insulin responsive individuals, the body is able to reach glucose homeostasis by striking a balance between glucose uptake and glucose output during insulin stimulation (Fig.1-1). However, in T2DM this balance is altered, resulting in a reduced level of glucose clearance and an elevated level of glucose in the circulation. This loss of balance in glucose homeostasis is largely attributed to insulin resistance, which is a state of impaired insulin ability that fails to bring about euglycemia.

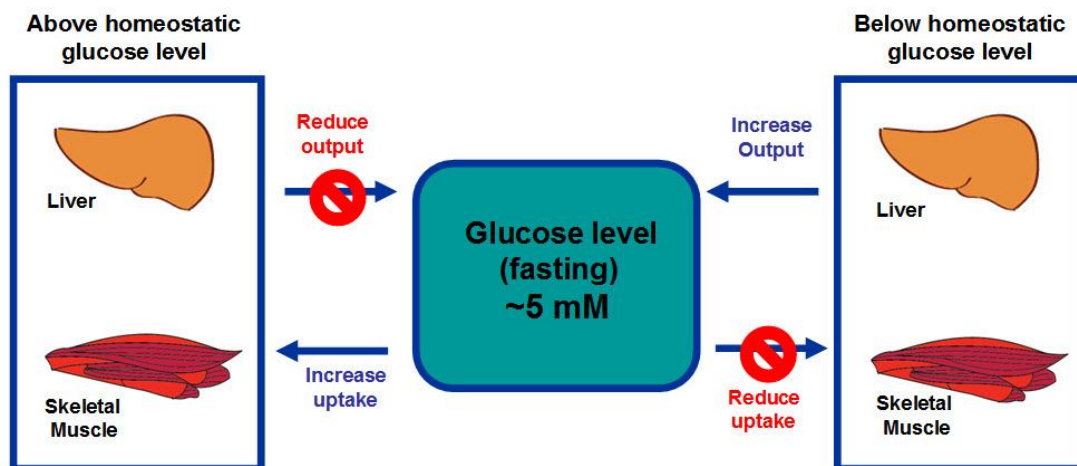


Fig.1-1. Regulation of blood glucose levels by liver and skeletal muscle in the presence of insulin during changes in homeostatic glucose level. During feeding, (e.g increase blood glucose) insulin levels are elevated, this leads to increased uptake of glucose by skeletal muscle. The liver, in turn, suppresses glucose release to prevent further raising blood glucose levels. The converse occurs when glucose levels fall below homeostatic levels and the liver releases glucose while skeletal muscle suppress glucose uptake.

1.2.3 Insulin action and mechanism

A key molecular player in insulin signal transduction is AKT, which is also known by its historical name of protein kinase B (PKB). During insulin stimulation, a cascade of signalling activity is activated. Insulin receptors activate IRS-1/2, which in turn complexes with PI-3K to convert membrane bound PIP₂ to PIP₃ causing PDK-1 and mTORC2 (PDK-2) activation. This results in phosphorylation of AKT at Ser 473 and Thr 308. The activated AKT allows GLUT-4 sequestered by AS160 to separate and translocate to the cell membrane which brings glucose into the cell^{41,42} (Fig.1-2).

Full activation of AKT occurs when both these two residues, Ser 473 located at the hydrophobic C-terminal regulatory domain and Thr 308 found at the activation loop, are phosphorylated during insulin stimulation⁴³.

This process involves phospholipid phosphatidylinositol (3-4-5)-trisphosphate (PIP₃), synthesized at the membrane by phosphoinositide 3-kinase, which causes the translocation of pleckstrin homology domain-dependant AKT to the plasma membrane. The pleckstrin homology domain of AKT has high binding affinity to PIP₃. When bound, a structural change occurs that leads to the phosphorylation of AKT at Thr308 by the enzyme PDK 1 (also known as 3-phosphoinositide-dependent protein kinase 1)⁴⁴. Studies suggest that activation of AKT at its Ser 473 residue, depends on cell type and agonist⁴⁵.

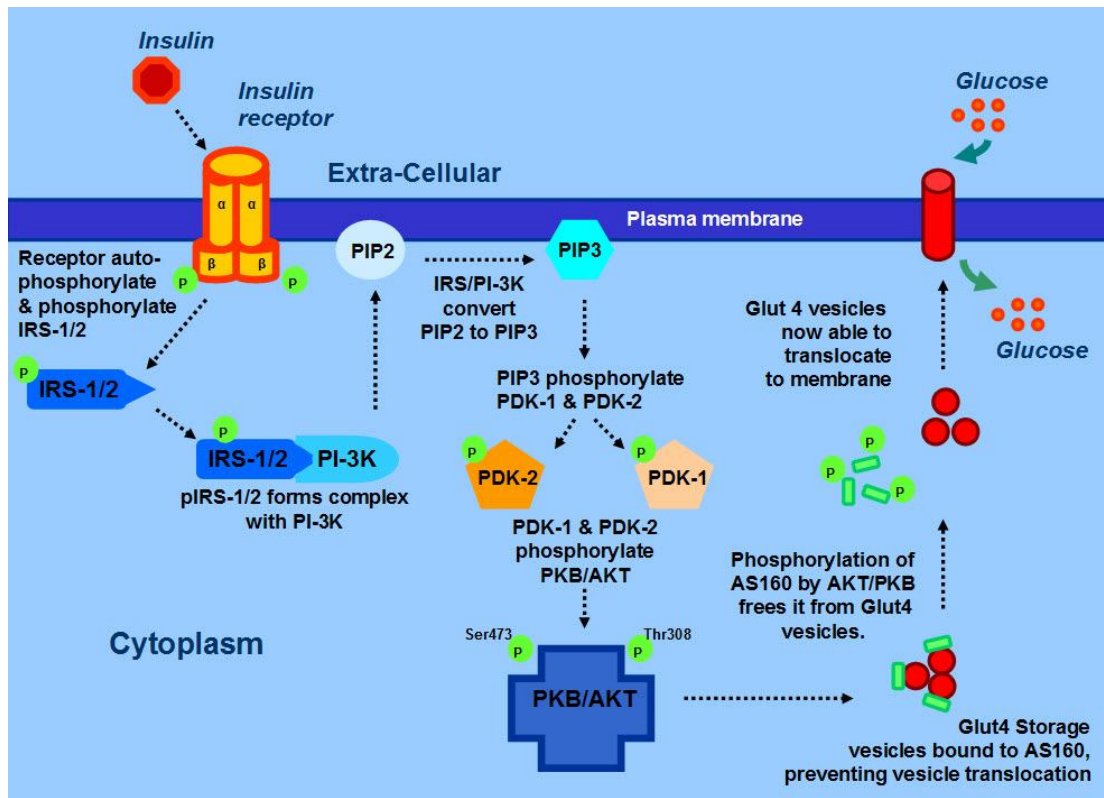


Fig.1-2. *Insulin signalling transduction in skeletal muscle. During insulin stimulation, insulin receptor activates IRS-1/2. Activated IRS -1/2 proceeds to complex with PI-3K and converts membrane bound PIP₂ to PIP₃ causing PDK-1 and mTORC2 (PDK-2) activation, which results in phosphorylation of AKT at Ser 473 and Thr 308. Activation of AKT allows GLUT-4 to separate from AS160 and translocate to the membrane for glucose transport. IRS-1/2, insulin receptor substrate-1/2; PI-3K, phosphatidylinositol 3-kinase; PIP₂, phosphatidylinositol 4,5-bisphosphate; PIP₃, phosphatidylinositol-3,4,5 trisphosphate; PDK1, 3-phosphoinositide-dependent protein kinase 1; PDK2, phosphoinositide-dependent protein kinase 2; PKB, protein kinase B; AS160, Akt substrate of 160 kDa; Glut4, glucose transporter type 4.*

1.2.4 Lipid-induced insulin resistance: Lipid toxicity

Euglycemia is the normal homeostatic concentration of glucose in blood (~5mM during fasting). Insulin resistance occurs when a normal post-prandial insulin dose is unable to achieve optimal glucose uptake in insulin dependent glucose clearing tissues and to suppress gluconeogenesis in liver to achieve euglycemia. Various studies have shown that dysfunctional insulin signalling is highly associated with T2DM^{46,47}. At a

molecular level, insulin resistance is the diminished ability of insulin to signal through its cascade, due to agents that impede its transduction. While glucocorticoids and TNF α count among the provocateurs of insulin resistance^{8, 48}, there is compelling evidence that an excess of lipids beyond normal requirements is also a cause of insulin resistance^{49, 50}.

It is well documented that 'ectopic' lipid accumulation in peripheral insulin sensitive tissues, such as skeletal muscle and liver, induces insulin resistance by interfering with insulin signal transduction⁵¹. Additionally, cumulative evidence provides support for the role of elevated plasma free fatty acids as a cause of lipid induced insulin resistance in obesity. Firstly, the majority of obese subjects have elevated free fatty acids in the plasma^{52, 53}, secondly, in both diabetic and non-diabetic patients, acute elevation of FFA in plasma produces dose-dependent insulin resistance^{47, 49, 54, 55, 56} and thirdly, obese diabetic patients with chronic high levels of FFA in the circulation, show significant improvement in insulin sensitivity when plasma FFA levels are lowered overnight (from ~600 to 300 $\mu\text{mol/l}$) using pharmaceuticals⁵⁷.

The non-immediate effect of plasma FFA in causing insulin resistance (2-4 hours) and the equivalent delay for insulin resistance to recede, suggest that FFA induced insulin resistance is an indirect rather than a direct effect⁵⁶. The insulin inducing effect observed in FFA may possibly be due to generation of other lipid metabolites intracellularly which antagonize the insulin signal propagation.

1.3 Ceramides and its intracellular synthesis.

1.3.1 Ceramides

The sphingolipid, ceramide, is a bioactive lipid metabolite, comprising a variable 14-24 carbon length fatty acid, held to a sphingoid base by an amide bond (Fig 2). Within cells, ceramides can be found in lysosomes and the endoplasmic reticulum, however, they are mainly localised within caveolae, which are 50-60nm diameter invaginations of the plasma membrane⁵⁸. Initially, ceramide was thought to only serve a structural role in the membrane lipid bilayer. However, studies using artificial water soluble

short chain ceramides have document in much detail the myriad physiological process that this sphingolipid is able to modulate⁵⁹⁻⁶². These processes range from apoptosis, cell survival, inflammatory responses, mitochondrial function and insulin sensitivity^{3, 59, 60, 63}. Intracellularly, ceramides can be generated by three different pathways, namely, the sphingomyelinase pathway, the *de novo* pathway and the salvage/recycle pathway.

1.3.2 Sphingomyelinase pathway

In the sphingomyelinase pathway, ceramide synthesis occurs via the hydrolysis of phospholipid sphingomyelin found at the plasma membrane, by acid or neutral sphingomyelinase⁶⁰. The acid sphingomyelinases convert sphingomyelin to ceramide, while sphingomyelin synthase converts ceramide back to sphingomyelin⁶⁴ (Fig 1-3). The activity of the sphingomyelinase pathway can be further modulated by factors such as TNF α , Fas ligand, phorbol ester, heat stress, oxidative stress, ionizing radiation and chemotherapeutics^{59-62, 65-71}.

1.3.3 *De novo* pathway

The *de novo* pathway is a multi-stage substrate dependent process that relies on several enzymes and takes place in the endoplasmic reticulum⁷². The long chain fatty acid palmitate serves as the key substrate for *de novo* synthesis of ceramide^{60, 62}. When this pathway is initiated, serine and palmitoyl-CoA undergo condensation by the rate limiting enzyme of *de novo* synthesis, serine palmitoyl-CoA acyltransferase (SPT), which is localized in the endoplasmic reticulum⁷². Only in the presence of saturated long chain fatty acids (LCFAs) and not unsaturated fatty acids, is SPT activated^{8, 73}. The condensation of serine and palmitoyl-CoA forms 3-ketosphinganine. 3-ketosphinganine is then reduced to dihydrosphingosine (sphinganine) by 3-ketosphinganine reductase and subsequently acylated to dihydroceramide by dihydroceramide synthase which, depending on its isoform, produces dihydroceramide with distinct fatty acyl lengths^{74, 75}. Finally, dihydroceramides with different fatty acyl chain lengths are desaturated by dihydroceramide desaturase to form the corresponding fatty acyl chain ceramide (Fig.1-3). There is ample documentation showing that stimulation of SPT and dihydroceramide synthase in the *de novo* pathway causes an increase in ceramide production^{6, 76, 77}. Other stimuli such

as chemotherapeutics, heat stress, oxidised low density lipoprotein (LDL) and cannabinoids^{69, 76, 78, 79} can also interfere with this pathway. In addition, studies have shown that *de novo* generated ceramide can, in turn, be modified and converted to alternative forms such as glucosylceramide, ceramide 1-phosphate and sphingosine 1-phosphate which can, by itself, have distinct effects in apoptosis and stress responses^{69, 76, 78}.

1.3.4 Salvage/recycle pathway

The characteristic feature of the salvage pathway is how a number of different enzymes interplay to recycle existing complex sphingolipids, sphingosine and modified ceramide (glucosylated and phosphorylated) to generate ceramide. Enzymes involved in this pathway include, sphingomyelinases, ceramidases, acid- β -glucosidase, ceramide synthases and ceramidases (Fig.1-3).

In this pathway, the breakdown of complex sphingolipids and glycosphingolipids occurs in endosomes and lysosomes. During catabolization of these sphingolipids, ceramides are left behind in the lysosome, while fatty acids and sphingosine are released⁸⁰. The liberated long chain sphingosine bases, which are now located at the endoplasmic reticulum or at endoplasmic reticulum-associated membranes, then re-enter other pathways for ceramide or sphingosine-1-phosphate synthesis^{81, 82}. The long chain sphingoid bases are picked up and recycled by ceramide synthase to generate more ceramide via re-acylation.^{83, 84} In the case of glucosphingolipids, the enzyme β -glucosidase removes monosaccharides from the oligosaccharide end of these glucosphingolipids, breaking them down until they are converted back into ceramide⁸⁴. This pathway, which provides long-chain sphingoid bases for reconstruction of various sphingolipids, like ceramide, accounts for 50% to 90% of all sphingoid biosynthesis^{85, 86}.

While free dihydrosphingosine is mostly manufactured by the *de novo* pathway, a contrast should be noted on how free sphingosine is derived intracellularly. That is, free sphingosine availability for shunting into other sphingolipid generation pathways, stems exclusively from the turnover process of the salvage pathway⁸⁴. The turnover of sphingolipids and glucosphingolipids, to yield free sphingosine, has been shown to

occur independently of exogenously added sphingolipid. Sonnino and associates, utilising a cell culture model system, demonstrated that, while exogenously added sphingolipids to serum in cell culture media end up in lysosomes, they are broken down into small fragments and water, while the majority of endogenous sphingosine is recycled⁸³.

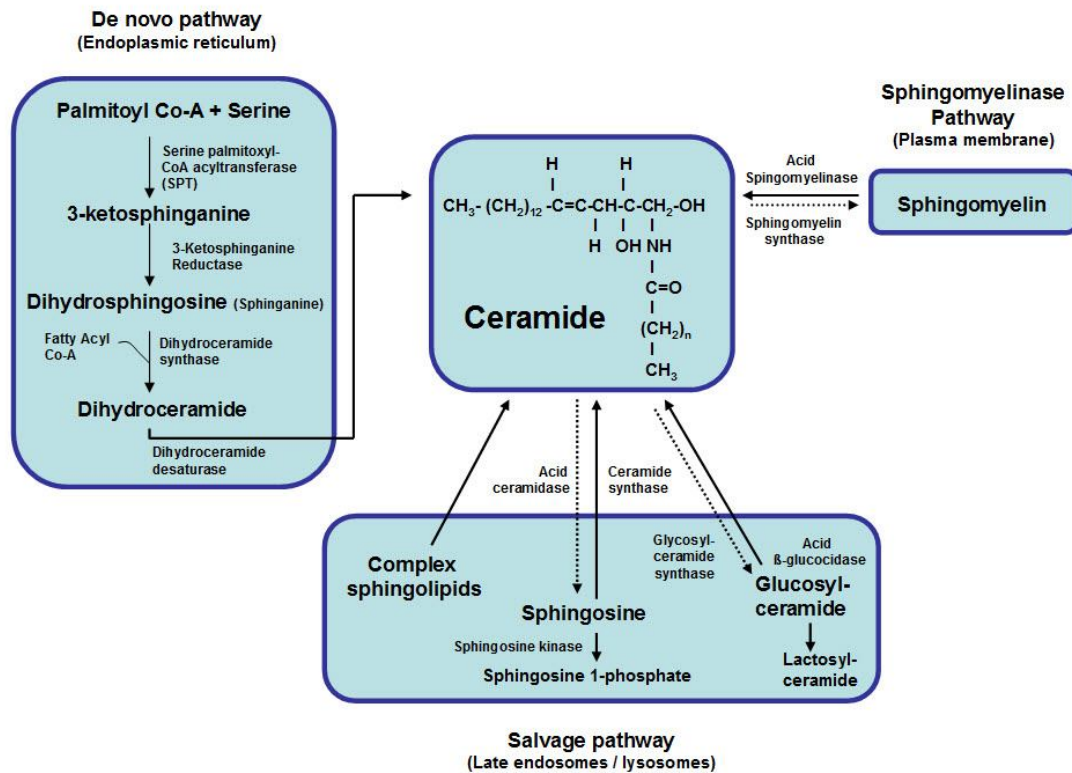


Fig. 1-3. Ceramide synthesis and its derivatives. This scheme shows the three main pathways of ceramide synthesis; the de novo pathway, which is substrate dependent; the spingomyelinase pathway which is activated by hydrolysis of spingomyelin by spingomyelinases; and a salvage pathway which occurs in late endosomes and recycles complex sphingolipids, sphingosine and glucosylceramide to reform ceramide. In addition, ceramide can be further modified (i.e by glucosylation and phosphorylation), to produce ceramide sub-species that have distinct biological effects.

1.3.5 Variable acyl-chain ceramides

Cloning studies have shown that, in mammals, six genes code for ceramide synthase. These genes are known both as longevity-assurance homologues (LASSs: ranging from LASS 1-6) and also known as ceramide synthases (CerSs: ranging from CerS1-6)^{75, 87-89}. These individual ceramide synthase isoforms have preference for specific acyl CoA substrates that they use for acylation of dihydrosphingosine. LASS1 significantly prefers to use long chain C_{18:0} fatty acid CoA, while LASS5 and LASS6 use myristoyl, palmitoyl and steroyl CoA^{74, 75}. This selective utilisation of different length fatty acyl CoA by the different isoforms of ceramide synthase is the reason why ceramide species of different acyl-chain lengths exist.

1.4 Observations implicating ceramide in insulin resistance.

1.4.1 In vitro observations implicating ceramide in insulin resistance.

In vitro observations have shown that ceramide accumulation during palmitate treatment is responsible for insulin resistance in several cell culture models^{3, 7-9}. Consistent with rodents studies, it appears that the mechanisms of lipid induced insulin resistance in human myoblast are distinct from each other, depending on the fat source that is available⁹⁰.

Using palmitate as a saturated fat source and myriocin and fumosin B as inhibitors for suppressing SPT and ceramide synthase activity, it has been shown that production of ceramide from palmitate is necessary for the induction of insulin resistance in human myoblast cells. In addition, this group recapitulated these observations using C2-ceramide, an artificial water soluble ceramide that causes insulin resistance in human myoblasts⁹⁰.

In C2C12 mouse myotubes, ceramide levels were increased 2 fold during palmitate treatment and exogenously added C2-ceramide mimics the effects of palmitate induced insulin resistance by inhibiting PKB activation and stimulating MAP kinases⁹. However, in L6 rat myotubes, C2-ceramide was shown to cause insulin resistance

by impairing insulin dependent recruitment of PKB, resulting in a loss of downstream signalling³.

1.4.2 *In vivo* accumulation of ceramide decreases insulin sensitivity.

One of the initial *in vivo* observations, which suggested that ceramide might be involved in the development of insulin resistance, was when skeletal muscle became insulin resistant when challenged chronically with non-esterified fatty acids (NEFAs). This insulin resistant state coincided with an increase in intramuscular ceramide and diacylglycerol (DAG) content²⁻⁶. However, this was confounded by the observation that endurance-trained athletes continue to have normal insulin sensitivity despite having elevated intramuscular triacylglycerol (IMTG) content (known as the athletes paradox), suggesting that IMTG by itself might not be directly involved and that some other lipid species which accumulate intramuscularly during lipid loading^{91, 92} maybe involved instead.

Following these observations, there was evidence suggesting that there are two possible mechanisms for lipid-induced insulin resistance that is dependent on the type of lipid. One study showed that, while infusion of both saturated and unsaturated oils decreases the rate of insulin-stimulated glucose uptake in rat soleus muscle, only lard (saturated fat) increased intramuscular ceramide content, while DAGs accumulated when the fat source was non-saturated (soy-based cocktail)⁷. Indeed, this observation is to be expected, as SPT, the enzyme for *de novo* ceramide synthesis, is reliant solely on saturated fatty acids as substrates^{8, 73}.

Several notable studies from the Summers group used myriocin, a specific inhibitor of SPT, as a strategy to examine whether a ceramide dependent mechanism of insulin resistance is involved during an oversupply of saturated fat. They showed how lard oil infused rats treated with myriocin had reduced ceramide content in soleus muscle and enhanced insulin sensitivity, as measured by hyperinsulinemic-euglycemic clamps. This was in contrast to non-myriocin treated controls, which had higher ceramide content and decreased insulin sensitivity^{7, 8}. In addition, they showed that myriocin did not improve soy-induced (non-saturated fat) insulin resistance, nor reduced DAG levels⁷. Their data suggest that ceramide generation is essential for saturated fat

induced insulin resistance, but not for unsaturated fat induced insulin desensitization. Collectively, these *in vitro* and *in vivo* observations strongly implicated ceramide in the development of lipid induced insulin resistance.

1.5 Mechanism of ceramide induced insulin resistance.

1.5.1 Ceramide mediated PP2A activation leads to AKT deactivation.

While it is now well accepted and widely documented that ceramide can down-regulate expression of insulin signalling molecules, such as AKT, and suppress activation of phosphoinositide 3-kinase, it appears that ceramide does not interfere directly with these key signalling events to evoke insulin resistance^{3, 63, 93}.

One proposed mechanism involves ceramide indirectly inhibiting AKT phosphorylation by activating the serine/threonine phosphatase protein phosphatase 2A (PP2A). PP2A inhibits AKT activity by causing dephosphorylation of AKT at Thr 308 and Ser 473^{94, 95}.

Studies that provide evidence for this mechanism come in the form of cell culture studies using brown adipocytes and C2C12 myotubes treated with okadaic acid, a protein phosphatase inhibitor^{96, 97}. While okadaic acid does not inhibit specific protein phosphatase isoforms, when used in conjunction with small t-antigen, which displaces subunits of PP2A, okadaic acid was shown to directly inhibit PP2A activity and prevent ceramide induce AKT inactivation⁶³.

However, this mechanism of ceramide induced inhibition of AKT through PP2A does not appear to be pleiotropic. Ceramide mediated AKT inactivation could not be blocked using okadaic acid in L6 myotubes or in white adipose tissue^{3, 98}, implying that this is not the sole mechanism by which ceramide inactivates AKT.

1.5.2 Ceramide activates aPKC λ/ξ associates with AKT and causes repression.

When activated by ceramide, atypical protein kinase C (aPKC) λ/ξ associates and forms a complex with AKT. When bound as a complex, AKT membrane localisation is disrupted and signalling to downstream events becomes suppressed (Fig.1-5). This indirect effect of ceramide causing disruption on insulin signalling via aPKC λ/ξ was also shown to be specific to AKT and not via an effect on membrane bound phosphoinositides, which are also part of the insulin signalling cascade⁹³.

The use of PKC activators and inhibitors in human muscle strips were among the initial studies that demonstrate this direct ability of PKC to deactivate AKT⁹⁹. It was shown that activation of aPKC λ/ξ , suppresses insulin activated AKT, while inhibition of aPKC resulted in enhanced insulin sensitivity⁹⁹⁻¹⁰². Furthermore, in isolated human adipocytes and L6 myotubes, inhibiting PKC was sufficient to safeguard against ceramide induced AKT deactivation during insulin stimulation^{101, 103}.

While there is evidence that shows aPKC repression of AKT activation, the link between ceramide and aPKC activation was established in studies which demonstrated ceramide binding directly to the cysteine-rich domain of aPKC λ/ξ ¹⁰⁰. Subsequent work from this group showed that aPKC λ/ξ , associates with AKT at the pleckstrin homology domain of AKT, the region used by AKT for membrane translocation. The region then becomes unavailable for AKT during translocation to the plasma membrane and results in suppressed AKT activity¹⁰¹.

1.5.3 Caveolae influences aPKC λ/ξ and PPA2 activation

Caveolae, a structural region of the plasma membrane enriched with ceramide, have been documented to influence the activation of aPKC λ/ξ and PPA2, the two mechanisms which are responsible for ceramide mediated AKT inactivation.

The plasma membrane does not exhibit a homogenous architecture but rather comprises a fluid base containing different proteins and micro-domains of lipids known as lipid rafts¹⁰⁴. Caveolins (consisting of caveolin 1-4)¹⁰⁵ are cholesterol binding integral membrane proteins that are responsible for giving caveolae their

characteristic pit-like appearance and they are found in a type of lipid rafts known as cholesterol-enriched membrane micro-domains (CEMs). The caveolin, contained in CEMs, act as a scaffold to which signalling complexes assemble, thus playing an important role in myriad signalling processes, including insulin mediated responses^{105, 106}.

α PKC λ/ξ becomes activated in the presence of ceramide when it translocates to CEMS of caveolae. Activated α PKC λ/ξ proceeds to bind with AKT and in so doing, suppresses AKT activity. Indeed, α PKC λ/ξ is recruited to CEMs following acute ceramide treatment¹⁰³. To further demonstrate the importance of the role of CEMs in α PKC λ/ξ recruitment, this same study showed that cholesterol-depleting agents which disrupted CEMs stopped recruitment of these kinases to the membrane and reduced ceramide induced AKT inactivation¹⁰³.

It has been postulated that caveolin-1 serves to assist in connecting the AKT- α PKC λ/ξ complex to CEMs¹⁰³. Although no evidence exists to show α PKC λ/ξ or AKT directly associating physically to CEMs, there is evidence of ceramide enhancing AKT- α PKC λ/ξ and α PKC λ/ξ - caveolin 1 association in 3T3L1 adipocytes¹⁰³. This bridging effect is believed to be due to regions in caveolin proteins known as caveolin scaffolding domains, which give them the ability to directly associate with α PKC λ/ξ ¹⁰⁷. Additional studies have also shown that cellular CEM abundance is directly connected to ceramide mediated AKT inactivation and it appears the mode between PP2A or α PKC λ/ξ mediated AKT inactivation switches, depending on the abundance of CEMs⁹⁴.

In a study involving the use of differentiated 3T3-L1 adipocytes which have plentiful caveolae, ceramide induced AKT inhibition was found to occur via the formation of the α PKC λ/ξ -AKT complex which sequesters AKT and prevents its activation⁹⁴. However, in the case of CEM-deficient 3T3-L1 pre-adipocytes, the mechanism switches instead to the PP2A mode of AKT deactivation, as using okadaic acid to inhibit PP2A ameliorated AKT deactivation by ceramide. In this same study, a different cell line was also used which showed that in fibroblasts with low CEMs, the mechanism for ceramide induced AKT inactivation is via the PP2A route but following over expression of caveolin-1 the mechanism switches instead to the

aPKC λ/ξ pathway. Why this switching mechanism occurs is not fully understood, however some clues can be gleaned from prostate cancer cells which showed that caveolin-1 has suppressive effects on PP2A¹⁰⁸.

Unlike the aPKC λ/ξ pathway, PP2A does not inactivate AKT by interfering with the region required by AKT for membrane translocation, as it was shown that ceramide activated PP2A was still able to dephosphorylate a cytosolic AKT construct lacking the pleckstrin homology domain during insulin stimulation⁶³.

Although these mechanisms involving ceramide activated aPKC λ/ξ and PPA2 activation were highlighted separately, it is highly possible that they are working in combination, but to lesser degrees when one mode is predominately in operation. However, what is clear is that disruption or the lack of caveolae prevents ceramide induced AKT inactivation.

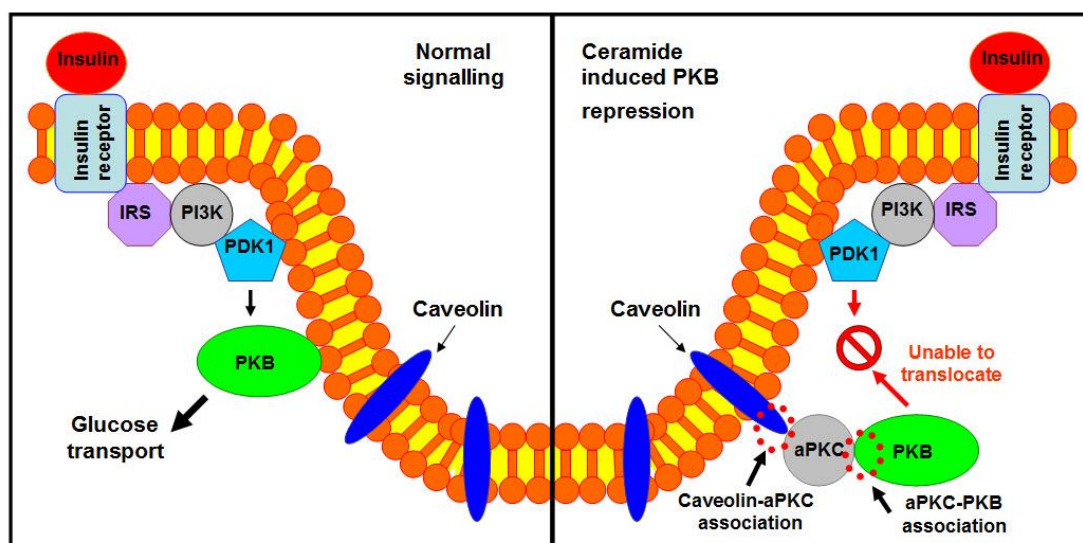


Fig.1-4. Mechanism of PKB (AKT) repression via aPKC λ/ξ complex formation. Normally, when insulin signalling is initiated PIP₃ levels increase causing PKB to translocate to the plasma membrane and be activated by PDK1. However, increased caveolar ceramide activates aPKC λ/ξ , resulting in formation of a complex that puts PKB in a repressed state. Caveolin-1 is believed to bridge the PKB -aPKC λ/ξ complex to caveolae. PIP₃, phosphatidyl-inositol-3,4,5 trisphosphate; PDK1, 3-phosphoinositide-dependent protein kinase 1.

1.6 Observations implicating ceramide to inflammation

1.6.1 Inflammation and insulin resistance.

Two schools of thought exist to explain impaired insulin action due to an oversupply of lipids. One is the idea of lipotoxicity, that is, where oversupply of lipids in non-adipose tissue directly impairs insulin action. The other idea is inflammation, in that, a hyper-activated immune system over-produces inflammatory cytokines which antagonize insulin signal transduction. Evidence now exists to show that there is a continual relationship between inflammation and insulin action and that these two theories are not exclusive singular events but instead are intertwined and work in concert to cause insulin resistance.

The obese T2DM state is characterized by a low grade chronic inflammatory state which has been proven to be causative to insulin resistance ¹. Pro-inflammatory cytokines are known to be involved in systemic insulin resistance. Such examples include the cytokine TNF- α , which activates JNK to disrupt insulin signalling by phosphorylating serine residues on IRS-1 that causes reciprocal suppressive effects in decreasing tyrosine phosphorylation, which is required for insulin signal transduction in the PI3K-AKT pathway of insulin action ¹⁰⁹.

1.6.2 Ceramide activates pro-inflammatory NF- κ B pathway and JNK

One of the first clues that link ceramide to inflammation was not based on studies directly with ceramide, but rather on examining intracellular effects of tumour necrosis factor- α (TNF- α), a pro-inflammatory cytokine ¹¹⁰⁻¹¹³. In these pioneering studies, it was found that TNF- α generated intracellular ceramide by activating acid sphingomyelinase ^{114, 115}, which in turn activated nuclear factor-kappa- β (NF- κ B) a pro-inflammatory transcription factor which is ubiquitously expressed in mammalian cells ⁷⁰. TNF- α in itself is a potent activator of NF- κ B, and NF- κ B in turn is an inducer of TNF- α , this positive feedback is key to many inflammatory conditions such as rheumatoid arthritis and inflammatory bowel disease ²². Interestingly, while TNF- α can activate both neutral and acid sphingomyelinase, only activation of acid sphingomyelinase resulted in NF- κ B activation¹⁹. Animal studies using TNF- α deficient mice have also showed increased insulin action¹¹⁶.

Normally, NF- κ B is rendered inactive in the cytosol, due to its coupling to a repressor protein known as inhibitor of NF- κ B ($\text{I}\kappa\text{B}\alpha$). When phosphorylated by $\text{I}\kappa\text{B}$ kinases (IKK), $\text{I}\kappa\text{B}\alpha$ dissociates from NF- κ B. The uncoupled NF- κ B is then free to translocate to the nucleus to upregulate genes¹¹. $\text{I}\kappa\text{B}\alpha$, once separated from NF- κ B then becomes degraded by proteasomes^{10, 20}. Stimuli known to degrade $\text{I}\kappa\text{B}\alpha$, include, stress responses, viral infections, ultraviolet radiation, free radicals, the cytokines TNF α and IL-1 β , acidic sphingomyelinase and ceramide^{10, 14, 15, 19, 20}. When NF- κ B translocates to the nucleus, it can upregulate the expression of over 150 genes, among them the cytokines and chemokines connected to inflammation. Pro-inflammatory proteins known to be up-regulated by NF- κ B include: interleukin-1b (IL-1b), IL-6, IL-8, monocyte chemo-attractant protein-1 (mcp-1) and COX-2 (also known as prostaglandin-endoperoxide synthase 2, PGHS-2)¹¹⁷.

There is increased JNK activity in muscle, liver and fat in obese insulin resistant individuals¹¹⁸. Additionally, JNK1 null mice are protected against obesity and insulin resistance by process that are both genetic and environmental in origin, although there are no changes in mice that do not express JNK2¹¹⁸. Cell culture models show that ceramides can activate JNK¹¹⁹. JNK is implicated as an agent of insulin resistance, since activated JNK disrupts insulin signaling by phosphorylating serine residues on IRS-1. This leads to a suppressive effect causing a decrease in tyrosine phosphorylation which is required for insulin signal transduction in the PI3K-AKT pathway of insulin action¹⁰⁹.

The mechanism by which ceramide activates JNK is via an intermediate enzyme. The mixed lineage kinase-3 (MLK3) enzyme, a ubiquitous serine/threonine kinase is believed to be the intermediate that connects ceramide to activation of JNK. *In vitro* and *in vivo* studies have shown that ceramide activates MLK3¹²⁰ and overexpression of MLK3 was also found to significantly activate JNK¹²¹. Given that the JNK signalling cascade responds to multiple stimuli, the specificity of ceramide induced MLK3 activation of JNK but not ERK and p38¹²⁰ provides a clue to a mechanism whereby a specific MPKKK under the influence of an “bridging intermediate” (i.e ceramide) can regulate the different MAPK pathways.

1.6.3 Ceramide activates c/EBP and COX-2 pathway

In addition to activating the pro-inflammatory NF- κ B pathway, ceramide also modulates CCAAT/Enhancer binding proteins (c/EBPs), a family of transcription factors that regulate inflammation.

In rat primary hepatocytes, C2 ceramide treatment increased nuclear phosphorylated c/EBP β protein content, although transcript levels were not altered¹³, and while C2-ceramide was unable to induce pro-inflammatory COX-2 directly in RAW 264.7 macrophages, C2-ceramide enhanced the effect of the endotoxin, lipopolysaccharide (LPS) in increasing c/EBP mediated COX-2 induction in this cell line model. This suggested that ceramide can exacerbate pre-existing inflammatory conditions via a secondary effect¹².

While COX-2 was not directly induced in macrophages, in a human mammary epithelial cell line (184B5 cells), treatment with C2 and C6 ceramide directly induced COX-2 protein through activation of several mitogen-activated protein kinases (MAPK) such as ERK, JNK and p38¹²². Ceramide induced COX-2 expression, leading to inflammatory prostaglandin E₂ (PGE₂) release, was also shown in a study utilizing A549 lung adenocarcinoma cells¹²³.

1.6.4 Ceramide activated protein kinase the link between MAPK inflammatory signalling and ceramide.

During an inflammatory response various intracellular signalling pathways are activated that convey signals to produce myriad inflammatory mediators. One such cascade, which is activated by ceramide during an inflammatory event, is the mitogen-activated protein kinases (MAPKs) pathway.

The MAPK signalling cascade consists of a three tier protein kinase sequential system of signal activation. When activated by GTPases, other kinases, oligomerization or trans-phosphorylation²⁷, MAPKK-kinases (also known as MAPKKKs, MEKK or MKKK) phosphorylate and activate MAPK-kinases (also known as MKK, MEK or MKKs), which in turn activate MAPKs by phosphorylating threonine and tyrosine residues. Once activated, MAPKs then proceed to phosphorylate transcription factors

present in the cytoplasm or nucleus, which leads to expression of target genes, giving rise to a biological response. 14 MAPKKKs (ASK1, Tpl-2, MEKK1-4, MST, SPRK, MUK, TAK1, Mos, B-raf, A-raf, raf-1), 7 MAPKK (MKK4, MKK6, MKK3, MKK7, MEK5, MEK2, MEK1) and 12 MAPK (ERK1-5, JNK1-3, p38 α , β , δ , γ) have been identified thus far ²⁷.

The 12 MAPKs fall under one of three major groups, they are; the extracellular signal regulated kinases (ERK), c-jun N-terminal kinase (JNK) and p38. The later two classes are also known as stress activated protein kinases (SAPKs). The ERKs are activated upstream by MEK1 and MEK2, JNKs by MKK4 and MKK7, and p38s by MKK3, MKK4, MKK6 ^{22, 24, 25}.

Various inflammatory cytokines have been documented to be activated during MAPK activation. ERK activation has been shown to upregulate IL-6, IL-12, IL-23 and TNF- α ^{21, 124} while p38 inhibition has been shown to block TNF- α , IL-1, IL-8 and COX-2 production in monocytes ^{23, 26}. Studies show that JNK contributes to IL-2 secretion and proliferation of thymocytes ¹²⁵ as well as the observation that activating transcription factor-2 (ATF2), a downstream target of JNK in a knockout mouse model, do not express E-selectin ¹²⁶, a leukocyte adhesion molecule, important in the infiltration step of leukocytes to sites of tissue injury ¹²⁷. Anti-inflammatory pyridinyl imidazole drugs known to inhibit MAPKs, have also been shown to inhibit some JNK isoforms¹²⁸. Given the roles of MAPKs in mediating inflammatory processes, the question arises, what is the evidence linking ceramide to the activation of the MAPK pathway?

One well documented target for ceramide action on proteins involved in the MAPK signalling cascade is a membrane associated 97 kDA Ser/Thr protein kinase known as ceramide activated protein kinase (CAP kinase), which is alternately known as kinase suppressor of Ras (KSR) ^{115, 129, 130}. While the usual activation of Raf-1 (a MAPKKK), is through tyrosine kinase receptors involving adaptor proteins, in the presence of pro-inflammatory TNF- α , Raf-1 is instead activated by CAP kinase. CAP kinase sits upstream of Raf-1, and when activated by ceramide, forms a complex which phosphorylates Raf-1 at Thr 269 ¹³¹. Activated Raf-1 then proceeds to activate MEK1, which subsequently activates pro-inflammatory ERK targets, such as phospholipase

A₂ (PLA₂)^{19, 132}. In HL-60 cells, it was shown that CAP kinase activation occurs in a ceramide dependent manner and is essential for TNF induced RAF-1 activation¹³¹. This same group also performed over expression of CAP kinase and showed how it continually stimulates Raf-1 activity, further strengthening the observation on the importance of CAP kinase in modulating Raf-1.

These observations documenting ceramide's ability to activate NF-κβ, c/EBP, COX-2 and MAPK signalling, provide evidence that ceramide can mediate inflammatory responses (Fig.1-4).

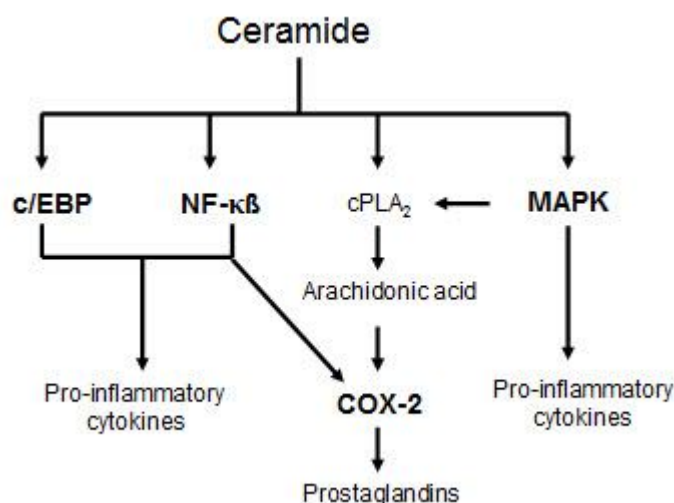


Fig.1-5. Inflammatory pathways documented in literature known to be induced by ceramides¹⁰⁻²⁷. c/EBP, CCAAT/enhancer binding proteins; NF-κβ, nuclear factor-kappa-β; cPLA₂, cytosolic phospholipase A₂; COX-2, cyclooxygenase-2, MAPK, mitogen activated protein kinase.

1.6.5. Toll-like receptor-4 signalling mediates ceramide accrual during lipid loading.

In the inflammation theory of the development of insulin resistance, it is suggested that whole skeletal muscle consists of myocytes and a variety of immune cells such as resident macrophages¹³³⁻¹³⁷. Immune cells increase in abundance during myositis, where they cause specific muscle immune reactions^{133, 137, 138}. Given the evidence showing that immune cells are associated with inflammatory lesions in skeletal muscle¹³⁷, it is suggested that these immune cells may also generate cytokines that

interfere with insulin signal transduction. However, there is no definite evidence supporting this mechanism.

TLR4 is a member of the Toll-like receptor family, which are pattern-recognition receptors that act as sensors to detect and mount inflammatory responses against pathogens. While TLR4 is commonly found in macrophages, there are studies showing that they are also found in myotubes and are upregulated in muscle cultured from obese and insulin-resistant humans¹³⁹. While lipopolysaccharides (LPS) and bacterial cell surface proteins are the better known ligands of TLR4, saturated fatty acids (SFAs) are also known agonist for TLR4¹⁴⁰⁻¹⁴⁴ and it has been shown that TLR4 is required for lipid induced insulin desensitisation¹⁴⁰. There is also documented evidence of TLR4 inducing expression of SPT, in a variety of tissues¹⁴⁵⁻¹⁴⁷, as well as activating sphingomyelinase, which hydrolyses sphingomyelin to generate ceramide¹⁴⁸.

One unusual observation was that several long-chain SFAs which were not substrates for SPT, the rate limiting enzyme for *de novo* pathway of ceramide synthesis, could still induce ceramide accumulation¹⁴⁹. While substrate alone was long thought to be the sole force driving *de novo* ceramide synthesis, this might not always be the case. An alternative mechanism of ceramide accrual in the face of lipid oversupply has been linked to Toll-like receptor-4 (TLR4) in a recent study⁷.

In a series of elaborate animal and cell culture experiments, Summer's group showed that SFAs, including palmitate, do not exclusively upregulate ceramide synthesis by loading the *de novo* pathway with substrate, but rather by triggering the TLR4 cascade, which induces NF- κ B activation and upregulation of genes associated with ceramide synthesis such as different SPT and CerS isoforms⁷. This same study also showed that sodium salicylate, a IKK β inhibitor, led to enhanced glucose and insulin tolerance and blocked accumulation of ceramide in soleus muscle, liver and hypothalamus of high fat fed mice. Together, these studies show that IKK β is essential for TLR4-mediated insulin resistance and ceramide synthesis. Furthermore, these studies highlight one pathway through which hyperlipidemia and inflammation converge to cause insulin resistance.

1.7 Ceramide in systematic circulation

1.7.1 Plasma ceramide

While important proof of principal concepts have been drawn from utilising water soluble short-chain ceramides to examine the role of ceramide in physiological processes²⁰⁻²³, including insulin resistance^{7, 9, 90}, these studies are not entirely reflective of natural ceramides, which have long acyl chains and are extremely hydrophobic. However, it is well documented that even though natural ceramides are hydrophobic, they circulate in the blood^{28, 29}. In addition, elevated plasma ceramide levels have even been correlated with many pathological disorders, such as coronary artery disease^{150, 151}, atherosclerosis¹⁵²⁻¹⁵⁴, obesity^{30, 151} and insulin resistance in type 2 diabetic patients³⁰.

1.7.2 Sub-species of ceramide in plasma.

Analytic techniques such as electrospray tandem mass spectrometry (ESI-MS/MS)^{155, 156}, gas chromatography mass spectrometry (GC-MS)¹⁵⁷, high-performance liquid chromatography (HPLC)¹⁵⁸ and high-performance liquid chromatography mass spectrometry (HPLC-MS)¹⁵⁹⁻¹⁶¹, have identified the individual ceramide species found in plasma.

Ceramides identified in plasma include, C14:0, C16:0, C18:0, C18:1, C24:0, C24:1, C24:2 ceramide¹⁵⁵⁻¹⁶². The sub-species of ceramide are named accordingly to the number of carbon atoms and the carbon double bonds present in the fatty acid component of ceramide. C16:0 and C24:0 ceramide are the two major sub-species of ceramide in plasma with C16:0 ceramide making up approximately 37% and C24:0 ceramide 28% of the entire ceramide pool¹⁵⁶. C18:0 ceramide contribution is approximately 14%, while the other ceramide contribution are minor (C14 ~ 5% , C18:1 ~1%, C20 ~7%, C24:1 ~9%)¹⁵⁶.

1.7.3 Lipoproteins are transporters of plasma ceramide.

Given the hydrophobic nature of natural ceramide, it was presumed that ceramide in plasma was transported via a carrier protein. In rats, it was demonstrated that nearly

all plasma ceramide are associated with and transported by lipoproteins, such as low-density lipoprotein (LDL), high-density lipoprotein (HDL) and very low-density lipoprotein (VLDL)¹⁶³. Two human studies^{28, 29} also suggest that, similar to rats, ceramide, along with other sphingolipids are also transported by the LDL, HDL and VLDL in the plasma of humans. It is highly plausible then, that, since these lipoproteins function as carriers for plasma ceramides, their levels in circulation may be implicated in pathological conditions associated to ceramides.

1.7.4 Lipoproteins

The circulatory system is a highly aqueous environment. As such, lipids, which are hydrophobic need to rely on carriers to be transported in plasma. Herein lies the importance of lipoproteins which are responsible for circulating lipids in plasma.

Lipoproteins are spherical macromolecular assemblies of protein and lipids. They comprise a non-polar core coated with an amphipathic shell. The non-polar core consists of hydrophobic lipids, such as cholesteryl esters, triacylglycerols and sphingolipids, shielded by a hydrophilic shell coating comprising phospholipids, free cholesterol and apoproteins directed towards the aqueous salt-water environment of plasma. This structural arrangement allows the lipoproteins to remain soluble in plasma (Fig.1-6).

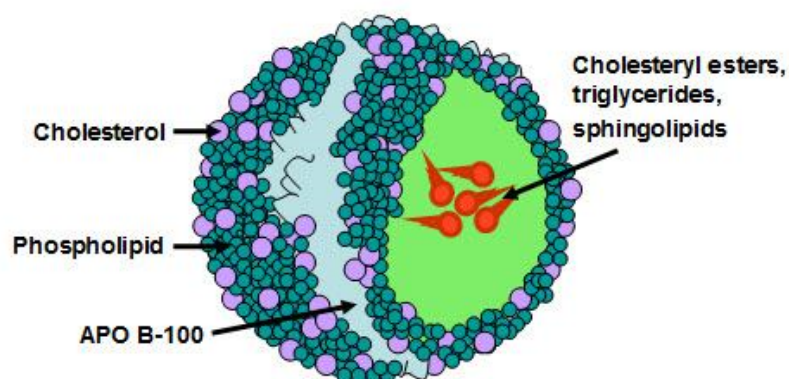


Fig.1-6. Structure of low density lipoprotein (LDL). LDL exhibit typical lipoprotein structure, i.e. an amphipathic shell layer comprising of cholesterol, phospholipids, and protein, encapsulating a hydrophobic core (green area) containing cholesteryl esters, triglycerides and sphingolipids in a sphere configuration.

Five major groups of lipoproteins exist in plasma, classified by size and density based on ultracentrifugation procedures which sort these lipoproteins according to hydrating densities ¹⁶⁴. From the largest to the smallest particle size they are: chylomicrons, very low density lipoproteins (VLDL), intermediate density lipoproteins (IDL), LDL and HDL. These five classes have distinct protein and lipid component configuration (Table.1-1)

Characteristics	Major plasma lipoproteins in human				
	Chylomicrons	VLDL	IDL	LDL	HDL
Density range (g/mL)	<0.94	0.94-1.006	1.006-1.019	1.019-1.063	1.063-1.21
Molecular weight (kD)	(0.4-30) x 10 ⁹	(10-80) x 10 ⁶	(5-10) x 10 ⁶	2.76 x 10 ⁶	(1.75-3.6) x 10 ⁵
Diameter (nm)	75-1200	30-80	25-35	18-25	5-12
Apolipoprotein present	A(1,2,4), B-48, C(1,2,3)	B-100, C(1,2,3), E (2,4)	B-100, C(1,2,3), E (2,4)	B-100	A(1,2,4), C(1,2,3), D, E(2,4)
Protein composition	1-2%	5-12%	10-12%	20-22%	55%
Triglyceride composition	85-88%	50-55%	24-30%	10-15%	3-15%
Cholesterol composition	~1%	8-10%	8-10%	8-10%	2-10%
Cholesteryl esters composition	~3%	12-15%	32-35%	37-48%	15-30%
Phospholipid composition	~8%	18-20%	25-27%	20-28%	26-46%

Table.1-1. Characteristic of major plasma lipoproteins in humans. Adapted from ¹⁶⁵⁻¹⁶⁷.

1.7.5 Low-density lipoprotein clearance in plasma.

In all mammalian cells lipids are essential for normal physiological function (e. g. membrane synthesis). Except for the liver and small intestine, which produce lipoproteins, others cells which cannot synthesize lipids must rely on an external source for their requirements ¹⁶⁸. These cells accomplish this predominately through the uptake of LDL from plasma^{169, 170}. Thus, it is proposed that ceramide localised in LDL could possibly be internalised by cells during the uptake process.

The contributions of each organ to whole body LDL clearance have been examined in the hamster using radio-labelled LDL. The vast majority of LDL cleared from plasma is via the liver (73%), with a minimal role contributed by other organs (Table.1-2). Of particular note is skeletal muscle. While it represents the largest organ in the body, it accounts for only 2.1% of total plasma LDL uptake ¹⁷¹.

Liver	73%	Lung	1.5%
Ovary	0.2%	Kidney	0.8%
Spleen	3.8%	Heart	0.3%
Adrenal	0.1%	Colon	0.4%
Ileum	4.1%	Stomach	0.3%
Jejunum	2.5%	Skin	3.0%
Fat	1.3%	S.muscle	2.1%
Brain	<0.1%	Urine	1.5%

Table 1-2. Percentage of whole-body clearance rate of plasma LDL in hamster. Data from ¹⁷¹.

LDL uptake occurs via receptor-dependent and receptor-independent mechanisms that are predominant according to tissue type. In the receptor-dependent process, LDL binds with high affinity to the low-density lipoprotein receptor (LDL-R) on the cell membrane and is internalized^{172, 173}. This process is saturable. The receptor-independent uptake is a non-saturable process, whereby LDL is passively transported into the cell¹⁷⁴. The liver, ovaries, adrenal gland, lung and kidney primarily use the receptor-dependent pathway to take up LDL, while the other organs appear to rely on a receptor-independent process¹⁷⁴.

1.7.6 Modified LDL potential in eliciting pathological states.

Macrophages are responsible for clearing LDL that have infiltrated through damaged endothelium. The uptake of LDL by macrophages occurs via LDL receptors, which is modulated by a negative feedback mechanism^{172, 173, 175, 176}. When LDL is modified into an oxidised form (ox-LDL), macrophages preferential take this up, because macrophages possess more receptors for altered lipoproteins than they do for native LDL¹⁷⁶. To exacerbate this situation further, the uptake of ox-LDL is not down regulated with increasing intracellular cholesterol content^{175, 176}. The influx of cholesteryl ester rich LDL, leads to a massive build-up of intracellular lipids, transforming the macrophage into atherosclerotic foam cells that release pro-inflammatory cytokines to elicit pathological inflammatory conditions¹⁷⁵. This is in contrast to a fully functional negative feedback system, where uptake of native LDL by macrophages does not result in foam cell formation¹⁷⁷.

While, the dangers of LDL oxidation should be acknowledged, the presence of fully oxidized LDL existing in circulation is very minimal, accounting for only 0.001% in healthy patients¹⁷⁸, while in patients with acute coronary events it is approximately 5%¹⁷⁹. The low level of ox-LDL in circulation is attributed to anti-oxidants which are abundant in plasma and the liver which rapidly clears ox-LDL¹⁸⁰.

1.8 Summary and research aims

In summary, the actions of ceramide are clearly associated with inflammation and suppression of insulin signal transduction. Furthermore, a large body of literature investigating *in vitro* and *in vivo* effects of ceramide have provided compelling evidence implicating intracellular ceramide accumulation with insulin resistance.

In contrast, only associative studies describing the link between circulating ceramide and insulin resistance exists. The mechanisms underpinning plasma ceramide induced insulin resistance and inflammation remains unresolved.

This thesis seeks to investigate the role of circulating ceramide in the development of insulin resistance and inflammation. The specific aims of this thesis are:

1. To determine the nature of ceramide transport in plasma and the lipoprotein-ceramide profile of insulin resistant patients with T2DM.
2. To create a model to mimic the natural ceramide-lipoprotein system for use in subsequent studies of lipoprotein-ceramide biology.
3. To examine the biology of LDL-ceramide *in vitro*. The specific aim was to examine insulin resistance in skeletal muscle myotubes, hepatocytes and adipocytes and to examine inflammation in macrophages.

CHAPTER 2

**Elevated lipoprotein-ceramides
in plasma is associated with
type 2 diabetes in humans**

2.1 Introduction

Insulin resistance is a state of subnormal responses of tissues to the action of insulin to achieve euglycemia and is a central feature in patients with T2DM. While there are numerous factors proposed that contribute to insulin resistance, one such factor is obesity. There is compelling evidence that an oversupply of non-esterified fatty acids (NEFAs) in tissues contributes significantly to insulin resistance^{49, 50}. Since these initial observations, there has been much progress in clarifying the causes of NEFA-induced insulin resistance.

While adipose tissue NEFA production and plasma concentrations are reported to be elevated in obese and insulin resistant individuals^{181, 182}, this is not always the case and adipose tissue NEFA output (lipolysis) is not necessarily increased per unit weight of tissue in insulin resistant states^{183, 184}. In this regard, insulin resistance is often associated with a generalised dyslipidemia and other circulating lipids may provide a signal that impact on insulin sensitivity.

For example, triacylglycerols that circulate within lipoproteins are a known risk factor for insulin resistance¹⁸⁵. Interestingly, plasma ceramides are also increased in genetically obese, T2DM mice¹⁸⁶ and obese subjects with T2DM³⁰, although others have reported no effect of obesity¹⁸⁴ or high-fat feeding¹⁸⁷ on circulating ceramide levels. The hypothesis that circulating ceramides are involved in the aetiology of insulin resistance is attractive, given that intra-myocellular ceramide accumulation causes insulin resistance^{8,9}.

Previous studies have examined ceramide concentrations in plasma. However, ceramide is highly hydrophobic and is presumably transported via a carrier protein. Indeed, nearly all plasma ceramide in rats is incorporated in and transported by lipoproteins¹⁶³. As such, determining the exact lipoprotein fraction enriched with ceramide in human blood is important for understanding how circulating ceramides might signal to other tissues and cause insulin resistance.

2.2 Aims

To determine the lipoprotein fractions in human plasma responsible for ceramide transport and to quantitatively assess which lipoprotein fractions have altered plasma ceramide levels in obese patients with T2DM.

2.3 Materials and methods

The following section describes materials and methods used for chapter 2. Additional or variation of material and methods used in other chapters will be contained within their respective sections.

2.3.1 Subjects and experimental procedures

Twenty-seven male subjects were recruited for the study. All samples were under the same conditions at medical screening and included samples from obese, T2DM patients (T2DM, n=13) and lean, aged matched non-diabetic individuals (Lean, n=14). The categorisation of patients to the T2DM group was determined by patients having a fasting plasma glucose >7 mmol/l and/or plasma glucose levels of >11.1 mmol/l 2 hours after a 75 g oral glucose load. None of the patients received insulin treatment, nor were any of them taking oral hypoglycemic agents or other medication known to alter carbohydrate metabolism. Samples were collected by Dr. Darren Hentsridge and Prof. Bronwyn Kingwell (Baker IDI).

Participant characteristics are summarized in Table 2-1. All volunteers were non-smokers and free of overt coronary disease (based on lack of symptoms at clinical examination and a normal 12-lead ECG). Patients medicated for other conditions were excluded. All participants were normally active but were not specifically exercise trained. The protocol was approved by the Alfred Hospital Ethics Committee, and conducted in accordance with the Declaration of Helsinki of the World Medical Association. All volunteers provided written informed consent prior to participation.

Participants were requested to refrain from exercise, alcohol, caffeine for the 24 h prior to the experimental trial. After an overnight fast (~12 h), participants attended the Alfred Hospital at 0800 h. Subjects were weighed and BMI was calculated by

dividing mass (kg) by the square root of height (m²). Blood samples were drawn from an antecubital vein and immediately inverted and placed on ice.

2.3.2 Blood sampling and analysis

Resting blood samples for biochemical analysis were centrifuged at 1500 x g with the plasma frozen at -80°C for later analysis. Plasma total cholesterol (intra- and inter-assay variation ≤2.5 and 2.7%, respectively), LDL cholesterol (intra- and inter-assay precision ≤4.9 and 4.3%, respectively), HDL cholesterol (intra- and inter-assay precision ≤3.4 and 4.5%, respectively) and triglycerides (intra- and inter-assay precision is ≤1.6 and 2.3%, respectively) were measured with an enzyme based assay using a Cholestech LDX (Cholestech Corporation, Hayward, CA, USA). These analyses were performed by Dr. Darren Hentsridge and A/Prof Matthew Watt.

Glucose concentrations were measured using enzymatic, spectrophotometric techniques with a Cobas-BIO centrifugal analyzer (Roche Diagnostic Systems, Basel, Switzerland) (intra- and inter-assay precision is ≤1.0 and 1.7%, respectively) or by utilizing a Radiometer EML 105/100 (Radiometer Medical A/S, Copenhagen, Denmark). Plasma insulin concentration was measured in duplicate by radioimmunoassay (Linco Research, Inc, St.Charles, MO, USA) (RIA; intra- and inter-assay precision ≤4.4 and 6%, respectively). The glucose and insulin measures were conducted by Dr. Darren Hentsridge. Insulin resistance was determined by using the homeostasis model assessment (HOMA)-IR¹⁸⁸. Software is available at www.dtu.ox.ac.uk/index.php?maindoc=/homa/.

2.3.3 FPLC isolation of lipoproteins.

Lipoproteins from human plasma (200 µl) were isolated by fast protein liquid chromatography (FPLC). Samples were loaded onto an ÄKTA purifier-900 pump (GE Healthcare Life Sciences, Australia) connected to two Superose-6 columns in series, previously equilibrated with 0.15 M NaCl, 0.01 M Na₂HPO₄, 0.1 mM EDTA (pH 7.5). 1 ml fractions were eluted in buffer at a flow rate of 0.4ml/min. The eluted fractions containing lipoproteins were identified by analysis of the UV absorption chromatogram and confirmed by measuring cholesterol in each fraction as per the manufacturer's instructions (Calbiochem Cholesterol Detection Kit, Merck, Victoria,

Australia) (Figure 1). The lipoprotein isolations were conducted by Dr. Jonathan Oakhill (St Vincent's Institute of Medical Research and A/Prof Matthew Watt (Monash University). Ceramide concentrations were determined in fractions as described below.

2.3.4 Ceramide quantification

Lipids corresponding to VLDL, LDL and HDL by size fractionation were extracted according to the methods of Priess et al ¹⁸⁹. The organic phase was evaporated under nitrogen and ceramides were determined using a radiometric method (γ - ³²P ATP) catalysed by diacylglycerol kinase (DAG-K). This reaction phosphorylates both diacylglycerol and ceramide, which are separated by thin layer chromatography. The ³²P-labelled ceramides (ceramide-1-phosphate) were visualised via autoradiography, scrapped from the plates and quantified by scintillation counting.

2.3.5 Statistical analysis

Data are presented as mean \pm SEM. Comparison between groups was performed by unpaired t-tests. Correlations were performed using Pearson correlation coefficient.

2.4 Results

2.4.1 Type 2 diabetic patients and lean patients' characteristics

The characteristics of the subjects are described in Table 2-1. While a BMI of 27 falls in the overweight category, the “lean” subjects are only mildly overweight compared with the overweight cohort. In addition, the highest BMI in the “lean” group is less than the lowest BMI in the obese group. The patients with T2DM had increased BMI, plasma glucose, insulin, cholesterol and triacylglycerols. HOMA IR was also increased in the patients with T2DM indicating reduced insulin sensitivity as expected.

Characteristic	Lean	T2DM	P value
Age (years)	46 ± 3	49 ± 4	0.19
Weight (kg)	86 ± 5	113 ± 6	<0.001
BMI (kg/m ²)	27.0 ± 0.9	34.1 ± 2.9	<0.001
Plasma glucose (mmol/l)	4.7 ± 0.1	10.2 ± 0.9	<0.001
Plasma insulin (pmol/l)	46 ± 6	199 ± 45	0.016
OGTT (2h post)	5.4 ± 0.3	ND	ND
HOMA-IR	0.9 ± 0.1	3.46 ± 0.47	<0.001
Cholesterol	4.91 ± 0.16	4.86 ± 0.45	0.021
Plasma triacylglycerol (mmol/l)	1.06 ± 0.11	2.70 ± 0.52	0.003
LDL	3.18 ± 0.15	2.62 ± 0.31	0.720
HDL	1.26 ± 0.06	0.93 ± 0.08	0.018

Table.2-1. Patient characteristics. BMI, body mass index; OGTT, oral glucose tolerance test; HOMA-IR, Homeostasis Model Assessment insulin resistance. (n=14 lean and n=13 T2DM patients).

2.4.2 Majority of circulating ceramides are localized to lipoproteins

Plasma ceramide levels in lean insulin responsive and obese insulin resistant individuals were assessed after FPLC. Six random samples from each group were selected for FPLC and its subsequent quantification of ceramide. The eluted fractions containing lipoproteins were first identified by analysis of the ultraviolet absorption

spectrum and confirmed by measuring cholesterol in each fraction by ELISA (Fig 2-1). FPLC revealed that 98% of plasma ceramides were incorporated into lipoproteins.

In lean insulin responsive individuals, of the total plasma ceramide, $9.1 \pm 1.6\%$ was contained in VLDL, $47.4 \pm 7.4\%$ in LDL and $43.5 \pm 10.1\%$ in HDL (Fig 2-2A). In insulin resistant obese T2DM, of the total plasma ceramide, $13.8 \pm 3.6\%$ was contained in VLDL, $50.6 \pm 6.0\%$ in LDL and $35.6 \pm 5.6\%$ in HDL (Fig 2-2B).

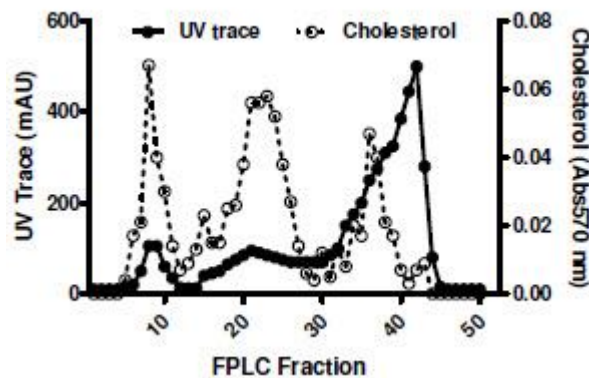


Fig 2-1. Validation of FPLC separation. Representative UV trace of lipoprotein peaks (closed circles) from FPLC and an overlay of cholesterol determined within these fractions by ELISA (open circles)

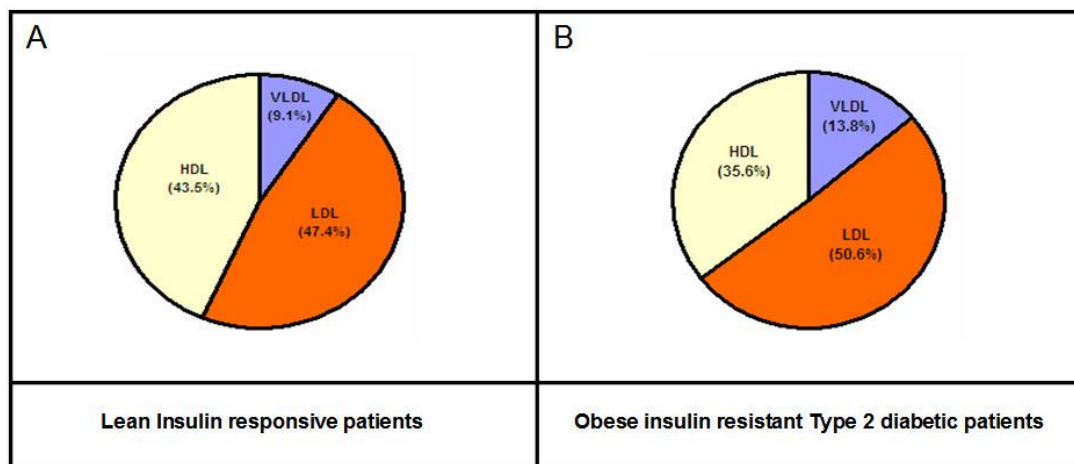


Fig 2-2. Distribution of ceramides in lipoprotein fractions of plasma. A: Ceramide distribution in lipoprotein fractions of lean insulin responsive patients ($n=6$). B: Ceramide distribution in lipoprotein fraction of obese insulin resistant T2DM ($n=6$).

2.4.3 Circulating ceramides are elevated in obese type 2 diabetic patients

Circulating ceramides are elevated in obese patients with T2DM. Total plasma ceramides averaged $13.8 \pm 1.1 \mu\text{mol/l}$ in lean participants and were elevated by 26% in patients with type 2 diabetes ($17.4 \pm 1.3 \mu\text{mol/l}$, $P=0.02$) (Fig 2-3). Specifically, ceramides were increased in LDL (55%, $P = 0.006$) but not in VLDL ($P = 0.76$) or HDL ($P = 0.16$) as shown in Fig 2-4. $n=14$ for lean and $n=13$ for T2DM, $*P < 0.05$.

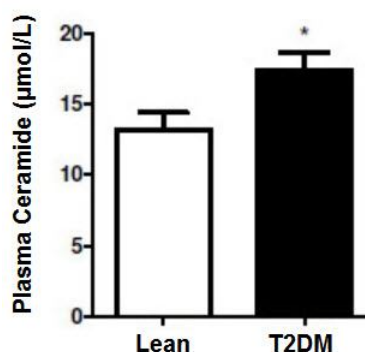


Fig 2-3. Total plasma ceramide content in lean patients and obese patients with T2DM. ($n=14$ for lean and $n=13$) for T2DM, $*P < 0.05$.

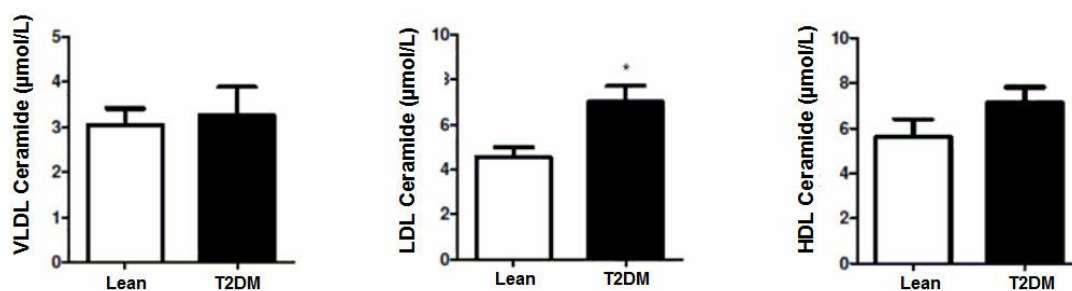


Fig 2-4. Plasma ceramide content in lipoproteins fraction of lean patients and obese patients with T2DM. Venous plasma was obtained from subjects, separated via FPLC and ceramide content quantified by radiometric enzymatic methods. Ceramides were increased significantly in LDL (55%, $P = 0.006$), but not in VLDL ($P = 0.76$) or HDL ($P = 0.16$) fractions. $n=14$ for lean and $n=13$ for T2DM, $*P < 0.05$.

2.4.4 Circulating ceramides correlate with plasma insulin and whole body insulin sensitivity

The potential relationship between plasma ceramide and aspects of glucose homeostasis were examined using correlation analysis. Within the entire cohort, ceramide was positively associated with insulin resistance (HOMA IR, $r = 0.45$, $P = 0.03$), plasma glucose ($r = 0.43$, $P = 0.03$) and plasma insulin ($r = 0.41$, $P = 0.04$) (Fig 2-5A-C). Interestingly, ceramide did not associate with BMI ($r = 0.24$, $P = 0.25$), suggesting that obesity *per se* does not account for increased plasma ceramide levels in patients with T2DM. Total ceramide did not associate with age across the entire cohort ($r = 0.21$, $P = 0.30$) and no correlations were found between total ceramide and plasma triacylglycerol or total, LDL and HDL cholesterol. When correlations were examined for the individual lipoprotein-ceramide fractions vs other variables, only LDL ceramide vs. HOMA ($r = 0.58$, $P = 0.003$) was found to be significant. No other significant correlations were detected among the other lipoprotein-ceramide fractions.

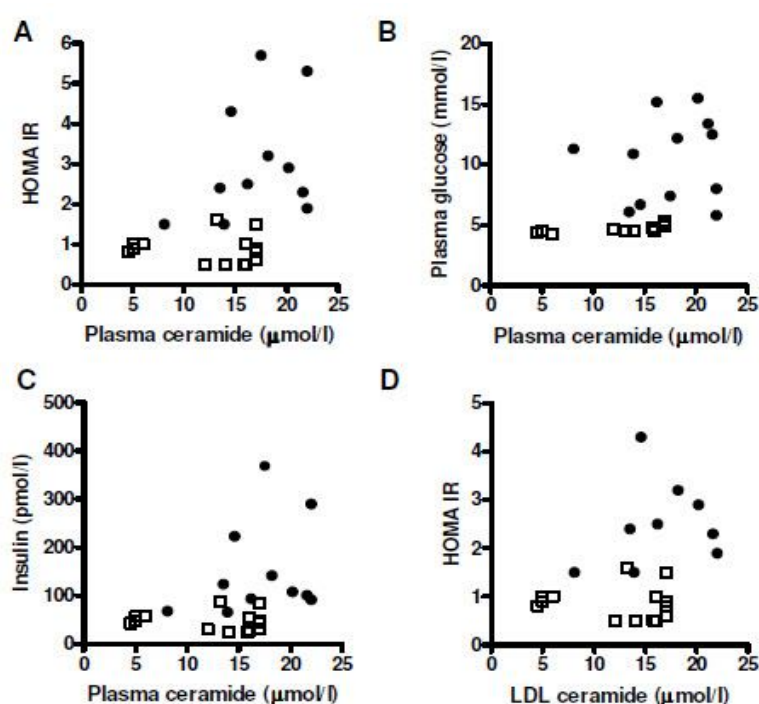


Fig 2-5. Plasma ceramide correlation to (A) HOMA IR, (B) plasma glucose, (C) plasma insulin and (D) LDL-ceramide. Pearson's correlation analysis was used to assess the relationships in the dataset ($n=27$). Closed circles = obese type 2 diabetic patients, open squares = lean insulin responsive patients.

2.5 Discussion

Intracellular ceramide accumulation induces insulin resistance in several tissues, most notably skeletal muscle and liver, which have been well documented^{8, 9, 51, 190}. Most studies, however, use water soluble ceramide analogues, whereas natural ceramides are hydrophobic. Yet the existence of ceramide has been verified in highly aqueous plasma^{28, 29}. While the precise role of plasma ceramide remains unresolved, it appears they may be pathogenic as they are elevated in obese and insulin resistant phenotypes^{30, 186}.

Previous human studies examining plasma ceramide used an initial extraction with organic solvents, which separates lipids from proteins and other potential binding partners, thereby providing information regarding total ceramide levels in blood^{30, 184, 187}. This study extended on this approach and has identified how ceramides are transported in human plasma. Whole plasma was fractionated using FPLC prior to lipid extraction and the present results show that plasma ceramides are almost exclusively associated with lipoproteins. These observations are consistent with previous rodent studies showing ceramide as a substantial component of lipoproteins^{145, 163}, as well as in a recent human study³⁰.

A major unanswered question is from where are these ceramides derived? The logical thought is that ceramides produced in the liver are associated with lipoproteins before their release into the systemic circulation. In support of this premise, the predominant ceramide species in liver and plasma are C24:0 and C24:1^{30, 191} whereas C16:0 and C18:0 are the predominant species in most other tissues such as skeletal muscle¹⁹²⁻¹⁹⁴. Also, cultured hepatocytes secrete ceramide and the predominant fatty acid chain lengths are C20 and C24¹⁶³ while ceramide is not detected in the culture medium from skeletal muscle myotubes or 3T3-L1 adipocytes (unpublished observation, A/Prof. Matthew Watt).

If one assumes that the liver is a primary source of lipoprotein-ceramide, another major question is what is driving the biosynthesis of ceramide in the liver? Serine palmitoyl-CoA transferase (SPT) catalyses the *de novo* synthesis of ceramide, which involves the condensation of long-chain fatty acids to serine. The degradation of

sphingomyelin by sphingomyelinases (SMase) is also a possible source of ceramide. It seems unlikely that an increase in dietary fatty acid availability provides precursors for *de novo* synthesis in the liver because SPT is highly specific for fatty acyl-CoAs of chain length 16 ± 1 ⁷³ and these fatty acids are not abundant in liver or plasma ceramide. However, SPT deficient mice have reduced plasma and liver ceramide¹⁹¹ and intralipid infusion in humans increased plasma ceramides 2-3-fold, indicating that *de novo* synthesis may be relevant in some physiological settings¹⁸⁴.

T2DM has been described as a low-grade inflammatory state¹ and pro-inflammatory cytokines (e.g. IL-1) increase SPT1 mRNA and activity, which produces lipoproteins enriched in ceramides¹⁴⁵. Moreover, cytokines such as TNF α can trigger ceramide accumulation by activating neutral and acid SMase, which hydrolyse sphingomyelin to ceramide¹⁹. A very recent study reported that TLR4 signalling, which is usually associated with the innate immune system in detecting pathogens, was found to mediate ceramide accrual during lipid loading⁷. In addition, ceramide itself can induce a TLR4 response¹⁹⁵ thus creating a positive feedback for ceramide accumulation. Hence, there is a possibility that plasma lipoprotein ceramide may act as a TLR4 ligand that induces insulin resistance in muscle and other tissues.

Thus, the combination of enhanced fatty acid flux and pro-inflammatory cytokines in T2DM may promote ceramide generation and release via both *de novo* synthesis and sphingomyelin degradation and the subsequent release of ceramide in lipoproteins. Sphingomyelin is a major component of cell membranes in most tissues and it is possible that stimulation of membrane SMase provides ceramide, which may bind to/be incorporated into lipoprotein carriers of ceramide such as LDL. Interestingly, neutral SMase is activated by a number of factors including oxidized LDL and TNF- α ¹⁹⁶, suggesting an interaction between defective lipoprotein metabolism, inflammation and plasma ceramide production.

The second major finding from this investigation is that plasma ceramide is increased in the patients with T2DM and the severity of insulin resistance positively associates with the plasma ceramide concentration. Plasma ceramide was not associated with BMI, suggesting that obesity does not drive the defective ceramide metabolism in T2DM. Also, plasma ceramide was not related to plasma cholesterol or triacylglycerol

levels, indicating that altered ceramide is not simply a reflection of a generalised dyslipidemia, but rather a specific defect of T2DM. The negative relationship between plasma ceramide and insulin sensitivity was reported by another group while our studies were being completed³⁰ and agree with a 2-fold increase in plasma ceramide in insulin resistant *ob/ob* mice¹⁸⁶.

Ideally, comparison between lean insulin sensitive versus a lean insulin resistant group would be a more vigorous approach in examining the association of plasma ceramides to insulin resistance in humans. However, we were not able to obtain insulin resistant patients who were lean. All insulin resistant subjects were found to be obese. As such, comparisons between insulin sensitive vs insulin resistant patients could only be done using lean insulin sensitive and obese insulin resistant groups. The relatively small sample size is another limitation in these findings thus requiring confirmation in larger cohorts.

While ceramide is clearly a negative regulator of insulin action in muscle and liver^{8,9}, acute insulin administration does not suppress muscle ceramide content^{192, 194, 197}. Whether this holds true for liver and plasma is unknown. Similarly, how plasma ceramide mechanistically affects insulin signal transduction is unknown.

Ceramides circulates at relatively high concentrations ($\mu\text{mol/l}$) and it is possible that they are transported across the muscle sarcolemma. LDL-derived ceramide uptake was demonstrated in endothelial cells and was dependent on the presence of the LDL receptor¹⁹⁸. Whether this mechanism occurs in key tissues involved in whole-body glucose metabolism remains to be determined.

In summary, ceramides are transported by lipoproteins in human plasma and circulating ceramides are positively associated with insulin resistance in patients with T2DM. In particular, plasma ceramide is increased in LDL of patients with T2DM, suggesting that circulating LDL-ceramides could cause insulin resistance in insulin responsive tissues. Whether circulating ceramide is an exact cause or consequence of insulin resistance remains to be answered. Mechanistic studies will be pertinent in elucidating this question.

CHAPTER 3

Design and construction of reconstituted LDL-ceramide preparation

3.1 Introduction

It is now firmly entrenched in the literature that ceramide accrual can cause insulin resistance and inflammation^{7,9,90}. However, the drawback of such studies is that they utilise short acyl chained ceramide analogues, which not only do not exist naturally, but are water soluble. This is in contrast to natural ceramides which have long acyl chains and are extremely insoluble in an aqueous environment. While proof of principle concepts can be drawn from the use of short chain ceramides, caution must be taken from extrapolating these results back to natural ceramides in the circulation.

This thesis (Chapter 2) and other studies involving humans³⁰ and rodents¹⁶³, have shown that natural ceramides are transported predominantly by lipoproteins. In addition, the previous chapter of this thesis has identified LDL as the exact lipoprotein fraction which is enriched with ceramide in insulin resistant patients with T2DM. While an associative link between plasma ceramide and insulin resistance was shown by the results, whether circulating ceramides are mechanistically involved in eliciting insulin resistance or if they are a consequence of T2DM remains to be answered.

The role of LDL-ceramide in insulin resistance and inflammation can be examined by testing LDL-ceramide on various *in vitro* and *in vivo* models to assess if LDL-ceramide can mechanistically cause such conditions. As such, the procurement of a consistent and reliable supply of LDL-ceramide is essential to perform such mechanistic studies. However, obtaining a constant supply of native LDL-ceramide is hindered on many fronts, such as the availability of constant volunteers, time and cost prohibitive methods of obtaining LDL-ceramide and the high possibility of cross contamination during processing. Additionally there are no commercial sources of LDL-ceramide.

To overcome these difficulties it is necessary to design and create a model which mimics circulating ceramides, where a known amount of exogenously added natural long chain ceramide can be reliably associated to LDL.

3.2 Aims

The aim is to design, create and validate an LDL preparation containing ceramide that mimics the natural LDL-ceramide. The purpose of creating this model is to use this for *in vitro* and *in vivo* mechanistic studies which will test the role of LDL-ceramide in insulin resistance and inflammation.

3.3 Materials and methods

The following section describes materials and methods used for chapter 3. Additional or variation of material and methods used in other chapters will be contained within their respective sections.

3.3.1 Associating exogenous long chain ceramide with human LDL

The ceramide species chosen for association with human LDL were C16:0 ceramide and C24:0 ceramide as they represent the two major sub-species of ceramide in plasma¹⁵⁶. Both these ceramide were purchased from Avanti Polar Lipids (Avanti Polar Lipids, Alabama, USA).

All preparations were done in 12 x 75 mm glass tubes. Lyophilized human LDL (Sigma-Aldrich, Missouri, USA) was first dissolved in de-ionised water and vortexed gently until the solution turned milky and particulate free. 0.5mg/500 μ L of this LDL solution was added to a glass tube containing 6.25mg of potato starch powder (Sigma-Aldrich) and vortexed vigorously before plunging the glass tube into liquid nitrogen to snap freeze the sample before the starch powder settle out. The snap frozen sample was then dried under vacuum in a miVac quattro centrifugal evaporator (Genevac, Ipswich, UK) at room temperature for a minimum of 8 h or until completely dry. Once dried the glass tube containing the LDL-potato starch complex was stored at 4°C in an air-tight container with desiccant (Drierite (Sigma-Aldrich), and gassed with nitrogen. The dried LDL-potato starch complex was not stored longer than 24 h before proceeding to the next step.

To deplete endogenous cholesterol from the LDL-potato starch complex, 1.5mL of heptane (Sigma-Aldrich) was added to each glass tube containing the dried LDL-potato starch complex. The sample was vortexed for 2 min until the LDL-potato

starch complex broke into a fine grain like slurry. The preparation was then chilled at 4°C for 15 min, after which it was vortexed for 2 min and re-chilled again at 4°C for 15 min. This process was repeated for a total of four times, at the end of which, the sample was centrifuged at 2000 rpm, for 10 min at 4°C to pellet the LDL-starch complex. After centrifuging, heptane but not the LDL-potato starch slurry was removed and 1.5 mL of fresh heptane was added to the sample. This entire process constitutes one cycle of the extraction process and a total of three cycles were performed. At the end of the third cycle the heptane was removed and ceramide was ready to be added.

Prior to the addition of ceramide to the LDL-potato starch complex, both C24:0 ceramide and C16:0 ceramide were dissolved in heptane. Both ceramide species were heated to 72°C as they do not dissolve completely in heptane at room temperature. Next, the key step of the protocol involved cooling the dissolved ceramide to 40°C and before the ceramide precipitated out of solution, the LDL-potato starch complex was quickly added and mixed vigorously by vortexing for 2 min. To each reaction tube containing the LDL-potato starch complex, 500µL of 0.4 mg ceramide in heptane was added. The sample was then incubated at -10°C for 1 h, after which time the heptane was evaporated under a steam of nitrogen gas at RT. It is essential for the sample to be thoroughly dry and free of non-polar heptane, otherwise the subsequent hydrating step which utilizes a polar hydrating solution to release the LDL-ceramide preparation from the potato starch powder will not be efficient.

The LDL-ceramide was then hydrated in 1 mL of the hydration solution (pH 8.8), comprised of 0.12M NaCl (Sigma-Aldrich.) and 10 mM Tricine (Sigma-Aldrich) in de-ionised H₂O. The preparation was incubated in the hydration solution for a minimum of 18 h at 4°C to allow good release of LDL-ceramide from the potato starch powder into the hydration solution.

To remove the potato starch powder from the LDL-ceramide preparation, a three step centrifugation process was used to pellet out the insoluble potato starch powder and ceramide which did not associate with LDL. Firstly, the sample was centrifuged at 2000 rpm for 10 min at 4°C to pellet the bulk of the potato starch powder and ceramide precipitate. The supernatant containing LDL-ceramide was then transferred

to a clean 1.5 mL centrifuge tube (Eppendorf, Hamburg, Germany) and further centrifuged at 13,000 rpm for 20 min at 4°C to remove any residual potato starch powder. This step was repeated one more time before the LDL-ceramide was stored under nitrogen gas and kept at 4°C until ready to use. The LDL-ceramide preparation was not kept longer than 3 days.

3.3.2 Quantification of LDL-ceramide via DAG-K assay

The diacylglycerol kinase assay (DAG-K) utilizes the ability of DAG-K to phosphorylate ceramide and, together with [γ -³²P] ATP as a reaction substrate, allows radio labelling of ceramide for quantification. Prior to the DAG-K assay reaction, all lipids were extracted in glass tubes (12 x 75 mm). To 1 mL of each sample 1.9 mL of chloroform: methanol:PBS +0.2% SDS (1: 2: 0.8) was added and vortexed before incubated for 1 h at RT. Thereafter, 0.5mL chloroform was added to each tube and vortexed, after which 0.5mL of 1% perchloric acid (v/v) was added and the samples vortexed again. The phases were then separated by centrifuging at 1000 rpm for 10 min. 0.9 mL of the lower organic phase was removed and transferred to a fresh glass tube then evaporated under nitrogen at 40°C using a sample concentrator.

The extracted lipid samples were resuspended in 20 μ l of octylglucoside: cardiolipin (10:1 w/w) in 1 M DETAPAC (pH 7.0) which was prepared 1 h before use. The samples were vortexed vigorously before the addition of the DAG-K reaction mixture.

The DAG-K reaction mixture was prepared with 100 mM imidazole, 100 mM NaCl, 25 mM MgCl₂, 2 mM EGTA, 20 mM DTT, 20 mM ATP and 5 μ g of DAG kinase purified from *Escherichia Coli* (Sigma-Aldrich). [γ -³²P] ATP (Amersham Bioscience, Giles, UK) was added to a final activity of 0.5 μ Ci/ μ l, and 100 μ L of this reaction mixture was added to the samples and gently mixed. After a 3 h incubation at RT the reaction was terminated by the addition of 2 mL of chloroform: methanol (2:1). 500 μ L of 1% perchloric acid (v/v) was added and the organic and aqueous phases were separated by centrifugation at 1000 rpm for 10 mins at RT. 1 mL of the organic phase was removed and transferred to a new glass tube and the solvent was evaporated under nitrogen at 37°C using a sample concentrator. This dried lipid sample contained radio-labelled diacylglycerol and ceramide.

To separate the lipid species, thin layer chromatography (TLC) was used. The dried lipids were constituted in 40 µl chloroform:methanol (2:1), mixed, then spotted onto scored silica gel 60 coated aluminium plates (Merck, Darmstadt, Germany). This process was repeated for each sample and the plate was loaded into a TLC tank containing chloroform:acetone:methanol:aceticacid:water (50:20:15:10:5). The solvent front was run to three quarters of the length of the plate ensuring sufficient separation of the lipid species. The silica gel plate was air-dried and the radioactively labelled lipids were visualised via autoradiography with films. The position on the TLC plate corresponding to ceramide were scrapped and the radioactivity were assessed via scintillation analysis and calculated by first subtracting a reaction blank then dividing by the specific activity.

3.3.3 Bicinchoninic acid (BCA) protein assay

The BCA_{TM} Protein Assay Kit (Pierce, Illinois, USA) which measures total protein content, was used to quantitatively measure ApoB-100 protein amount in the LDL-ceramide preparation, since ApoB-100 is the sole protein found in LDL. Bovine serum albumin standards provided in the kit were made to concentrations of 0, 25, 50, 100, 200, 300, 500 and 1000 g/ml, and 25 µL of each standard or the lysed samples were added to a 96 well microtitre plate in duplicate. 200 µL of the BCA buffer, composed of 98 parts kit reagent A and 2 parts kit reagent B, was added to each well and the plate was incubated for 30 min at 37°C. Absorbance was determined at 540 nm on a SpectraMax Plus 384TM spectrophotometer (Molecular Devices, California, USA). The protein standards produced a linear relationship between protein concentration and absorbance, and from this information the absorbance of the unknown samples was used to determine their protein concentration.

3.3.4 Western blotting

To further verify the presence of ApoB-100 in the LDL-ceramide preparation western blot was performed. Western blotting is a technique used to detect the presence of specific protein in a protein sample by first separating proteins using gel electrophoresis before transferring the proteins to a membrane where antibodies specific to the target protein are used to probe for the protein of interest.

Several LDL-ceramide preparations were pooled together and dried under vacuum in a miVac quattro centrifugal evaporator (Genevac, Ipswich, UK) before the samples were lysed in 40 μ L of lysis buffer containing 50 mM HEPES, 150 mM NaCl, 100 mM NaF, 10 mM sodium pyrophosphate, 5 mM EDTA, 250 mM sucrose, 1 mM DTT, 1% (v/v) Triton-X 100, 1 mM sodium orthovanate, 1% protease inhibitor cocktail (Roche, Basel, Switzerland) and 1% phosphatase inhibitor, PhosSTOP (Roche). The samples were added to Laemmli's buffer containing 0.5 M Tris-HCl, 2% SDS (w/w), 20% glycerol (v/v), and 1% bromophenol blue dye (w/w), pH 6.8.

The samples were then separated by sodium dodecyl sulphate polyacrylamide gel electrophoresis (SDS-PAGE) using the Invitrogen X Cell Sure Lock system. Samples were heated for 3 min at 95°C, prior to loading on the SDS-PAGE gel.

The solutions used in electrophoresis are outlined in Table 3.1. For separating ApoB-100, gel acrylamide were made to 3% with the following reagents 1.5M Tris pH 8.8, Bis-Acrylamide (BioRad California, USA), 10% SDS (Sigma-Aldrich), 50% sucrose (Sigma-Aldrich), TEMED (BioRad), 1% Ammonium Persulfate (APS) (Sigma-Aldrich.) and H₂O.

Solutions /Buffer	Components
Electrophoresis running buffer	3 g/L Tris-HCl, 14.4 g/L glycine, 1 g/L SDS, pH 8.8
Wet Dry transfer buffer	3 g/L Tris-HCl, 14.4 g/L glycine, 20% methanol.
TBST wash buffer	0.5 M Tris-HCl, 8 g/L Sodium Chloride, 0.1% Tween, pH 7.6.
Block buffer	TBST + 5% skim milk

Table 3.1. Solutions and buffers used in Western blotting.

The electrophoresis of the acrylamide gel was run at 150 volts (Power Pac 300, BioRad) for ~ 9 h. Proteins were then transferred onto polyvinylidene difluoride (PVDF, Pall Biosciences, New York, U.S.A.) membranes using a BioRad semi-dry transfer system. Prior to transfer the PVDF membranes were soaked in methanol until translucent. The wet-dry transfer was undertaken at 75 mA per membrane for 5 h in transfer buffer. At the end of the transfer, the membrane was blocked for 1 h at RT in block buffer, and then rinsed 4 times for 10 min each in TBST. The membrane was then incubated overnight at 4°C with a primary antibody directed against Apo B-100

(Biodesign International, Saco, Maine, USA) diluted 1:300 in TBST containing 1% BSA. The next day the primary antibody was removed and the membrane rinsed 4 times for 10 min each in TBST before the membrane was incubated with a HRP-conjugated protein G (BioRad) secondary antibody diluted 1:4000 in block buffer for 2 h at RT. A final series of 4 washes each at 10 min was performed to remove unbound secondary antibody, before visualisation with an ECL kit (Sigma-Aldrich).

3.3.5 Transmission electron microscopy

A 2% solution of phospho-tungstic acid (pH 7.4) dissolved in water was mixed 1:1 (v/v) with the LDL-ceramide sample to negatively stain the sample before transmission electron microscopy. After staining, a small drop of the stained sample was placed on a carbon coated copper grid and left to air-dry. The grid was viewed under vacuum in a Hitachi T7500 transmission electron microscope at 30,000 times magnification.

3.3.6 Analysis of lipid composition of LDL-ceramide by mass spectrometry.

Analysis of lipid composition of the final LDL-ceramide preparation was performed as described in Chapter 4, section 4.3.6 of this thesis.

3.3.7 Analysis of LDL-ceramide oxidation status.

Positive controls of oxidized LDL (oxLDL) were first prepared as follows: freshly prepared LDL was adjusted to 1.2g/L final concentration of proteins in TBS with a copper sulfate solution (final concentration, 5 $\mu\text{mol/l}$) for 24 h at 37°C. At the end, oxidation was stopped by the addition of EDTA (final concentration, 200 $\mu\text{mol/l}$) and oxLDLs were kept at 4°C. The extent of oxidation in the LDL-ceramide preparation was investigated by measuring the amount of thiobarbituric acid reactive substances (TBARS) generated with a colorimetric assay for malondialdehyde¹⁹⁹. This assay was performed by Alaina Natoli (Baker IDI).

3.4 Results

3.4.1 Amount of exogenous ceramide associated with LDL.

Ceramide used as starting material that is not associated with LDL will remain precipitated together with potato starch at the end of the protocol.

Quantification of ceramide content in the LDL-ceramide preparation using mass spectrometry showed, using 0.4 mg of exogenous ceramide as starting material, that approximately 319 ± 50 μmol of ceramide associated with LDL.

There was a maximum amount of exogenous ceramide that could be used as starting material (0.4 mg/ 500 μL) before the collection of the LDL-ceramide product at the end of the procedure became unfeasible. This was due to excessive unassociated ceramide precipitation that remained suspended in the hydration solution which could not be pelleted down by centrifugation.

3.4.2 ApoB-100 is present in LDL-ceramide preparation.

The BCA assay measures total protein content in the preparation and since ApoB-100 is the only protein in LDL, by extension the BCA assay was used to quantify the amount of ApoB-100 present. The total amount of protein recovered at the end of the procedure tested using the BCA assay was ~56% of the amount of LDL used in the beginning.

Since the BCA assay did not specifically validate the presence of ApoB-100 in the preparation, Western blot analysis using an antibody directed against ApoB-100 was used to confirm ApoB-100 in the LDL-ceramide preparation. A single band representing ApoB-100 was detectable in the LDL-ceramide preparation as well as the unprocessed LDL positive control, indicating that the LDL-ceramide procedure did not alter ApoB-100 electromobility.

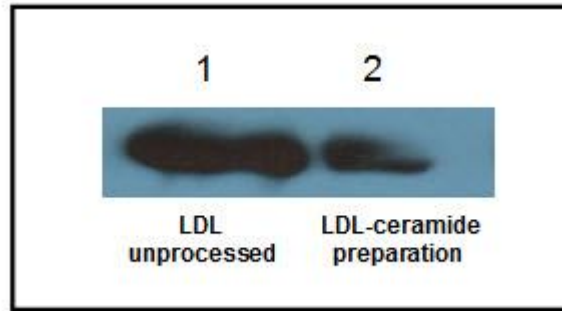


Fig 3-1. ApoB-100 is present in LDL-ceramide preparation. Lane 1 represents unprocessed human LDL. Lane 2 represents pooled samples (n=15) of the LDL-ceramide preparation. 20 μ g of sample was used.

3.4.3 Ceramide content in the LDL-ceramide preparation is dependent on the initial amount of exogenous ceramide, but not LDL amount.

Increasing the starting amount of ceramide used in the procedure leads to increased ceramide content in the preparation (Fig 3-2). Curiously, increasing the initial amount of LDL used as starting material did not lead to increased levels of ceramide in the preparation. This indicated that ceramide association to LDL did not follow LDL saturation kinetics, but was instead reliant on exogenous ceramide.

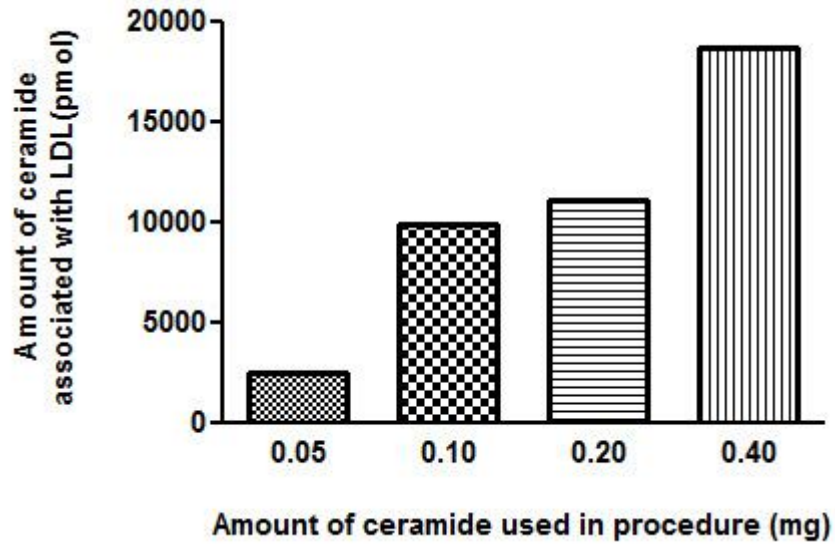


Fig 3-2. Increasing the amount of exogenous ceramide as starting material leads to increase association with LDL. Amount of LDL used as starting material was fixed at 0.5mg while varying amounts of ceramide (0.05 mg, 0.1 mg, 0.2 mg, 0.4 mg) were used as starting material to create the LDL-ceramide preparation.

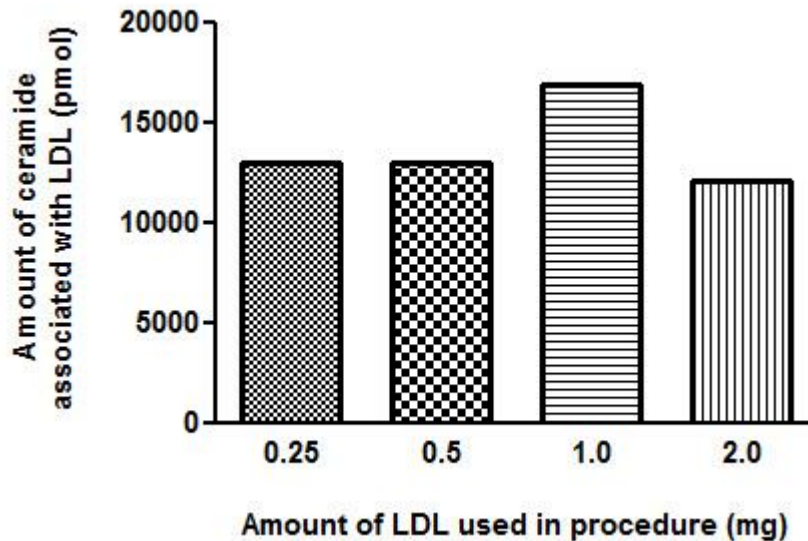


Fig 3-3. Increasing amount of LDL as starting material does not lead to increase association with LDL. Amount of ceramide used as starting material was fixed at 0.2 mg while varying amounts of LDL (0.25 mg, 0.5 mg, 1.0 mg, 2.0 mg) were used as starting material to create the LDL-ceramide preparation.

3.4.4 LDL-ceramide preparation is similar in shape to LDL

To determine if the preparation altered LDL from its spherical shape, transmission electron microscopy (TEM) was performed to examine the shape of the reconstituted LDL-ceramide particle. TEM revealed that the LDL-ceramide preparation had a similar spherical shaped as native LDL (Fig 3-3), indicating that the procedure did not disrupt the shape of LDL. Clumping of native LDL samples occurred during air drying of samples. This gives the impression that native LDL appears to be larger than the LDL-ceramide preparation.

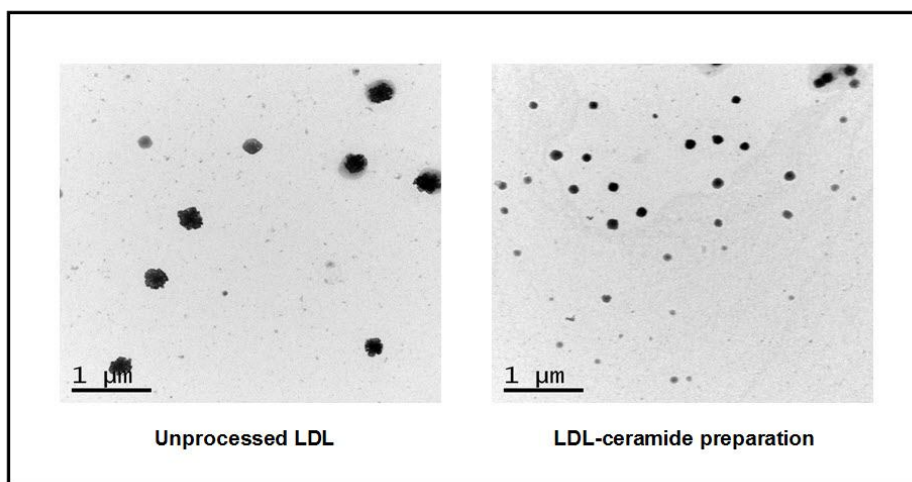


Fig 3-3. *Transmission electron microscopic image of LDL-ceramide preparation. The LDL-ceramide preparation shares a similar spherical appearance with native LDL. Unprocessed LDL and LDL-ceramide preparation samples were viewed under vacuum in a Hitachi T7500 transmission electron microscope at 30,000 x magnification. Scale bar represents 1 μm.*

3.4.5 LDL is not oxidized during LDL -ceramide preparation.

The protocol described in this chapter to create artificial LDL-ceramide does not result in oxidization of LDL as assessed by a colorimetric assay for malondialdehyde as a measure of thiobarbituric acid reactive substances (TBARS). (Fig 3-4)

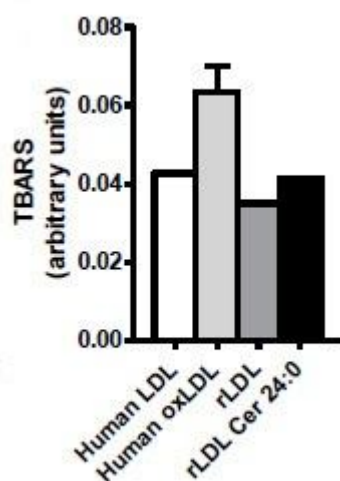


Fig 3-4. Thiobarbituric acid reactive substances (TBARS) in LDL-ceramide, normal LDL, and oxLDL. No TBARS was detected in LDL-ceramide and normal LDL. (n=2) LDL in the preparation is not oxidized. LDL was assessed for oxidation using the thiobarbituric acid reactive substances (TBARS). Human LDL and LDL oxidized by myeloperoxidase (oxLDL) were used as control samples. rLDL refers to reconstituted LDL depleted of endogenous TGs and cholestrols using the preparation protocol minus ceramide. rLDL-Cer24:0 refers to the LDL-ceramide preparation.

3.4.6 Lipid composition of LDL -ceramide preparation.

The breakdown of lipid concentrations of the LDL-ceramide preparation in comparison to depeleted LDL is summarized in table 3.4-1.

	Lipid concentration (pmol/mL)					
	Dihydro-Ceramide	Total Ceramide	Phospho-lipids	Cholesteryl-Esters	Diacylglycerol	Triglycerides
LDL (depleted)	40.8	6417.7	629.4	2165.2	16036.7	0.0
LDL-Ceramide	511.2	42956.1	695.3	927.2	21373.9	0.0

Table 3.4-1 Lipid composition in LDL-ceramide preparation and depleted LDL analysed by mass spectrometry.

3.5 Discussion

To examine the biological role of LDL-ceramide, an appropriate LDL-ceramide preparation had to be developed and validated. Several logistical challenges are presented when obtaining a constant and reliable supply of LDL-ceramide. Among them include the difficulty in obtaining constant human volunteers, the variability of samples, time and cost prohibitive issues, perishability and the likelihood that the LDL is variably oxidized. As such, the design and construction of a reliable model of LDL-ceramide, which would mimic how ceramides are naturally transported in plasma was conceptualized as a strategy to bypass these problems and to provide a reliable platform to test the biological roles of LDL-ceramide.

Several notable challenges were presented during the design of this LDL-ceramide model. One such problem was that LDL dissolves in an aqueous solution and long chain ceramides, which are extremely hydrophobic, do not dissolve in water based solvents. The conundrum then was how to associate these two substances when each of them dissolves in different solvents. In addition, the solvent used to solubilize ceramide must not denature ApoB-100, the protein in LDL, as evidence shows that the protein component of LDL is required by LDL receptors for recognition in tissues which use the receptor dependent method of LDL uptake²⁰⁰⁻²⁰².

The lyophilized human LDL used in the procedure was found to dissolve completely only in double distilled deionised water and not in phosphate buffered saline (PBS), which would result in undissolved particulate if used. Thus, the choice of solvent to dissolve the purchased LDL was limited. Exogenous ceramide (C24:0 and C16:0 ceramide) dissolved completely in chloroform. However, the use of chloroform as a solvent to dissolve ceramide was ruled out, as denaturation of LDL proteins would occur should a ceramide-chloroform solution be used during the association process. An alternative solvent was required, one that had to fulfil the criteria of being able to dissolve both ceramide and at the same time not denature the protein in LDL.

Another issue that was taken into account during the design of the LDL-preparation was that commercially purchased human LDL would inevitably be variable in its lipid content depending on batch sample. To solve this problem of inconsistency, it was

decided that that LDL must first be depleted of its endogenous lipids before ceramide could be associated with it. Also, this step was required to successfully associate ceramide with LDL.

As such, the extraction step of endogenous lipids was deemed necessary as part of the protocol. The question then arose as to how endogenous lipids could be extracted from LDL without the removal of LDL in the process. In addition, the extraction process must not alter ApoB-100.

As first described by Gustafson²⁰³ and used on VLDL and later by Krieger²⁰⁴ on LDL, potato starch powder can be used as an anchor to hold down protein and phospholipids and to stabilize the lipid-depleted apoproteins such that aggregation will not occur during lipid extraction. In the described technique it was found that the majority of the phospholipids and protein remained associated with the insoluble starch powder²⁰⁴. The initial part of the procedure for the creation of this LDL-ceramide preparation in the present study borrowed from this concept and involved combining LDL with potato starch powder, so that the protein and phospholipid components of LDL would be anchored to the insoluble potato starch powder and would not be washed away while the endogenous lipids were removed.

The non-polar solvent heptane selectively extracts endogenous lipids from a combined potato starch-lipoprotein complex without damaging the protein component of VLDL and LDL^{203, 204}. As such, heptane was deemed safe for use during the removal of endogenous lipids from LDL and was used as the extracting solvent of choice.

While heptane is a non-polar solvent, and was expected to fully dissolve both C24:0 ceramide and C16:0 ceramide, this was not entirely the case. Both ceramide species did not dissolve in heptane at room temperature. However, they dissolved to a clear solution when heated to 72°C. This temperature was chosen because it was below both the melting point of the ceramide species (99°C) and the boiling point of heptane (98°C), and yet capable of completely dissolving the long chain ceramides.

Although both of these long chain ceramides could be dissolved in heptane at 72°C,

adding the solution at such temperatures to LDL would disrupt the protein confirmation of ApoB-100 protein. Calorimetric and spectroscopic investigation of the unfolding of ApoB-100 in human LDL have showed that from 5°C to 40°C the secondary and tertiary structural organization of ApoB-100 in LDL remains unchanged, but at temperatures between 48°C to 57°C, a reversible structural re-organisation occurs²⁰⁵. To prevent the unfolding of ApoB-100 due to excess heat, a key step of the protocol involved cooling the dissolved ceramide in heptane from 72°C to 40°C and quickly adding it to the LDL-potato starch complex before the ceramide fully precipitated out of solution.

To liberate the LDL-ceramide from insoluble potato-starch powder, a polar hydrating solution was utilized. Initially, double distilled ionised water was used as a hydrating solution. However, it was found that the ceramide content in the final LDL-ceramide product was low when this was used as a hydrating agent. This was attributed to the insufficient release of the LDL-ceramide particle from the potato starch powder. This appeared to be the case as it has been reported that hydration buffers with high salt content increase recovery of LDL protein (ApoB-100) from starch by 40-47%, compared to buffers without salt²⁰⁶. As such, a hydrating solution prepared from tricine and NaCl was used to increase the liberation of LDL-ceramide from the potato starch. The LDL-ceramide preparation was left to incubate in the hydrating solution for a minimum of 18 h to facilitate the release of LDL-ceramide from the insoluble starch powder, as it was shown in previous time course studies conducted by other groups that this time results in the maximal release of LDL-protein from starch during the hydration process²⁰⁴.

During optimisation of the procedure to increase ceramide content in the final LDL-ceramide product, it appears that there is a maximum amount of ceramide that can be used as starting material before excessive unassociated ceramide appears in suspension at the final step of the protocol which renders the collection of the final product unfeasible.

The question then arises, is saturation of ceramide occurring because there is insufficient LDL present for association? To answer this question, a series of LDL-preparations were made with a fixed amount of ceramide in each preparation but

varying amounts of LDL as starting material. Curiously, increasing the amount of LDL did not increase the amount of ceramide in the final LDL-ceramide solution. This suggests that association of ceramide to LDL in this procedure is not reliant on LDL saturation kinetics. This contrasts with another set of experiments where several preparations were made using fixed amount of LDL as starting material but varying the initial amounts of ceramide. It was shown that increasing the amount of ceramide in the starting material lead to an increase in ceramide content in the final product. Whether the addition of more than 0.4 mg of ceramide per preparation as starting material would lead to increase ceramide content in the final LDL-ceramide product is unclear from these experiments. However, this cannot be assessed adequately, because beyond this amount excessive unassociated ceramide precipitates will appear in suspension which renders collection of the final LDL-ceramide product unfeasible.

To examine whether the LDL-ceramide preparation was similar in shape to native LDL, TEM was first used to show that the preparation has the same spherical appearance as LDL. Transmission electron microscopy samples are viewed in vacuum and some clumping of native LDL samples occurred during air drying of samples. This gives the impression that native LDL appears to be larger than the LDL-ceramide preparation. Western blot analysis was then performed to verify that the protein in the preparation was ApoB-100.

Some schools of thought believe that LDL must be oxidized for it to be taken up by macrophages. Macrophages take up both normal and modified LDL, the difference is that macrophages possess more receptors for modified lipoproteins than they do for native LDL¹⁷⁶. In the case of encountering modified LDL, the normal negative feedback mechanism which prevents over engorging of the LDL particle is ignored^{172, 173, 175, 176}. In addition, reports show that oxLDL make up a miniscule fraction of total LDL, accounting for only 0.001% in healthy patients¹⁷⁸, while in patients with acute coronary events it is approximately 5%¹⁷⁹. This suggests that the impact of oxLDL is likely to be very minimal compared to the effects of normal LDL even though they are preferentially taken up by macrophages.

In either case, since the LDL-ceramide prepared in this chapter was intended to be tested on macrophages in subsequent studies, the oxidation status of the LDL-

ceramide preparation was investigated by examining the preparation for thiobarbituric acid reactive substances (TBARS), which is a measure of oxLDL. The artificial LDL-ceramide created by the methods described does not result in the oxidation of LDL.

Mass spectrometry analysis of the lipid composition of the LDL-ceramide preparation showed that heptane extraction effectively removed all triglycerides (TG). The lack of unesterified cholesterol in the LDL-ceramide preparation bears similarity to the LDL particle made by Krieger, which used a similar approach to reconstitute LDL²⁰⁴. It was important to deplete LDL of TG, so as to enable the individual effects of ceramide in LDL to be examined without the bias of TGs, which have been shown to correlate directly with insulin resistance in muscle of humans²⁰⁷.

The main limitation in generating LDL ceramide with this procedure is there appeared to be a maximum amount of ceramide that could be used as starting material to associate ceramide with LDL before collection of the final LDL-ceramide product became unfeasible due to suspended ceramide precipitates in the hydration solution.

Nonetheless, despite this drawback, this protocol provides a method for safely associating a fixed amount of ceramide to LDL without disrupting the native apoprotein component. In so doing, this procedure provides a quality controlled supply of LDL-ceramide for use in mechanistic studies.

CHAPTER 4

**LDL-Ceramide decreases
insulin action in cultured
myotubes & skeletal muscle**

4.1 Introduction

While T2DM is clearly multifactorial, insulin resistance is a key feature of this disease. Insulin resistance occurs when the biological effects of insulin become desensitised and this is reflected in the reduced efficacy of insulin to stimulate glucose clearance. At a cellular level, insulin resistance has been associated with dampened signal transduction as well as post-receptor cytoplasmic inhibition of insulin signalling molecules²⁰⁸.

In the case of patients with T2DM, numerous studies show a strong association between lipid oversupply and defective insulin action in insulin sensitive tissues such as skeletal muscle and liver²⁻⁶. This has resulted in significant research efforts aimed at identifying the exact lipid or lipid metabolites responsible for antagonizing insulin signaling. Among the best candidates as a lipid mediator of insulin resistance is the sphingolipid ceramide, such that the measurement of ceramide content in various models of insulin resistance and in human studies is common place^{3, 7-9, 30, 48, 51, 209}.

While it is highly likely that intracellular ceramide accumulation is involved in the pathogenesis of insulin resistance, the biological relevance of plasma ceramides which are elevated in patients with T2DM³⁰ is unknown. While chapter two of this thesis showed that plasma ceramides are associated with insulin resistance and identified the lipoprotein fraction in patients with T2DM that is elevated with ceramide, that study nor the study by Haus³⁰ address the biological role of plasma ceramides.

An important question is, are plasma ceramide levels a reflection of intracellular ceramide concentrations in the pathological state of T2DM or are they directly causative of insulin resistance?

To resolve whether circulating ceramides are involved in the development of insulin resistance, the LDL-ceramide preparation created (as per chapter 3) was used in functional assays to test the direct effects of LDL-ceramide on insulin stimulated glucose disposal in cultured myocytes, adipocytes and hepatocytes. Finally the LDL-

ceramide was injected into mice to examine if it induces insulin resistance in various tissues.

4.2 Aims

To determine whether LDL-ceramides alter insulin action in cultured myocytes, adipocytes and hepatocytes as well as determining whether *in vivo* infusion of LDL-ceramide induces insulin resistance in tissues of mice.

4.3 Materials and methods

The following section describes materials and methods used for chapter 4. All treatments with the LDL-ceramide preparation (C24:0 ceramide and C16:0 ceramide) used in this chapter were adjusted to a final working concentration of 2 μ M ceramide for all experiments, unless otherwise stated. All LDL controls used in this chapter refers to LDL depleted of endogenous TGs and cholesterol without addition of exogenous ceramide which was prepared at the same time alongside each LDL-ceramide preparation batch.

4.3.1 Cell culture

All cells were grown in a humidified Thermo™ Hera cell 150 incubator (Asheville, NC, USA) at 37°C and 10% carbon dioxide (CO₂). Cell culture medium was replaced daily for all cell lines unless otherwise stated. Prior to medium replacement, cells were rinsed twice with PBS containing magnesium and calcium (PBS +) (Gibco™, Invitrogen). All cells were grown on sterile non-coated tissue culture grade dishes or multi-well plates. For passaging, cells were first rinsed twice in PBS without calcium and magnesium (PBS -) (Gibco™), before addition of 1 X 0.05% Trypsin-EDTA (Gibco™.) for 4 min at 37°C to detach cells. Following this, medium specific for that cell line containing fetal calf serum (FCS) was used to neutralise trypsin. The cell suspension was then centrifuged at 1000 rpm for 4 min at RT and the supernatant discarded to remove all traces of trypsin. Fresh medium appropriate for the cell line was then added to re-suspend the cell pellet and cell suspensions were plated out on tissue culture plates or dishes according to the densities required. Cell line specific

maintenance and differentiation conditions are described in their respective subsections.

4.3.1.1 Standard L6 & L6 Glut4-myc skeletal myoblast cell culture

L6 Glut4-myc cells were a kind gift from Prof. Amira Klip (SickKids Research Institute, Toronto, Ontario, Canada). The L6 Glut4-myc skeletal myoblast cell is an immortalised myoblastic cell line which undergoes spontaneous differentiation to form myotubes through multiple cell fusion when cultured at high confluency in low concentrations of serum. Like skeletal muscle, these myotubes respond to insulin and stimulate Glut4 translocation to increase the rate of glucose uptake^{210, 211}. This cell line was derived from L6 myoblastic cells²¹² by stable expression of Glut4 tagged to a myc epitope in its large exofacial loop²¹³.

For propagation, both cell lines were grown in Dulbecco's Modified Eagle's Medium (DMEM) + GlutaMax™, 1 g/l D-glucose, 110 mg/L Na pyruvate, (Gibco™) containing 10% fetal calf serum (Gibco™) and 100 U/ml penicillin, 100 ng/ml streptomycin (Invitrogen). During maintenance, cells were passaged at not more than 75% confluence and were evenly spread to minimise clustering as a measure to prevent spontaneous differentiation, which would lead to loss of differentiation potential in later passages.

To differentiate the cells to myotubes, the cells were grown post confluence for 2 days before switching to differentiation medium comprising of DMEM + GlutaMax™, 1 g/l D-glucose, 110 mg/L Na pyruvate, 2% horse serum (Gibco™, New Zealand sourced) and 100 U/ml penicillin, 100 ng/ml streptomycin and (Invitrogen) for 8-9 days, with daily replacement of fresh differentiation medium. After this time frame approximately 65-70% of the myoblast were fused to form myotubes.

4.3.1.2 Primary mouse hepatocyte cell culture

Primary hepatocytes from 6-8 week old C57BL/6 mice were isolated by the two step collagenase A (0.05% w/v) perfusion method described by Seglen²¹⁴. Briefly, perfused livers were removed and minced with scalpel blades under aseptic conditions, washed extensively with Hank's buffered salt solution (HBBS) (Gibco™), and cultured in M199 medium (Gibco™), containing 10 % (v/v) FBS, 100 U/ml penicillin,

100 µg/ml streptomycin and 1 nM insulin. Using albumin as a marker of mature hepatocytes, FACS analysis suggested an absolute minimum of 85% of the cell population are hepatocytes after the procedure. Experiments were performed not more than 3 days after isolation of hepatocytes.

4.3.1.3 HepG2 hepatocyte cell culture

The HepG2 cells were a kind gift from Prof. Tony Tiganis (Department of Biochemistry and Molecular Biology, Monash University). The HepG2 cell line is an immortalized human liver carcinoma-derived cell line established from minces of human liver biopsies that were initially overlaid on feeder cultures of irradiated mouse cell layers and grown until they became feeder independent²¹⁵. Cells were grown in DMEM + GlutaMax™.

4.3.1.4 CRL 1439 hepatocyte cell culture

The CRL is an epithelial cell line derived from normal liver of a young male rats²¹⁶. Cells were grown in DMEM + GlutaMax™.

4.3.1.5 3T3-L1 adipocyte cell culture

3T3-L1 cells were a kind gift from Dr. Nicky Konstantopoulos (School of Medicine, Deakin University). This cell line is a well-established and widely used *in vitro* model for adipocytes studies. The 3T3-L1 is a mouse pre-adipocyte cell line that was developed through clonal isolation and is able to differentiate to mature lipid loaded adipocytes when subjected to a multi-step differentiation regime²¹⁷.

For propagation, the following 3T3-L1 growth medium comprising of DMEM + GlutaMax™, 4.5 g/L D-glucose, 110 mg/L Na pyruvate, 50 U/ml penicillin, 50 ng/ml streptomycin and 10% FCS was used.

To differentiate 3T3-L1 to mature adipocytes, cells were subjected to a regime following 2 days post-confluence as follows; growth medium was replaced with 3T3-L1 induction medium, made up of 3T3-L1 growth medium containing 2 mg/mL insulin, 0.25 mM dexamethasone and 0.5 mM 3-isobutyl-1-methylxanthine. After 3 days without any medium change, the induction medium was replaced with fresh 3T3-L1 growth medium containing 2 mg/mL insulin for a further 3-4 days. Medium

was refreshed only once during this period following which time the cells were switched to 3T3-L1 maturation medium made up as follows; DMEM + GlutaMax™, 4.5 g/L D-glucose, 110 mg/L Na pyruvate, 50 U/ml penicillin, 50 ng/ml streptomycin and 5% FCS. After 3-4 more days in maturation medium, approximately 80% of the cells were differentiated to lipid loaded adipocytes. The cells were maintained in maturation medium until ready to use for experiments. Medium was refreshed every 2 days and care was taken not to dislodge cells during medium change as the differentiated adipocytes peel off easily.

4.3.2 Insulin stimulated 2-deoxy-D-1[³H] glucose uptake assay

L6 Glut4-myc myotubes and 3T3-L1 adipocytes were used in the insulin stimulated 2-deoxy-D-1[³H] glucose uptake assay. Briefly, this assay works on the principle whereby, 2-deoxy-D-glucose (2DG) has the 2-hydroxyl group replaced by hydrogen so that it cannot undergo further glycolysis, thus when coupled with a radioactive label, makes it an ideal candidate to examine glucose uptake by cells or tissue.

Prior to the assay, LDL-ceramide treated myotubes and adipocytes were rinsed twice in 37°C PBS + to remove all traces of residual glucose from the cell culture medium. Cells were then added with pre-incubation buffer made up of glucose free DMEM 0.1% (w/w) bovine serum albumin (BSA, Bovogen, Victoria, Australia), 10 μM 2-deoxy-D-glucose (Sigma-Aldrich) and insulin (Actrapid®, Novo Nordisk, Bagsvaerd, Denmark) adjusted to a final concentration of 10 nM for 20 min at 37°C. Following this time the pre-incubation buffer was aspirated away and replaced with radioactive 2-deoxy-D-1[³H] glucose uptake buffer made up of no glucose DMEM, 0.1% (w/w) BSA, 1 mCi/mL 2-deoxy-D-1[³H] glucose (PerkinElmer) and 10 nM insulin (Actrapid®) for a further 20 min at 37°C. At the end of this step, the radioactive uptake buffer was removed and the cells were washed 5 times in ice cold PBS + to remove any residual radioactive deoxy-D-1[³H] glucose. The PBS + was removed and solubilising buffer, made up of 0.1% Triton-X (Sigma-Aldrich) in PBS + was added to myotubes. The cells were scrapped in an ice-filled tray and the lysate transferred to scintillation vials containing Ultima Gold scintillation fluid (Perkin Elmer) and radioactivity was quantified on a LS 6500 Multi-Purpose Scintillation counter (Beckman Coulter, California, USA).

4.3.3 Glut-4 translocation assay

This Glut-4 translocation assay works specifically on the L6 Glut4-myc cell line. These cells have an exo-facial myc epitope tagged to Glut4 and during a translocation event the exposed myc epitope can be quantified using an antibody-coupled colorimetric assay. A myc antibody linked to a secondary HRP secondary antibody will react with the reaction substrate buffer to give rise to colour development which can be quantified by a spectrophotometer.

Briefly, the assay was performed as follows; LDL-ceramide treated L6 Glut4-myc myotubes were rinsed twice in 37°C PBS + to remove all traces of residual glucose from cell culture medium. Insulin medium comprising of no glucose DMEM, 0.1% (w/w) BSA, 10 µM 2-deoxy-D-glucose and 10 nM insulin was used to stimulate the myotubes for 20 mins at 37°C. The medium was aspirated and the cells were rinsed twice in ice cold PBS + and fixed with 3% paraformaldehyde (PFA) (Sigma-Aldrich.) for 10 min at 4°C, then a further 20 min at room temperature.

After fixing, the myotubes were rinsed 5 times with 0.1M glycine in PBS + to quench any residual PFA and then incubated for a further 10 min in this solution at room temperature. 5% BSA (W/V) in PBS +, was added to the fixed myotubes as a blocking step before addition of C-myc (9E10) mouse monoclonal IgG1 antibody (Santa Cruz Biotechnology, California, USA) diluted 1:250 in PBS+ with 5% BSA for 90 min at room temperature. The samples were washed at least 6 times in PBS +, before a secondary antibody, mouse IgG, HRP linked whole antibody (GE Healthcare-Amersham, Buckinghamshire, UK.) diluted 1:5000 in PBS+ with 3% BSA (w/v) was added to the samples for 90 min at room temperature. 6 washes, with 3 min incubation per wash was performed after this step. To visualise the signal, a substrate buffer made up of 0.4mg/mL O-phenylenediamine dihydrochloride (OPD) (Sigma-Aldrich.) dissolved in 0.05M phosphate-citrate buffer, pH 5.0 (Sigma-Aldrich.) containing 30% fresh hydrogen peroxide per 100mL of substrate buffer was added to samples for 40 mins at room temperature. The reaction was stopped by adding 3M hydrochloric acid (HCL). The supernatant was collected and colour intensity was measured using a SpectraMax Plus 384™ spectrophotometer (Molecular Devices, California, USA) at 493 nM.

4.3.4 Bicinchoninic acid (BCA) protein assay.

BCA protein assay was performed as described in section 3.3.4. to quantify total protein so that a known amount could be loaded for Western blotting.

4.3.5 Western blotting

Western blotting was performed as per section 3.3.5, with the following changes in this chapter; acrylamide gels were made to 10% concentrations and the wet-dry transfer was performed for 90 min. 40 µg of protein sample were loaded into each well in all experiments. All primary antibodies used in this chapter were purchased from Cell Signalling (Cell Signaling Technology, Massachusetts, USA) and used at 1:1000 dilution in TBST containing 5% BSA. Primary antibodies used in this chapter include; phospho-Akt (Ser473) rabbit monoclonal antibody (mAb), phospho-Akt (Thr308) rabbit mAb, phospho-SAPK/JNK (Thr183/Tyr185) rabbit mAb, phospho-p44/42 MAPK (Erk 1/2) (Thr 202/Tyr204) rabbit mAb, Akt rabbit mAb, p44/42 MAPK (Erk 1/2) rabbit mAb. The secondary antibody used was anti-rabbit IgG, peroxidase-linked species-specific F(ab')₂ fragment (GE Healthcare-Amersham) diluted 1:4000 in block buffer.

4.3.6 Mass Spectrometric analysis

Ceramide content in L6 Glut4-myc myotubes following LDL-ceramide treatment was examined via mass spectrometry. L6-Glut4-myc myotubes were first lysed using a cell scraper in PBS and then sonicated for 10 sec. The sample extracts were reconstituted in 200 µL 10mM, NH₄COOH in methanol. Ceramide analysis was performed by liquid chromatography (LC), electrospray ionisation-tandem mass spectrometry (ESI-MS/MS) using a HP 1100 liquid chromatography system combined with a PE Sciex API 2000 Q/TRAP mass spectrometer with a turboionspray source (250°C) and Analyst 1.4.2 data system. LC separation of lipids was performed on an Alltima C18, 3 µm, 50 x 2.1 mm column using the following gradient conditions; 70% A/30% B reducing to 0% A/100% B over 3 min followed by 5 min at 0% A/100% B, a return to 70% A/30% B over 0.1 min then 1.9 min at 70% A/30% B prior to the next injection. Solvents A and B consisted of tetrahydrofuran:methanol:water in the ratios (30:20:50) and (70:20:10) respectively, both containing 10 mM NH₄COOH.

Quantification of individual species was performed using multiple-reaction monitoring (MRM) in positive ion mode. MRM product ions used were m/z 264 for Cer and GC, m/z 184 for SM. Each ion pair was monitored for 50 ms with a resolution of 0.7 amu at half-peak height and averaged from continuous scans over the elution period. Ceramide concentrations were calculated by relating the peak area of each species to the peak area of the corresponding internal standard. Lipid extractions from samples for mass spectrometry were performed by Dr. Clinton Bruce (Baker IDI / Monash University) and mass spectrometry by A/Prof. Peter Meikle (Baker IDI).

4.3.7 Caspase-3 assay.

Caspase-3, also known as CPP-32, Yama or Apopain is an intracellular cysteine protease that becomes activated during events associated with apoptosis²¹⁸. To examine whether the concentration of ceramide (2 μ M) used in all the experiments induces apoptosis, caspase-3 activity was measured using the EnzChek Caspase-3 Assay kit (Molecular Probes, Mt. Waverley, Australia). The assay was performed as per kit instructions. Briefly, LDL-ceramide treated L6 Glut4-myc myotubes, were washed twice in PBS + before caspase assay lysis buffer (5 mM EDTA pH 7.4, 5 mM TRIS-HCL pH 7.6, 10% NP-40) was added to the sample and left to incubate for 10 min at RT. Myotubes were then scrapped and subjected to a freeze-thaw cycle. After this, the protein lysate was centrifuged at 2,300 g for 5 min and the supernatant was transferred to a 96-well microtitre plate. The caspase-3 substrate buffer was added to each well, and the plate was incubated in the dark for 30 min at room temperature. Caspase-3 activity was fluorometrically determined at 342 ex /441 em using a Victor³ 1420 Multilabel Counter (PerkinElmer).

4.3.8 Glucose oxidase assay

The glucose oxidase (GO) assay kit (Sigma-Aldrich), was used to quantitatively measure glucose secreted by the hepatocytes in cell culture medium. In this assay, glucose oxidase is oxidized to gluconic acid and hydrogen peroxide by glucose oxidase. The generation of H₂O₂ is indirectly measured by oxidation of o-dianisidine which in the presence of peroxidase forms a coloured product which can be quantified. The intensity of the colour measured is proportional to the original glucose concentration in the cell culture medium.

Prior to the assay, hepatocytes were treated with LDL-ceramide for 24 h then the cells were rinsed 5 times with PBS + to remove residual LDL-ceramide medium. Glucose output medium comprising of no glucose DMEM, 2 mM Na pyruvate, and 20mM sodium-L-lactate (Sigma-Aldrich.) with 10nM insulin or without insulin was then added to the cells. The medium was left to incubate with the cells for 4 h or 8 h the supernate was collected and glucose assessed.

Glucose standards provided in the kit were made to concentrations of 0, 7.9, 15.6, 31.3, 62.5, 125, 250 and 500 µg/ml. To each well on a 96 well microtitre plate, 50 µL of standard or experimental samples were added together with 100 µL of GO assay kit reagent (glucose oxidase, peroxidase reagent, o-dianisidine) in duplicate. The plate was left to incubate for 1 h at 37°C and the reaction was stopped using 100 µL of 12M H₂SO₄. The colour intensity was measured using a SpectraMax Plus 384™ spectrophotometer (Molecular Devices.) at 540nm.

4.3.9 Statistical analyses

Statistical analysis was performed using Graphpad Prism program (Graphpad Software, California, USA). Unpaired Student's t-tests were used to compare one variable between two groups. Two-way analysis of variance (ANOVA) was used to compare two independent variables given one measurable variable, with Tukey's multiple comparison test incorporating Kramer's correction for unequal sample sizes used as a post-hoc test for differences between groups. Statistical significance was set at $p < 0.05$. All data are shown as mean \pm SEM.

4.4.0 LDL-ceramide infusion in to mice.

6-8 week old C57BL/6 mice was fasted 5 hours prior to experimentation. The jugular veins of the mice were catheterized under isoflurane anesthesia by Dr. Russell Brown (Dept of Physiology, Monash University) and this process took ~10min. The mice were restrained in a mouse holder and randomly assigned to be infused with either 15µmol/L LDL-C24:0 ceramide for 4 h or LDL for 4 h as the control. After the infusion, the catheter was closed off and the mice were housed individually overnight. The next morning, mice were anaesthetised with isoflurane, and insulin (0.5 U/kg) and 2-deoxy-D-1[³H] glucose (10 µCi) were administered together as an intravenous

bolus injected into the inferior vena cava. Mice were then killed by cervical dislocation and gastrocnemius, quadriceps, liver, heart, brown adipose tissue and epididymal fat pads were removed .

4.4.1 Plasma membrane fractionation.

All steps were carried out at 4°C. The plasma membrane fraction was prepared from 100-200 mg muscle tissue. Muscle tissue was powdered using mortar and pestle on dry ice and then dissolved in 1 ml buffer A, containing 0.25 M sucrose/1 mM EDTA/20 mM Tricine, pH 7.8. The lysate was further homogenized using a bead mill (Qiagen, Tissue Lyser) and 20-50 strokes of a Teflon homogenizer. Homogenate was transferred into an eppendorf tube and centrifuged at 1000 g for 10 min (Eppendorf). The postnuclear supernatant fraction (PNS) was removed and stored on ice. The pellet was resuspended in 1 ml of buffer A, homogenized with Teflon homogenizer, and centrifuged at 1000 g for 10 min. The two PNS were combined, layered on the top of 11 ml of 30 % Percoll (Sigma) in buffer A, and centrifuged at 22133 rpm (Beckmann, SW41 Ti rotor) for 30 minutes. The top layer is the plasma membrane fraction. This was collected with a pasteur pipette, adjusted to 1.7 ml with buffer A, and placed in an ultra-centrifuge (Beckmann, TLA-100.3) and centrifuged at 42 995 rpm for 1 hr. The pellet was washed and resuspended again in buffer A and re-centrifuged for 30 min. As a quality control for plasma membrane isolation the plasma membrane pellet was dissolved in 200 ul RIPA buffer and immunoblots were performed for plasma membrane markers but also markers for other cell organelles such as endoplasmic reticulum and mitochondria (cell signalling). This assay was performed by Dr Romana Stark (Monash University, Physiology Department).

4.4 Results

4.4.1 Testing basal glucose uptake in standard L6 Glut4-myc myotubes in response to insulin

Standard L6 myotubes exhibit low responsiveness to insulin; therefore the L6-Glut4-myc cells were used in these experiments. Myotubes differentiated from L6 Glut4-myc cells showed good uptake of 2DG following insulin stimulation (Fig 4-1). Insulin-stimulated glucose uptake was increased 43% above basal, demonstrating that this cell line was appropriate for further studies.

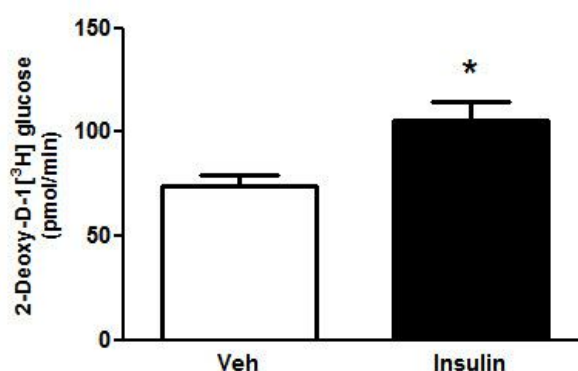


Fig 4-1. 2-deoxy-D-1[³H] glucose uptake in L6 Glut4-myc myotubes following 10nM insulin stimulation. There was a 43% increase in glucose uptake following insulin stimulation ($n=6$, 1 biological replicate with six technical replicates. $*P<0.05$ vs Veh by Student's t -test). Figure depicts mean \pm S.E.M

4.4.2 Increasing insulin concentration does not lead to increased glucose uptake in L6 Glut4-myc myotubes.

To examine whether increasing insulin concentration would lead to enhanced glucose uptake, 10 nM and 100 nM was used to stimulate the myotubes. There was no increase in 2DG uptake with 100 nM insulin (Fig 4-2), indicating that the effects of insulin in stimulating glucose uptake was saturating at 10nM in the L6 Glut4-myc myotubes.

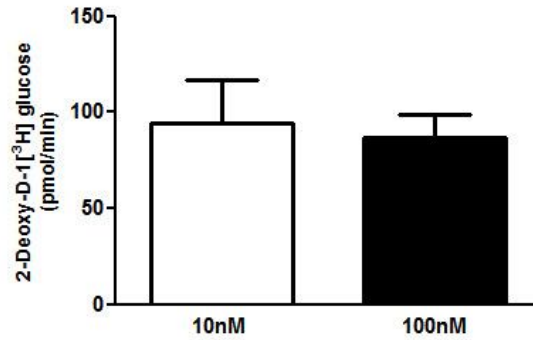


Fig 4-2. 2-deoxy-D-1[³H] glucose uptake in L6 Glut4-myc myotubes following 10nM and 2 μ M insulin stimulation (n=6). Figure depicts mean \pm S.E.M.

4.4.3 LDL treatment does not affect insulin stimulated glucose uptake in L6 Glut4-myc myotubes.

LDL was used as control against untreated myotubes to examine whether LDL treatment had an effect on insulin stimulated 2 DG uptake in L6 glut4-myc myotubes. L6 Glut4-myc cells were differentiated into myotubes and incubated with LDL for the same duration as that used in LDL-ceramide treatment (24 h). LDL alone did not reduce insulin stimulated glucose uptake in the myotubes (Fig 4-3). There was no effect of LDL alone on basal glucose uptake (data not shown).

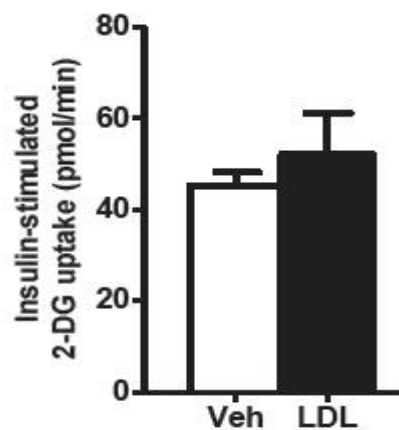


Fig 4-3. LDL administration does not influence insulin-stimulated 2-deoxy-D-1[³H] glucose uptake compared with untreated L6 Glut4-myc myotubes (n=6 per group). Each individual experiment was performed in triplicate. Figure depicts mean \pm S.E.M.

4.4.4 LDL ceramide decreases insulin stimulated glucose uptake in L6 Glut4-myc myotubes

L6 Glut4-myc myotubes were pre-treated for 6 or 24 h with LDL or LDL-ceramide, followed by measurement of 2-deoxy-D-1^[3H] glucose (2DG) transport after stimulation with insulin. Insulin stimulation of glucose uptake was not affected by 6 h LDL-ceramide treatment (Fig 4-4 A & B). Basal glucose uptake was not different between groups. In contrast, 24 h exposure to LDL-ceramide decreased insulin-stimulated glucose uptake by 25% with LDL-C24:0 ceramide (Fig 4-5 A) and 21% with LDL-C16:0 ceramide (Fig 4-5 B)

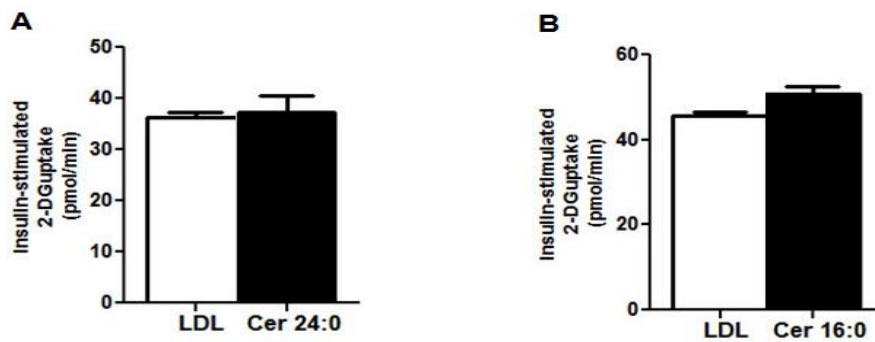


Fig 4-4. 6h LDL-C24:0 and C16:0 ceramide treatment does not decrease 2-deoxy-D-1^[3H] glucose uptake in L6 Glut4-myc myotubes. 2 μ M of LDL-ceramide was used as treatment and 10nM insulin was used for stimulation (n=9 per group), individual experiments were performed in triplicate. Figure depicts mean \pm S.E.M.

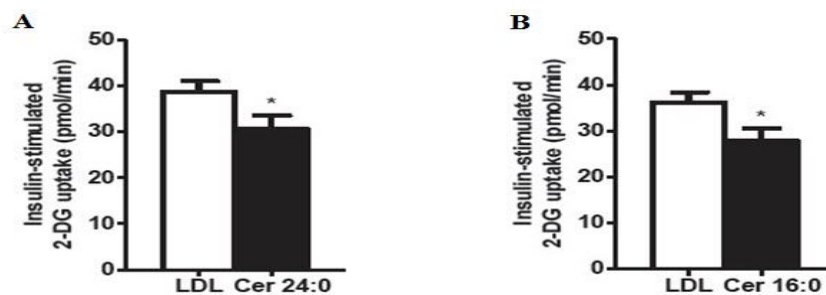


Fig 4-5. 24h LDL-C24:0 and C16:0 ceramide treatment decreases 2-deoxy-D-1^[3H] glucose uptake in L6 Glut4-myc myotubes. 2 μ M of LDL-ceramide was used as treatment and 10nM insulin was used for stimulation (n=9 per group), individual experiments were performed in triplicate, *P<0.05 vs LDL by Student's t-test. Figure depicts mean \pm S.E.M.

4.4.5 LDL-ceramide decreases AKT phosphorylation in L6 Glut4-myc myotubes.

AKT (also known as PKB) is essential for insulin signal transduction. In skeletal muscle, activation of AKT by phosphorylation ultimately leads to the translocation of glucose transporters to the cell membrane which brings glucose into the cell^{41,42} Full activation of AKT mechanistically occurs when both of its two residues Ser 473 and Thr 308 are phosphorylated during insulin stimulation⁴³.

To elucidate the mechanism of LDL-ceramide induced insulin resistance in L6 Glut4-myc myotubes, cells were treated with LDL-ceramide for 24 h, then stimulated with 1 nM insulin and AKT phosphorylation was examined by Western blotting. Phosphorylation of Akt was reduced in LDL-ceramide treated myotubes (Fig 4-6) 3E).

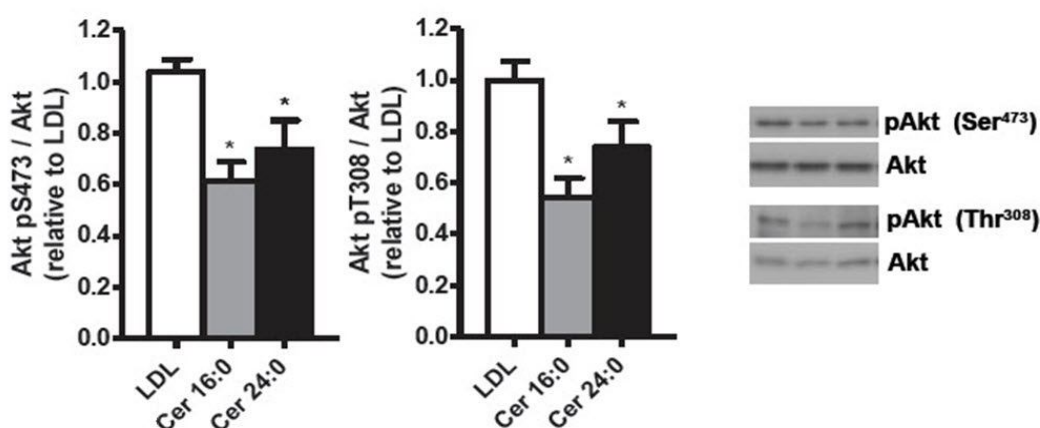


Fig 4-6. AKT phosphorylation (Ser⁴⁷³ and Thr³⁰⁸) is reduced in LDL-ceramide treated L6 Glut4-myc myotubes after 24h. Densitometry analysis of myotubes treated with LDL-ceramide for 24 h and stimulated with 1 nM insulin (n=9 per group, *P<0.05 vs LDL by Student's t-test). Right: representative immunoblots. Figure depict mean \pm S.E.M.

4.4.6 Testing viability of L6 Glut4-myc myotubes for use in insulin stimulated Glut4 translocation assay.

We next assessed the effect of LDL-ceramide on Glut4 translocation, an event that occurs distal to Akt. The L6 Glut4-myc cell line possesses an exo-facial myc epitope tagged to Glut4 which is exposed on the cell surface during Glut4 translocation,

thereby allowing detection. Plasma membranes Glut-4 content was increased in insulin treated cells (Fig 4-7) indicating that the cell line was appropriate for the assay.

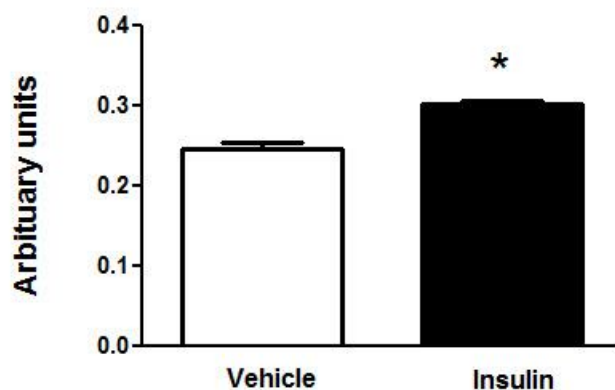


Fig 4-7. *Glut4-myc protein detected at cell surface of L6 Glut4-myc myotubes following 10 nM insulin stimulation (n=12, *P<0.05 vs vehicle by Student's t-test). Figure depict mean ± S.E.M.*

4.4.7 LDL-ceramide reduces insulin stimulated Glut4 translocation in L6 Glut4-myc myotubes.

L6 Glut4-myc myotubes were treated with LDL-ceramide for 24 h and then stimulated with insulin for 20 min. A significant decrease in Glut4-myc was detected at the cell surface of LDL-ceramide treated myotubes during insulin stimulation compared with LDL treated cells (Fig 4-8). The results indicate that the mechanism for LDL-ceramide induction of insulin resistance in myotubes is likely due to interference of Glut-4 translocation during insulin stimulation.

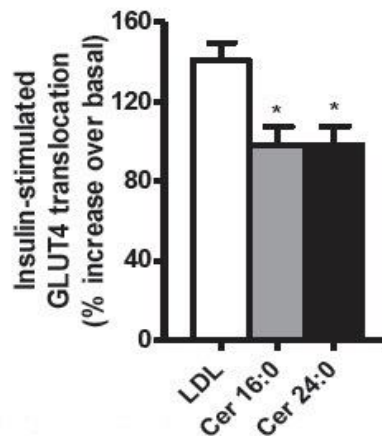


Fig 4-8. *Glut4-myc protein detected at cell surface of 24 h LDL-ceramide treated L6 Glut4-myc myotubes following 10 nM insulin stimulation (n=9 per group, *P<0.05 vs LDL using one-way ANOVA followed by Tukey's post hoc test.). Figure depict mean \pm S.E.M.*

4.4.8 LDL-ceramide does not influence JNK or NF κ B signalling in myotubes.

Extracellular regulated serine/threonine kinase such as JNK and ERK are known antagonists of insulin signal transduction. L6 Glut4-myc myotubes were examined to determine whether these kinases are increased after 24 h LDL-ceramide treatment. There was no effect of ERK, JNK and NF κ B activation as determined by immunoblots analysis (Fig 4-9).

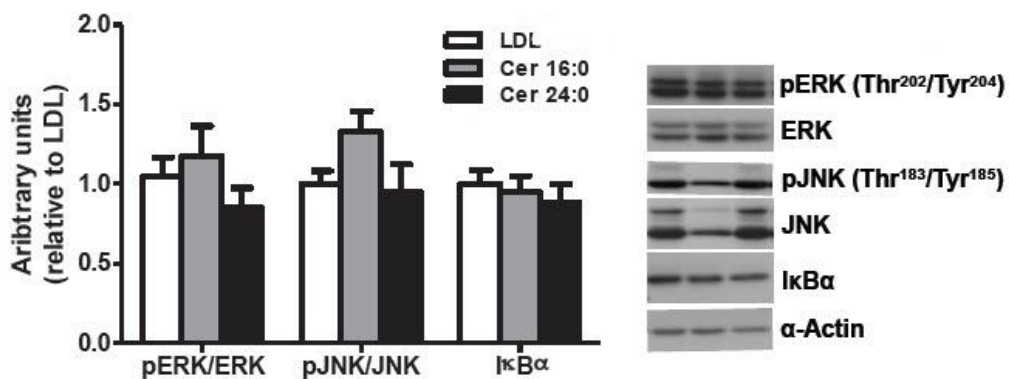


Fig 4-9 *LDL-ceramide has no effect on ERK, JNK and I κ B α . Densitometry analysis of immunoblots (n=6 per group). Analysis performed using one-way ANOVA followed by Tukey's post hoc test. Figure depict mean \pm S.E.M.*

4.4.9 LDL-ceramide treatment does not induce apoptosis via caspase-3.

Caspase-3 assay was performed to examine if LDL-ceramide induced apoptosis. Myotubes were treated with 2 μ M of LDL-ceramide for 24 h before analysis of caspase-3 activity. LDL-ceramide did not increase caspase-3 activity compared to LDL or untreated controls (Fig 4-10).

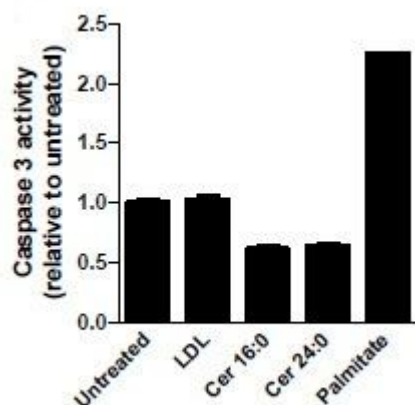


Fig 4-10. LDL-ceramide treatment does not increase caspase-3 activity. Caspase 3 activity in cell lysates in the culture medium 24 h after treating L6 Glut4-myc myotubes with LDL, LDL-ceramide 16:0, LDL-ceramide 24:0 and 0.75 mM palmitate ($n=3$).

4.4.10 LDL-ceramide treatment induces intracellular ceramide accrual in L6 Glut4-myc myotubes.

To examine whether intracellular ceramide content increased following LDL-ceramide treatment, myotubes were incubated with LDL-C16:0 ceramide or LDL-C24:0 ceramide for 24 h before cells were extensively washed, lysed and intracellular ceramide species content analysed via mass-spectrometry. Myotubes incubated with LDL-ceramide showed an increase in intracellular content of only the ceramide species that had been used for treatment. Treatment with LDL-C16:0 ceramide resulted in an increase in intracellular C16:0 ceramide levels (Fig 4-11). Similarly for LDL-C24:0 ceramide treated cells, intracellular C24:0 ceramide content was significantly increased (Fig 4-11). There was no increase in other ceramide species intracellularly. Sphingomyelin content was not decreased by LDL-ceramide treatment, suggesting that the increase in ceramide was not due to increased sphingomyelinase

activity. (Fig 4-12). The increase in specific ceramide species was also not due to *de novo* synthesis because there were no fatty acids present in the culture medium.

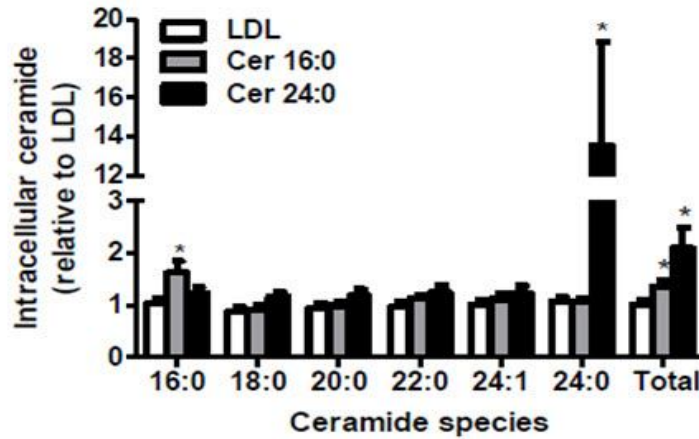


Fig 4-11. L6 *Glut4-myc* myotubes treated for 24 h with LDL-ceramide leads to increase in intracellular ceramide of the corresponding ceramide sub-species. Figure depicts mean \pm S.E.M. (n=12 per group, *P<0.05 vs LDL by Student's t-test).

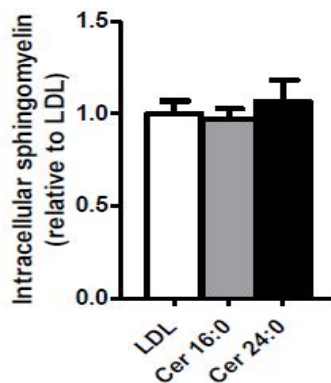


Fig 4-12. Sphingomyelin content in L6 *Glut4-myc* myotubes is not decreased by LDL-ceramide treatment (n=6 per group). Figure depicts mean \pm S.E.M.

4.4.11 Myriocin does not prevent ceramide accrual in LDL-ceramide treated L6 *Glut4-myc* myotubes.

Myotubes were treated with LDL-C24:0 ceramide and 10 μ M myriocin, a pharmacological inhibitor of serine palmitoyltransferase activity and *de novo*

ceramide synthesis. After 24 h, myotubes were lysed and analysed for intracellular C24:0 ceramide content by mass spectrometry. Intra-myocellular C24:0 ceramide increased when cells were incubated with LDL-C24:0 ceramide, even in the presence of myriocin (Fig 4-13). This indicates that that ceramide accrual in LDL-ceramide treated L6 Glut4-myc myotubes is not due to a *de novo* ceramide synthesis event.

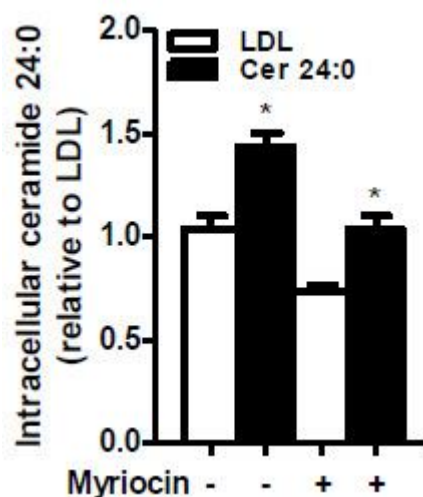


Fig 4-13. Myriocin does not prevent C24:0 ceramide accrual in LDL-C24:0 ceramide treated L6 Glut4-myc skeletal myotubes. Myotubes were pre-treated with SPT inhibitor myriocin, which blocks *de novo* synthesis, or vehicle for 10 min. Thereafter, myotubes were incubated with LDL or LDL-C24:0 ceramide for 24h and intracellular ceramide was analyzed via mass spectrometry ($n=3$ per group). Figure depicts mean \pm S.E.M. * $P<0.05$ vs. LDL by Student's *t*-test.

4.4.12 Anti LDL-receptor antibody does not prevent ceramide accrual in LDL-ceramide treated in L6 Glut4-myc myotubes.

LDL can be transported into cells by receptor-mediated and receptor-independent processes; however, skeletal muscle takes up virtually no LDL by receptor-mediated processes¹⁷¹. To address this problem, an anti-LDL receptor monoclonal antibody EP1553Y was used to block LDL receptor activity for 10 min to examine whether inhibition of LDL-R prevents intracellular C24:0 ceramide from increasing following LDL-C24:0 ceramide treatment. Blocking LDL receptor did not affect C24:0 ceramide accrual in L6 Glut4-myc myotubes following LDL-C24:0 treatment (Fig 4-14). Since we could not measure LDL uptake because of the extremely low uptake in

skeletal muscle, positive controls in this experiment were not implemented and the dose used was based on previous published experiments²¹⁹.

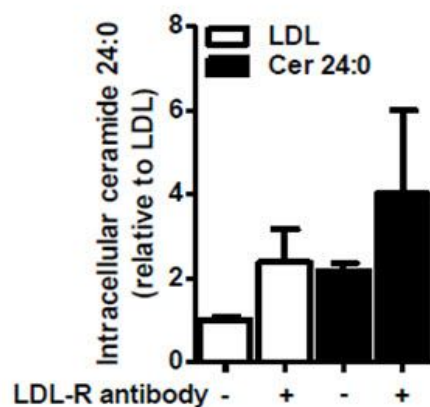


Fig 4-14. Anti LDL-receptor antibody does not prevent C24:0 ceramide accrual in LDL-C24:0 ceramide treated myotubes. Myotubes were pre-treated with a monoclonal rat LDL-receptor antibody or denatured antibody for 10 min. Thereafter, myotubes were incubated with LDL or LDL-C24:0 ceramide for 24 hr and intracellular ceramide was analysed via mass spectrometry. Figure depicts mean \pm S.E.M ($n=3$).

4.4.13 Testing insulin responsiveness of HEPG2 and CRL 1439 hepatocyte cell line in suppressing glucose output.

Two hepatic cell lines HEPG2 and CRL 1439, were tested for responsiveness to insulin before experiments with LDL-ceramide were performed. During insulin stimulation, hepatocytes suppress glucose release. Hepatic insulin resistance occurs when insulin has a diminished effect in suppressing hepatic glucose release. The HEPG2 hepatic cell line was not responsive to insulin and continued to secrete glucose even after insulin stimulation following 4 h and 8 h treatment (Fig 4-15). This was also the case for the CRL 1439 hepatic cells where insulin failed to reduce glucose output levels (Fig 4-16). The results indicate that these two cell lines are not suitable as a model to test for hepatic insulin resistance.

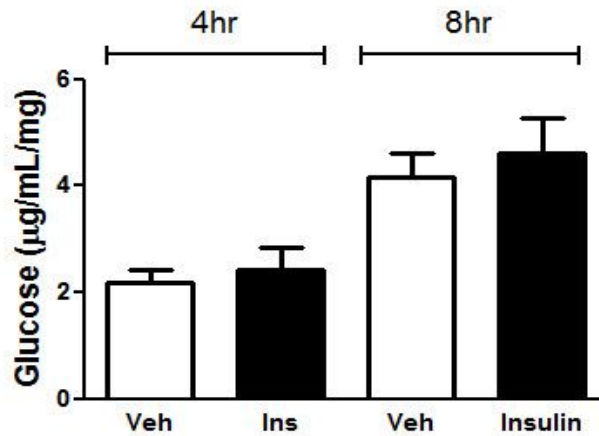


Fig 4-15. Glucose output in HEPG2 following 4 h and 8 h insulin stimulation. HEPG2 cells do not respond to insulin and suppress glucose release (n=3). Figure depicts Mean \pm S.E.M.

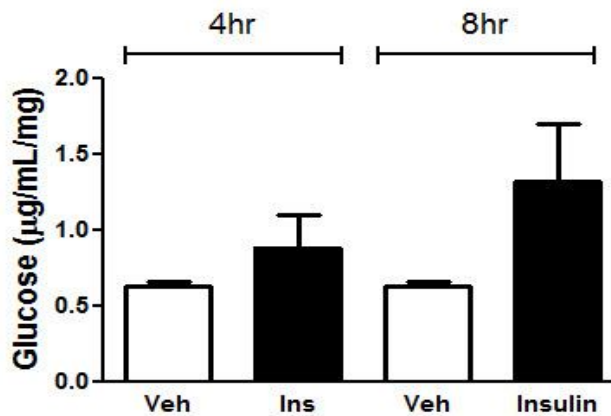


Fig 4-16. Glucose output in CRL 1439 following 4 h and 8 h insulin stimulation. CRL 1439 cells do not respond to insulin and suppress glucose release (n=3). Figure depicts Mean \pm S.E.M.

4.4.14 Testing insulin responsiveness of mouse primary hepatocytes in suppressing glucose output.

Mouse primary hepatocytes respond to insulin stimulation with suppression of glucose release (Fig 4-17). Glucose output was lower after 8 h in insulin stimulated cells compared with untreated controls. This indicates that primary mouse hepatocytes are suitable for use to examine LDL-ceramide effect on hepatic insulin resistance.

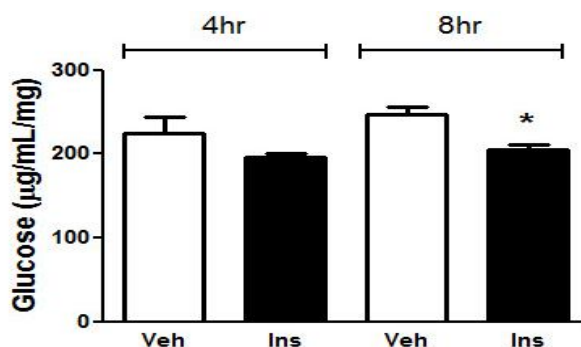


Fig 4-17. Glucose output in primary mouse hepatocytes following insulin stimulation. Primary mouse hepatocytes significantly suppress glucose release after 8 h stimulation with insulin ($n=4$, $p=0.0141$) but not at 4 h stimulation ($n=4$, $*P<0.05$). Figure depicts Mean \pm S.E.M.

4.4.15 LDL-ceramide does not cause insulin resistance in mouse hepatocytes.

As LDL was intended to be used as a control against ceramide treatment in mouse primary hepatocytes, LDL was tested to see whether it induces insulin resistance. Hepatocytes were incubated for 24 h with LDL and then stimulated with 10 nM insulin for 8 h, following which cell culture medium was collected and glucose levels examined. Glucose output was similarly suppressed upon insulin stimulation indicating that LDL treatment does not cause insulin resistance in hepatocytes (Fig 4-18A). 2 µM LDL-ceramide was then used to treat the hepatocytes with the same parameters as described with LDL testing. LDL-ceramide did not cause insulin resistance in treated hepatocytes as the cells continue to remain insulin responsive and suppress glucose release upon insulin exposure (Fig 4-18B & 4-18C).

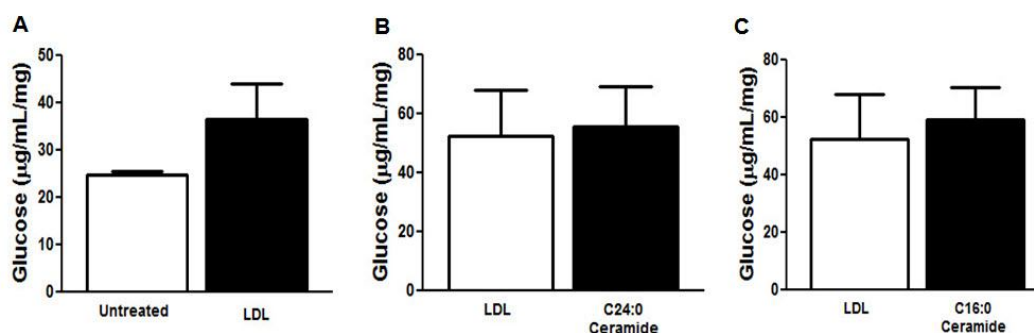


Fig 4-18. LDL-ceramide does not cause insulin resistance in primary mouse hepatocytes ($n=4$). Figure depicts mean \pm S.E.M.

4.4.16 LDL does not reduce insulin stimulated glucose uptake in 3T3-L1 adipocytes.

LDL was first tested to examine whether it induces insulin resistance in 3T3-L1 adipocytes before testing was done with LDL-ceramide. Differentiated 3T3-L1 adipocytes were treated for 24 h, after which an insulin stimulated 2-DG uptake assay was performed. LDL treatment does not reduce insulin stimulated 2DG uptake in mature 3T3-L1 adipocytes (Fig 4-19A). 2 μ M LDL-ceramide was then used to treat the adipocytes for 24 h. There was no significant reduction in insulin stimulated glucose uptake by 3T3-L1 adipocytes in both cases of LDL-ceramide treatment (Fig 4-19B & 4-19C). This suggests that LDL-ceramide has no effect in inducing insulin resistance in 3T3-L1 adipocytes.

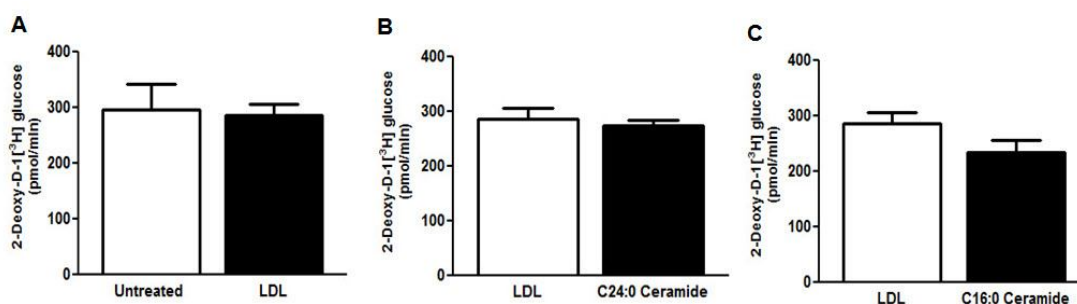


Fig 4-19. 24 h LDL-C16:0/C24:0 ceramide treatment does not reduce 2-deoxy-D-1[³H] glucose uptake in insulin stimulated 3T3-L1 adipocytes (n=6). Figure depicts mean \pm S.E.M.

4.4.17 LDL-ceramide infusion into lean mice causes insulin resistance.

To elucidate the physiological role of LDL-ceramide *in vivo*, LDL-ceramide was infused into the jugular vein of lean mice for 4 h, before assessing insulin-stimulated glucose transport 24 h later. LDL without ceramide was infused into control mice. The LDL-ceramide infusion reduced whole-body glucose clearance by 29% (Fig 4-20). This was accounted for by reduced glucose disposal specifically into skeletal muscle (Fig 4-21), which was accompanied by decreased phosphorylation of Akt (Fig 4-22). Surprisingly, there was no change in total muscle ceramide (Fig 4-23). Ceramide is a highly hydrophobic molecule and, as such, it is highly possible that ceramide remains localized to the plasma membrane, rather than diffusing into the cytosol. Consistent with this notion, ceramide tended (P=0.08) to be elevated in plasma membrane

enriched fraction from LDL-ceramide infused mice (Fig 4-24). The insulin-desensitizing effects of LDL-ceramide were specific to skeletal muscle because glucose disposal into white and brown adipose tissue, the heart and the liver was not different between groups (Fig 4-25).

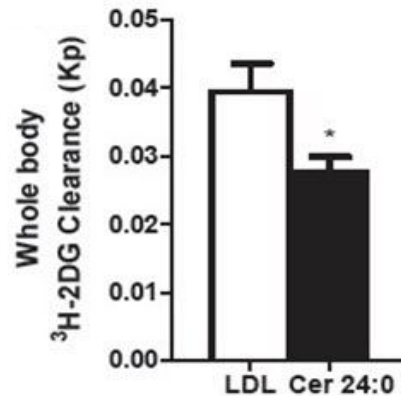


Fig 4-20. Rates of insulin stimulated ³H 2-deoxyglucose disappearance from blood of lean mice infused with LDL (white bar) or LDL-24:0 ceramide (black bar). (n=8 for LDL, n=9 for C24:0 ceramide, *P<0.05 vs LDL by Student's t-test.). Figure depicts mean \pm S.E.M

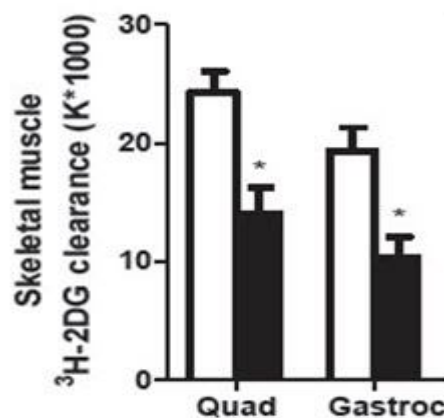


Fig 4-21. Rates of insulin stimulated ³H-2-deoxyglucose clearance into mixed quadriceps and mixed gastrocnemius skeletal muscle in lean mice infused with LDL (white bar) or LDL-24:0 ceramide (black bar). (n=8 for LDL, n=9 for C24:0 ceramide, *P<0.05 vs LDL by Student's t-test). Figure depicts mean \pm S.E.M

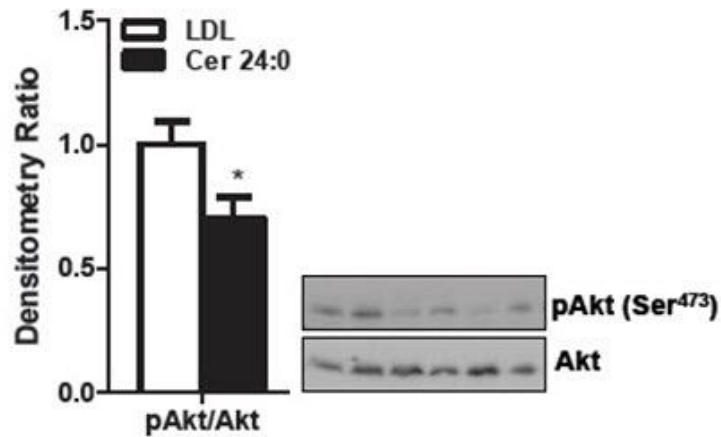


Fig 4-22. AKT (Ser⁴⁷³) phosphorylation is decreased in vastus lateralis muscle of LDL-C24:0 ceramide infused mice. Densitometry analysis of AKT (Ser⁴⁷³) in lysates of skeletal muscle obtained immediately after i.v insulin injection. Representative immunoblots to the right. (n=8 for LDL, n=9 for C24:0 ceramide, *P<0.05 vs LDL by Student's t-test). Figure depicts mean ± S.E.M.

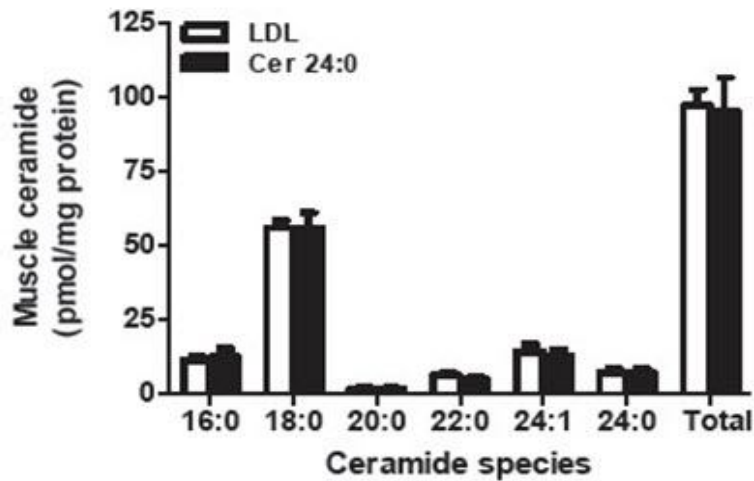


Fig 4-23. Ceramide content in mixed vastus lateralis muscle analysed by mass spectrometry (n=8 for LDL, n=9 for C24:0 ceramide). Figure depicts mean ± S.E.M.

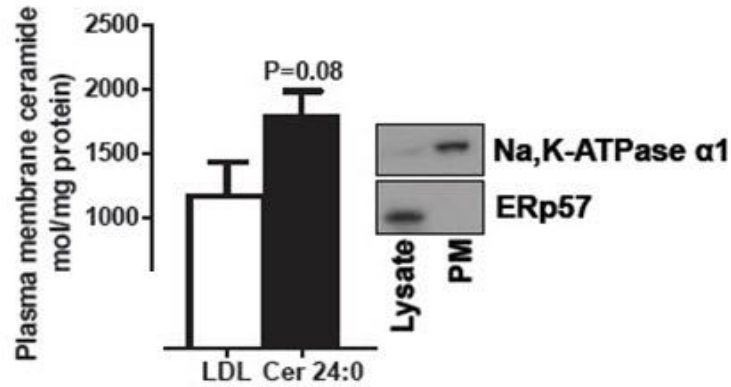


Fig 4-24. Ceramide content in plasma membrane enriched fraction of mixed vastus lateralis muscle measured by mass spectrometry. Right: Immuno blot of Na, K-ATPase and ERp57 demonstrating enrichment of the plasma membrane fraction and no contamination with endoplasmic reticulum. (n=8 for LDL, n=9 for C24:0 ceramide). Figure depicts mean \pm S.E.M.

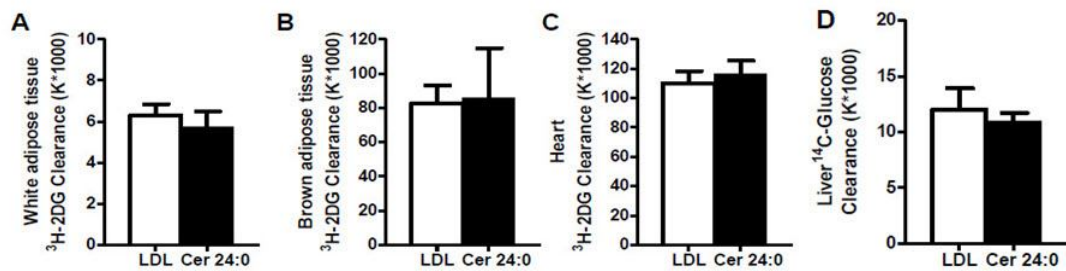


Fig 4-25. LDL-ceramide does not induce insulin resistance in adipose tissue, heart and liver. Mice were injected with insulin and ³H-2-deoxyglucose and uptake was assessed in (A) white epididymal adipose tissue (B), brown adipose tissue (C), heart (D), liver ¹⁴C-glucose clearance (D). (n=8 for LDL, n=9 for C24:0 ceramide). Figure depicts mean \pm S.E.M.

4.4.18 LDL-ceramide infusion cause inflammation in lean mice

Based on *in vitro* studies with L6 Glut4-myc myotubes which showed pro-inflammatory serine/threonine kinase phosphorylation increasing with LDL-ceramide treatment, it was reasoned that circulating ceramide may also regulate these pathways *in vivo*. Western blot analysis of muscle lysates revealed that LDL-ceramide increased IKK β signaling, as assessed by I κ B α degradation, but did not affect JNK

phosphorylation (Fig 4-26). The expression of NFκB target genes was also increased (Fig. 4-27). ELISA analysis of plasma pro-inflammatory cytokine showed that, while levels tended to increase with LDL-ceramide, these changes were not statistically significant (Fig 4-28).

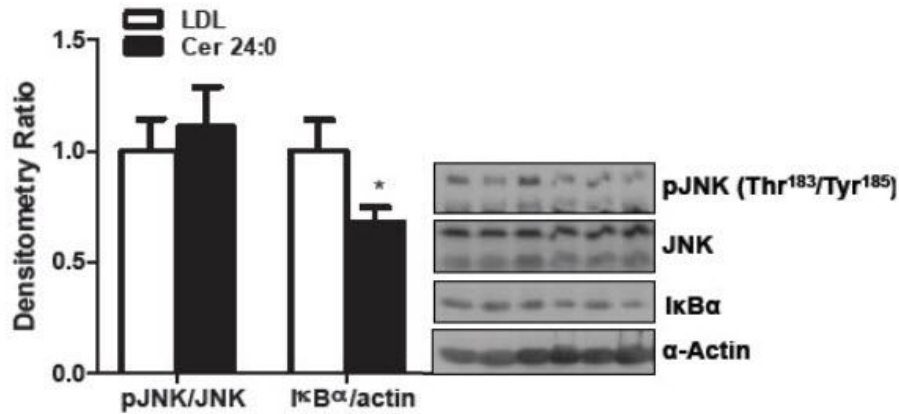


Fig 4-26. Quantification of immunoblot analysis of phosphorylated JNK (Thr¹⁸³/Tyr¹⁸⁵)/JNK and IκBα/α-actin in lysates of skeletal muscle obtain immediately after iv insulin injection. Representative immunoblots to the right (n=8 for LDL, n=9 for C24:0 ceramide, *P<0.05 vs LDL by Student's t-test). Figure depicts mean ± S.E.M.

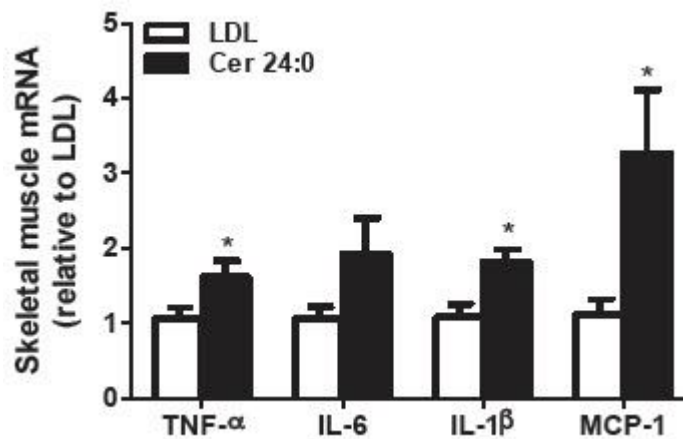


Fig 4-27. Transcript levels of pro-inflammatory cytokines in mixed vastus lateralis skeletal muscle (n=8 for LDL, n=9 for C23:0 ceramide, *P<0.05 vs LDL by Student's t-test). Figure depicts mean ± S.E.M.

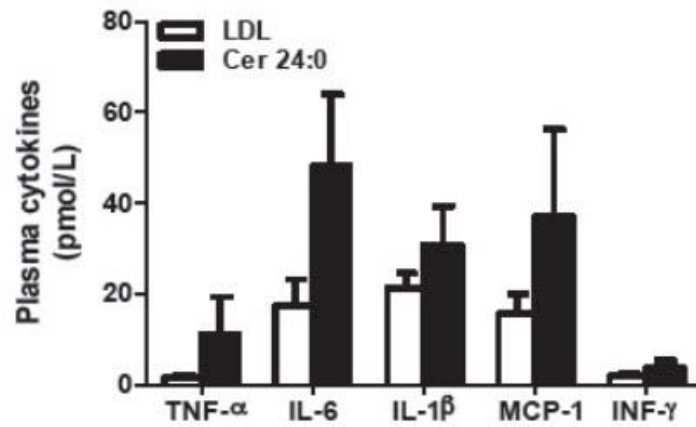


Fig 4-28. Plasma pro-inflammatory cytokine in lean mice infused with LDL or LDL-C24:0 ceramide for 4 h and intravenous insulin tolerance tests preformed 24 h later ($n=8$ for LDL, $n=9$ for C23:0 ceramide). Figure depicts mean \pm S.E.M.

4.5 Discussion

While various *in vitro* studies have examined the effects of ceramide, these studies use short chain ceramide analogues which are water soluble^{3, 9}. This is in contrast to an *in vivo* setting, where natural ceramides are long chain, hydrophobic and are transported in plasma via lipoproteins^{30, 163}. While studies exist which show an associative effect of plasma ceramide and insulin resistance in patients with T2DM³⁰, the question as to whether plasma ceramides are a cause or an effect of the insulin resistant T2DM state has yet to be answered.

Here for the first time, with the use of artificial constructed LDL-ceramides, proof-of-principal evidence is provided which shows that exposure to exogenous LDL-ceramide can induce a functional deficit in insulin stimulated glucose uptake in skeletal muscle cells, which is the main *in vivo* determinant of insulin mediated glycemic control. These results show that exogenous LDL-ceramide causes skeletal muscle insulin resistance and supports the contention that plasma ceramide may impair insulin action in human patients with T2DM (Chapter 2).

Skeletal muscle accounts for the majority of total glucose disposal (75-90%) during insulin stimulation³⁹. Skeletal muscle cells, like adipose cells, utilize Glut4 as the main glucose transporter, which translocates to the membrane surface from intracellular storage vesicles during insulin stimulation²²⁰⁻²²⁴. One major advantage in focusing on functional assays is that it represents the endpoint of multiple upstream signalling pathways. As such, the insulin stimulated 2DG uptake assay was chosen as the main read-out for examining LDL-ceramide effects in eliciting insulin desensitization.

During the course of the study, the L6 Glut4-myc skeletal muscle line was chosen as a replacement over the standard L6 cell line due to its robust performance in insulin stimulated glucose uptake. In addition, since the L6 Glut4-myc cell line possesses an exofacial myc epitope tagged to Glut-4, it offered the possibility of examining Glut4 translocation during insulin stimulation. It is important to note, however that, while the L6 skeletal muscle cell line is useful in examining insulin signalling that affects Glut4 translocation, the L6 skeletal muscle cell line do not develop the contractile

apparatus of sarcomere units²²⁵. Contractile studies are more suitable for skeletal muscle cell lines such as C₂C₁₂²²⁶⁻²²⁸ which, on the other hand, express low levels of Glut4 and are not ideal for use in examining insulin mediated lut-4 effects²²⁹.

Given that several *in vitro* studies show that ceramides inhibit insulin signalling in muscle cells by decreasing insulin-stimulated activation of Akt^{51,230}, it was logical to examine whether the mechanism behind LDL ceramide induced insulin resistance was due to suppression of AKT activity. The distal insulin signaling intermediate AKT was found to be reduced following LDL-ceramide treatment. Upstream signaling intermediates were not examined, however, since most previous studies suggest that ceramides do not induce defects in IR, IRS or PI3K signaling⁵¹.

While AKT is essential for most of the actions of insulin signal transduction, ultimately the translocation of Glut4 to the cell surface membrane is what transports glucose into the cell during insulin stimulation. As such, it might not be entirely prudent to rely solely on elements in the insulin signalling cascade as the major explanation of the mechanism behind insulin resistance. In fact, there are studies that show that insulin resistance is not always associated with defects in AKT signalling^{231,232}. Reports also exist which show that insulin triggered AKT activity and glucose uptake is non-linear²³³. In addition, a study using L6 myotubes showed that only 5% of the total AKT pool was required to be phosphorylated to have a maximal effect on Glut4 translocation²³⁴. Taken together, what these studies highlight is that relying solely on components upstream of the insulin signalling cascade to explain insulin resistance may not necessary equate to downstream defects of glut-4 translocation.

Glut4 translocation was examined as a possible downstream mechanism behind LDL-ceramide induced insulin resistance in L6 Glut4-myc myotubes. Treatment with LDL-ceramide suppresses Glut4 from translocating to the plasma membrane during insulin stimulation in the myotubes. While there is a growing literature that suggests Glut4 translocation alone does not fully account for the entire effects of insulin on glucose uptake²³⁵⁻²³⁹, a decrease in glucose uptake during insulin stimulation is the final outcome of any changes that affect the insulin signalling pathway.

While LDL-ceramide was shown to induce insulin resistance in skeletal myotubes by

interfering with AKT phosphorylation and Glut4 translocation, an unanswered question thus far is, are LDL-ceramides taken up by skeletal myotubes to exert their effects?

To address this, L6 Glut4-myc myotubes treated with LDL-ceramide were examined for differences in intracellular ceramide levels via mass spectrometry. Myotubes showed an increase in intracellular content of only the ceramide species that was used for treatment and there were no increase in other ceramide sub-species (i.e LDL-C24:0 ceramide treatment results in increased intracellular C24:0 ceramide only). However, a cautionary approach should be taken in interpreting the data. While a simplistic view could be that LDL-ceramides are taken up by myotubes, it is not entirely certain if this is the case, since the ceramide in the LDL-ceramide preparation was not labelled. Labelling of ceramide, either by fluorescent dye or radio-labelling could not be done due to the nature of the LDL-ceramide preparation protocol. Thus, it is possible that the increase in intracellular ceramide accrual from exposure to LDL-ceramide could result from inadequate washing of cells prior to extraction or due to ceramide synthesis via a process other than direct uptake of exogenous ceramide.

To further elucidate whether ceramide accrual in LDL-ceramide treated myotubes was due to intracellular ceramide synthesis, myriocin, a selective inhibitor of serine palmitoyltransferase (SPT)²⁴⁰, the rate limiting enzyme of *de novo* ceramide synthesis, was used. While the salvage pathway of ceramide synthesis is sensitive to the inhibitor fumonisin B1, and not to myriocin, when used over several hours myriocin will inhibit all sphingolipid synthesis and in so doing, inhibits the salvage pathway of ceramide synthesis indirectly by depleting the required precursor sphingolipids⁸⁴. As such, treating the myotubes for 24 h with myriocin would effectively inhibit both the *de novo* and salvage pathways of ceramide synthesis and would answer the question as to whether ceramide accrual in treated myotubes is due to an endogenous ceramide synthesis event. Ceramide accrual remained elevated, in spite of of myriocin treatment, indicating that increased ceramide content upon LDL-ceramide treatment was not due to a *de novo* synthesis event.

To determine whether LDL receptor activity is required for ceramide uptake, a monoclonal antibody against the LDL-receptor was used to block the LDL-receptor.

Blocking the LDL-receptor did not affect intracellular ceramide from accumulating when exposed to exogenously added LDL-ceramide. Viewed in conjunction with the myriocin results, one can conclude that intracellular ceramide increases in L6 Glut4-myc myotubes following treatment with LDL-ceramide is due to uptake of LDL-ceramide from culture medium.

Short chain ceramide analogues have been observed to induce apoptosis in cell models^{51, 59}. To rule out the possibility that the decrease in 2DG uptake is due to myotubes undergoing apoptosis and hence unable to efficiently uptake glucose²⁴¹, caspase-3 assay was preformed and showed the LDL-ceramide did not induce apoptosis in the myotubes. Additional work done by members of the group (data not part of this thesis) using lactate dehydrogenase (LDH) assay on culture medium of LDL-ceramide treated myotubes also ruled out cell toxicity effects and contamination of LPS in the LDL-ceramide preparation.

The liver works in conjunction with skeletal muscle to maintain glucose homeostasis. While skeletal muscle and adipose tissue take up glucose during insulin stimulation, the liver suppresses glucose release. The end point of insulin action in hepatocytes is the suppression of glucose release when challenged with insulin. As such, a functional assay examining glucose output in insulin stimulated primary murine hepatocytes was used as the main read-out to examine LDL-ceramide role in inducing hepatic insulin resistance.

Hepatocytes treated with LDL-ceramide maintained their insulin sensitivity, a result that agrees with previous reports that show mice with elevated hepatic ceramide content do not develop hepatic insulin resistance^{242, 243}. The liver itself does not exhibit full, but instead incomplete, insulin resistance. Proof exists which shows that while the liver may undergo impaired suppression of gluconeogenesis (glucose production), lipogenesis may not necessary be affected²⁴⁴. Gluconeogenesis and lipogenesis work together to bring about the sum of insulin resistance in the liver.

While the majority of glucose is cleared by skeletal muscle during insulin stimulation, approximately 10% is cleared by adipose tissue⁴⁰. Differentiated 3T3 L1 adipocytes

were used to assess whether LDL-ceramide was able to induce insulin resistance in adipocytes. There was no reduction in insulin stimulated glucose uptake in 3T3 L1 adipocytes treated with LDL-ceramide. These results contrast with studies which utilize cell permeable short chain ceramides, that show decreased insulin stimulated glucose uptake in 3T3 L1 adipocytes²⁴⁵. It is possible that the metabolic properties of short chain ceramide and natural long chain ceramide are different. This may indeed be the case, as short chain C2-ceramide deacylate much slowly compared to its long chain counterparts²⁴⁶ thus possessing a more direct effect compared to long chain natural ceramides that may be involved in metabolism to other sphingolipids forms such as sphingosine or sphingosine 1-phosphate^{246, 247}.

Ceramide induced insulin resistance is most commonly investigated via intracellular ceramide accumulation due to an endogenous synthesis event (i.e *de novo* ceramide synthesis), rather than an external source of ceramide (i.e plasma ceramide) as a cause of insulin desensitization. Various studies which adopt the former paradigm approach the topic by utilizing a nutrient overloaded model to drive substrate dependent ceramide synthesis before using inhibitors such as myriocin to block key enzymes of *de novo* ceramide synthesis such as SPT, to show that inhibition of intracellular ceramide accumulation improves insulin sensitivity^{7, 8, 62, 248}.

Reports arising from lipid infusion studies in rodents have provided evidence that insulin resistance can be invoked without any increase in tissue ceramide levels^{184, 249}. One possible explanation could be that nutrient overloading may not necessarily automatically translate into channelling of substrates towards the *de novo* pathway of ceramide synthesis but instead, they could be shunted into the creation of other lipid species which themselves are insulin desensitizing. In addition, a study demonstrated that long term suppression of SPT either pharmacologically or by short hairpin RNA-mediated silencing did not safeguard L6 myotubes against the insulin-desensitizing effects of palmitate⁶. These reports suggest that lipid-induced insulin resistance appears to have contingency routes, and is not solely reliant on endogenous intracellular *de novo* ceramide production. Perhaps then, in addition to intracellular ceramide accumulation, alternative routes for ceramide to cause insulin resistance may exist in the form of circulating ceramides.

There are reports of increased LDL (a native carrier of plasma ceramide) production in insulin resistant women without diabetes²⁵⁰. While it has been shown that LDL-ceramide can cause insulin resistance in *in vitro* cell culture models in this chapter, the true test of causality would be to show whether LDL-ceramide can induce the pathological state of insulin resistance in an animal model.

Infusion of lipid emulsions into rodents represents a commonly used *in vivo* approach to investigate the relationship between dyslipidemia and insulin resistance. While the components of these lipid emulsions may be known, it is difficult to dissect out individual lipid effects from the sum of total lipid effects in the emulsion. As such, infusion of the artificially created LDL-ceramide in this study into mice, would specifically mimic circulating ceramides *in vivo* and address the question whether LDL-ceramide is able to cause insulin resistance.

Studies report that insulin resistance in human patients takes approximately 2-4 h after acute elevation of plasma FFAs⁵⁶ to be invoked, as such, using this as a guideline, 4 h was chosen as the duration of the infusion of LDL-C24:0 ceramide into the mice.

The skeletal muscle of LDL-C24:0 ceramide infused mice showed a marked decrease in glucose uptake following insulin stimulation. Skeletal muscle accounts for the majority of total glucose disposal (75-90%) during an insulin stimulated event³⁹ and, given that LDL-C24:0 ceramide was able to induce insulin resistance in the skeletal muscle of mice, provides evidence that circulating ceramide is an agent of insulin resistance. This observation has not been previously shown in any *in vivo* model of insulin resistance.

No difference in glucose uptake levels were seen in the liver, white adipose (epididymal fat), brown adipose or heart of LDL-C24:0 ceramide infused animals was observed. This suggests that circulating ceramides do not have a pleiotropic insulin resistance inducing effect but is instead localized to specific tissues. Perhaps, tissues such as skeletal muscle which are main players of insulin stimulated glucose disposal are more susceptible to the insulin desensitizing effects of LDL-ceramide.

The absence of any insulin resistance effects in the liver and white adipose tissue of LDL-C24:0 ceramide infused mice bears similarity to the *in vitro* result where LDL-ceramide treatment was observed to have no effect in causing insulin resistance in mouse primary hepatocytes and 3T3-L1 adipocytes. It is possible that, since adipose tissue function as depots of lipids, they maybe innately more tolerant to insulin desensitizing by lipids.

In the case of liver, where LDL-ceramide appears to have no effect in inducing insulin resistance, proteins such as adipose differentiation-related protein (ADRP) and tail interacting protein of 47 kDa (Tip47) may possibly be conferring enhanced tolerance to ceramides by adding an additional layer of protection against the development of lipid induced insulin resistance in hepatic cells by re-packing lipids into smaller droplets, since studies utilizing combined knockdown of ADRP and Tip47, showed that the absence of these proteins resulted in insulin resistance and large lipid droplet formation²⁵¹.

Ceramides are known to activate proinflammatory serine/threonine signaling pathways that impede insulin signal transduction^{51, 252}. Among these pathways, activation of the MAP kinases (ERK1/2)²⁵³ and JNK are known to induce insulin resistance^{118, 254, 255}. LDL-ceramide did not affect JNK phosphorylation, although NF- κ B signaling and cytokine expression were increased in skeletal muscle *in vivo*. This pro-inflammatory effect is unlikely to result from direct LDL-ceramide action in skeletal muscle because there was no evidence of IKK/NF- κ B activation in cultured myotubes. Instead, the activation of NF- κ B signaling appears to be mediated by increased plasma cytokines produced by other tissues or, possibly, muscle-resident immune cells.

While these studies show that LDL-ceramide can cause insulin resistance in myotubes and in the skeletal muscle on lean, insulin sensitive mice *in vivo*, further studies showing that reducing ceramide in the blood improves insulin action in obese, insulin resistant mice would provide further support for this conclusion.

In summary, the work in this chapter provides evidence of the insulin desensitizing

effects of LDL-ceramide. LDL-ceramide induced insulin resistance via a reduction in AKT signaling as well as a concomitant decrease in Glut4 translocation in L6 Glut4-myc cells. The results presented here also provide insights into how ceramide accrual occurs in LDL-ceramide treated cells, that is, via a by a non-receptor mediated/*non-de novo* synthesis process, whereby ceramide is localized to the plasma membrane. Finally, infusion of LDL-ceramide into lean mice induced whole body and skeletal muscle insulin resistance and caused inflammation. Thus, this is the first study to show that LDL-ceramide cause insulin resistance in both *in vitro* and *in vivo* skeletal muscle systems. Whether intracellular ceramide accumulation is a pre-requisite for the insulin resistance and pro-inflammatory effects of the LDL-ceramide in myotubes remains a key unresolved issue and future studies would be required to address this.

CHAPTER 5

Inflammatory effects of LDL-Ceramide in macrophages

5.1 Introduction

Chronic inflammation is casually linked to obesity and T2DM¹ and studies have shown that white adipose tissue (WAT) in obese humans and mice contain increased numbers and activity of macrophages²⁵⁶⁻²⁵⁸. Pro-inflammatory cytokines secreted by activated macrophages such as TNF- α can trigger intracellular ceramide accumulation¹⁹. In addition, pro-inflammatory cytokines secreted by activated macrophages are known to directly induce insulin resistance both in skeletal muscle and liver by antagonizing insulin signal transduction²⁵⁹. As such, activated macrophages display a two-pronged mechanism of eliciting insulin resistance, by increasing ceramide and increasing pro-inflammatory serine/threonine signalling.

Toll-like receptors (TLR) are a family of pattern recognition receptors, which serve as the canonical sensors of macrophages to detect and mount inflammatory responses against pathogens. While these receptors are most commonly found in macrophages, they are also expressed and are upregulated in skeletal muscle cells cultured from obese and insulin-resistant humans¹³⁹.

Recent studies have examined the links between TLR-mediated inflammation and lipid metabolism. Saturated fatty acids (SFAs) are known agonists of TLR4¹⁴⁰⁻¹⁴⁴ and TLR4 is required for lipid-induced insulin desensitisation in mice¹⁴⁰. TLR4 signalling induces expression of serine palmitoyl transferase (SPT) in a variety of tissues¹⁴⁵⁻¹⁴⁷, and activates sphingomyelinase, processes which increase ceramide content via *de novo* synthesis and hydrolysis of sphingomyelin¹⁴⁸ respectively.

In a very recent study, it has been demonstrated that TLR4 signalling is a requisite for intracellular ceramide accrual in the face of lipid oversupply⁷. Additional studies have also demonstrated that short-chain ceramide analogues can directly induce a TLR4 response¹⁹⁵, thus creating a positive feedback for intracellular ceramide accumulation. These observations provide evidence linking TLR signaling to ceramide accumulation and, in turn, inflammation to insulin resistance.

Plasma ceramides are positively associated with inflammation³⁰, however, the role of

circulating ceramide on macrophage inflammation is currently unknown.

In this chapter of the thesis the previously developed (chapter 3) LDL-ceramide preparation will be utilized to investigate the role of LDL-ceramide in eliciting pro-inflammatory responses in macrophages, as well as examining whether LDL-ceramide activated macrophages secrete pro-inflammatory factors which cause insulin resistance in insulin sensitive cell types, such as skeletal muscle cells.

5.2 Aims

To determine whether LDL-ceramide elicits a pro-inflammatory response in macrophages and to examine whether the secretory products of LDL-ceramide treated macrophages causes insulin resistance in skeletal muscle cells.

5.3 Materials and methods

The following section describes materials and methods used for chapter 5. Additional or variation of material and methods used in other chapters will be contained within their respective sections. All treatments with LDL-ceramide (C24:0 ceramide and C16:0 ceramide) used in this chapter were adjusted to a final working concentration of 2 μ M ceramide for all experiments unless otherwise stated.

5.3.1 Cell culture

All cells were propagated in a humidified Thermo™ Hera cell 150 incubator (Asheville, NC, U.S.A.) at 37°C and 10% carbon dioxide (CO₂). Cell culture medium was replaced daily for all cell lines unless otherwise stated. Prior to medium replacement, cells were rinsed twice with PBS +. All cells were grown on sterile non-coated tissue culture grade dishes or multi-well plates. Cells were passaged at not more than 75% confluence and were dislodge in PBS – only with a cell scraper before seeding at desired densities. All macrophage cell line used in this chapter were grown in DMEM + GlutaMax™, 1 g/l D-glucose, 110 mg/L Na pyruvate, containing 10% fetal calf serum (Gibco™, Invitrogen, Australian sourced) and 100 U/ml penicillin, 100 ng/ml streptomycin (Invitrogen).

5.3.1.1 Raw 264.7 macrophage cell culture

The RAW 264.7 cells are an abelson leukemia virus transformed immortalised macrophage cell line derived from BALB/c mice²⁶⁰. The Raw 264.7 cells have receptors for immunoglobulin and produce lysozyme, and are one of the most commonly used macrophage cell lines used in inflammation and immunology studies throughout the literature. Culturing conditions for the Raw 264.7 cells are described in section 5.3.1

5.3.1.2 MyD88^{-/-} / TRIF^{-/-} macrophage cell culture

Cells were a kind gift from Dr Ashley Mansell (Centre for Innate Immunity & Infectious Disease, Monash Institute for Medical Research). This immortalised cell line was generated using the J2 retrovirus by Eicke Latz from bone marrow derived macrophages originating from C57BL/6 mice double deficient in MyD88 and TRIF, bred from matings of MyD88-deficient (MyD88^{-/-}) mice and TRIF-deficient (Ticam^{-/-}) mice. This double knockout (DKO) Myd88/TRIF macrophage cell line is a useful model to assess the role of toll-like receptors in inflammatory responses, as these two adaptor proteins encompass all possible combination of TLR based signalling downstream and thereby exhibit no TLR signaling. Culturing conditions for the Myd88/TRIF DKO macrophage are described in section 5.3.1

5.3.2 Isolation of mRNA

Cells cultured on 6 well dishes were lysed in 1mL QIAzol (QIAGEN, California, USA) per well and transferred into RNase-free 1.5 mL tubes. 600 µl of chloroform was added and the tubes were vigorously shaken for 15sec, then incubated at room temperature for 5 min. The tubes were centrifuged at 12,000 rpm for 15 min at 4°C. The clear upper phase supernatant was placed in a new tube and 600 µl isopropanol was added and the tube left to incubate for 10min at RT. The sample was then vortexed and centrifuged at 12,000 rpm for 10 min at 4°C. Following this a white RNA pellet could be visualized. The isopropanol was aspirated away and 1mL of 75% ethanol was added to the RNA pellet and vortexed. This was then centrifuged at 7,500 rpm for 5min at 4°C and the ethanol was removed and the RNA pellet air-dried. Finally, the pellet was resuspended in RNase free treated water and the mRNA concentration determined by the absorbance of the sample at 260 nm on a biophotometer machine (Eppendorf, Hamburg, Germany). A ratio of the absorbance

at 260 nm/280 nm between 1.8 and 2.0 was used as the cut off for acceptable purity of the extracted RNA.

5.3.3 cDNA synthesis

Extracted RNA was reverse transcribed to cDNA using the Thermoscript RT-PCR kit (Invitrogen). 2 µg of mRNA was diluted with H₂O to 9 µl and to this 1 µl of random hexamers and 2 µl of 10 mM dNTP mix were added. This was incubated at 65°C for 5 min. 40 U of RNase Out, 15 U of Thermoscript Gold and 1 µl of 0.1 M DTT in cDNA synthesis buffer were added to a final volume of 20 µl and this was heated at 25°C for 5 min, 50°C for 50 min to facilitate reverse transcription then 85°C for 5 min to terminate the reaction.

5.3.4 Quantitative real time polymerase chain reaction (qRT-PCR)

qRT-PCR reactions were undertaken to assess the levels of mRNA expression of specific genes. These data were used to compare expression of certain genes between control and treatment groups. The level of a housekeeping gene, ribosomal 18S, was used as an internal control to correct for differences in cDNA loading.

qRT-PCR was conducted using the AmpliTaq Gold with GeneAmp kit (Roche, Basel, Switzerland). 100 ng of cDNA was added to 200 µM deoxyribonucleotide triphosphate (dNTPs), 0.5 U Taq, 3mM MgCl₂ and 0.5 µl of the relevant primer in a final volume of 20 µl per well (96 well PCR plate, Eppendorf, Hamburg, Germany). Primers used were purchased as a commercially produced primer kit (Applied Biosystems, 26 2. Methods California, USA). The PCR running conditions were: an initial cycle of 50°C for 2 minutes to equilibrate our reaction mixtures, 95°C for 10 minutes to heat activate the polymerase enzyme, then 40 cycles of 95°C for 15 seconds, to denature our DNA template into single stranded DNA, and 60°C for 1 min to allow annealing of our primers and elongation of our target gene of interest. The relative quantities of each transcript were calculated using the comparative critical threshold ($\Delta\Delta C_t$) method

5.3.5 Enzyme-linked immunosorbent assay (ELISA)

ELISAs were performed to determine cytokine concentrations released into the medium by macrophages. Assays were performed as per instructions accompanying the IL-6 and TNF α ELISA kits (R&D Systems). Briefly, 50 μ l of assay diluent and 50 μ l of assay standard or sample was added to each well, gently mixed by tapping and incubated for 2 h at RT. This was aspirated and the wells washed 5 times before 100 μ l of assay conjugate was added to each well and the plate again incubated for 2 h at RT. Again this mixture was aspirated and the wells washed 5 times before 100 μ l of substrate solution was added to each well and incubated for 30 min at RT protected from light. Following the addition of 100 μ l stop solution absorbance was read at 450 nm on a SpectraMax Plus 384TM spectrophotometer to determine the concentration of cytokines in the medium.

5.3.6 Bicinchoninic acid (BCA) protein assay.

BCA protein assay was performed as described in section 3.3.4. to quantify total protein amount, so that a known amount can be loaded during in Western blotting.

5.3.7 Western blotting

Western blotting was performed as per section 3.3.5, with the following changes in this chapter; acrylamide gels were made to 10% concentrations and the wet-dry transfer was performed for 90 min. All primary antibodies used in this chapter were purchased from Cell Signalling (Cell Signaling Technology) and used at 1:1000 dilution in TBST containing 5% BSA. Primary antibodies used in this chapter are phospho-SAPK/JNK (Thr183/Tyr185) rabbit mAb and I κ B α rabbit mAB. The secondary antibody used was anti-rabbit IgG, peroxidase-linked species-specific F(ab')₂ fragment (GE Healthcare-Amersham, Buckinghamshire, UK.) diluted 1:4000 in block buffer.

5.3.8 Mass spectrometry analysis

Mass spectrometry analysis of ceramide accrual in Raw264.7 macrophages following treatment of LDL-ceramide was performed as per section 4.3.5.

5.4 Results

5.4.1 LDL-ceramide treatment upregulate M1 inflammatory genes and downregulate M2 anti-inflammatory genes in RAW 264.7 macrophages.

RAW 264.7 macrophage were treated with LDL or LDL-ceramide for 24 h then RNA was extracted and reverse transcribed. Following which, qRT-PCR was used to measure the expression of several M1 inflammatory transcripts such as TNF- α , MCP-1, IL-6 and the M2 anti-inflammatory gene IL-10. The expression of several classically activated M1 inflammatory genes, such as TNF- α and MCP-1 were increase by LDL-ceramide, and IL-6 tended (1.5-2 fold, P=0.12) to increase (Fig 5-1). The expression of M2 anti-inflammatory gene IL-10 was decreased by LDL-ceramide (Fig 5-1)

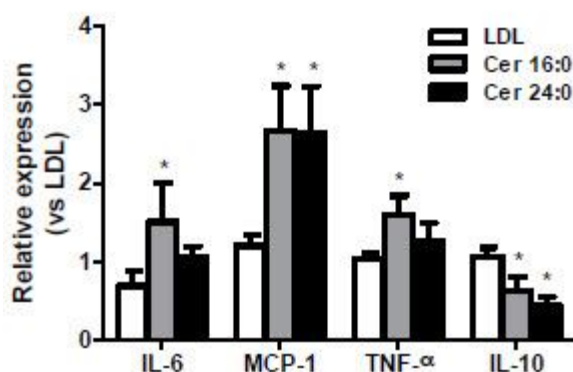


Fig 5-1 LDL-ceramide upregulates M1 inflammatory genes and downregulate M2 anti-inflammatory genes. Cells were treated with LDL or LDL-ceramide for 24 h. RNA was extracted, reverse transcribed and assessed by qRT-PCR. All data was normalized to 18S (n=9 per group, *P<0.05 vs. LDL by Student's t-test). Figure depict Mean \pm S.E.M.

5.4.2 Western analysis of TNF- α protein in RAW 264.7 cells follows LDL-ceramide treatment.

To confirm TNF- α transcript is translated to protein, western analysis of RAW 264.7 cells was performed. The precursor form of TNF- α (25kDa) is detectable at 4 h following LDL-ceramide treatment in RAW 264.7 macrophages and is less potent than palmitate in eliciting a TNF- α response. The precursor TNF- α is most strongly

detected at 8 h treatment. The mature form of TNF- α (17kDa) was only barely detectable after 8 h treatment. TNF- α , once processed into the mature form by the enzyme tumor necrosis factor- α -converting enzyme (TACE) from its precursor, is released from the cell to its external environment²⁶¹. Hence, this might explain why using intracellular protein lysates yielded poor detection, since the majority of TNF- α mature form is likely to be released into cell culture medium²⁶².

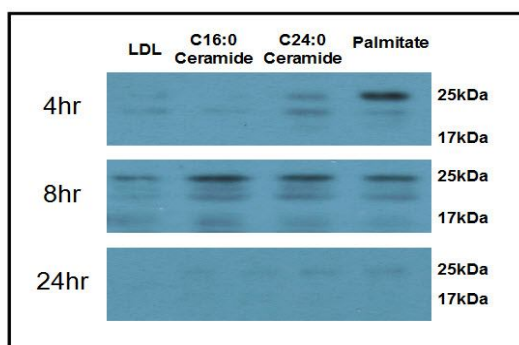


Fig 5-2 Western blot analysis of TNF- α in RAW 264.7 macrophage treated with LDL-ceramide for 4 h, 8 h, 24 h. 25 kDa is the precursor form of TNF- α while 17 kDa is the mature form. In LDL-ceramide treated macrophages, the precursor form is detectable most strongly at 8 h treatment, while the mature form of TNF- α is barely detectable at 8 h with western blot analysis. 0.75mM palmitate was used as positive control.

5.4.3 ELISA analysis of secreted inflammatory cytokines in LDL-ceramide stimulated RAW 264.7 cell culture medium.

To determine whether inflammatory cytokines are secreted into the medium of LDL-ceramide treated RAW 264.7 macrophages. Cells were treated with LDL or LDL-ceramide for 24 h, washed and the culture medium was replaced with fresh medium containing no LDL-ceramide. This ceramide free medium was then collected after 24 h, following which TNF- α and IL-6 were analysed by ELISA. The addition of LDL-ceramide increases the secretion of TNF- α and IL-6 into the culture medium (Fig 5-3).

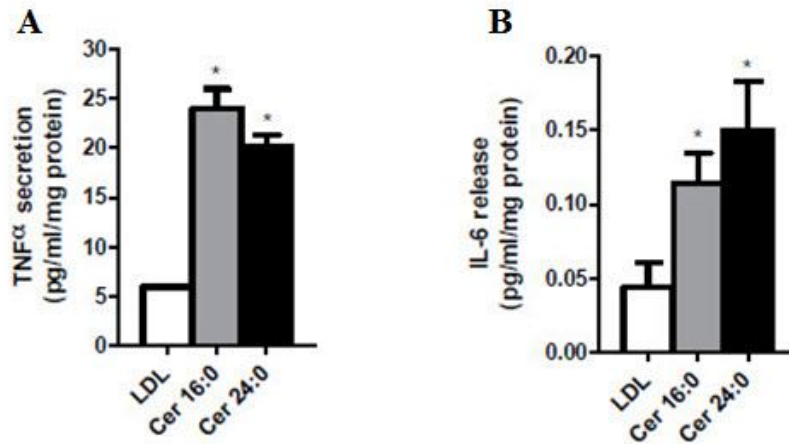


Fig 5-3. RAW 264.7 macrophage increase TNF- α and IL-6 secretion into culture medium following 24 h LDL-ceramide treatment. ($n=9$ per group, $*P<0.05$ vs. LDL by Student's t -test).

5.4.4 LDL-ceramide induces JNK activation in a time dependent manner in RAW 264.7 macrophages

To determine whether LDL-ceramide can activate JNK in RAW 264.7 macrophages, cells were treated with 2 μ M LDL-ceramide at 0.5 h, 2 h, 4 h, 8 h, and 24 h time intervals after which protein lysates were collected and examined for pJNK via Western blotting analysis. Densitometry was used to arbitrarily quantify the amount of pJNK detected.

pJNK protein expression was strongly expressed in RAW 264.7 macrophages within 0.5 h treatment with palmitate and LPS treatment and the increase was significantly increased for up to 8 h (Fig 5-4). While pJNK could be detected faintly following 0.5 h treatment with LDL-ceramide, a significant increase in pJNK could only be detected after 4 h of treatment (Fig 5-4). The time course of these effects suggest that the pro-inflammatory actions of LDL-ceramide are unlikely to be mediated via ligand activation of the toll-like receptors (which occurs in minutes), rather via the uptake and/or metabolism of LDL-ceramide.

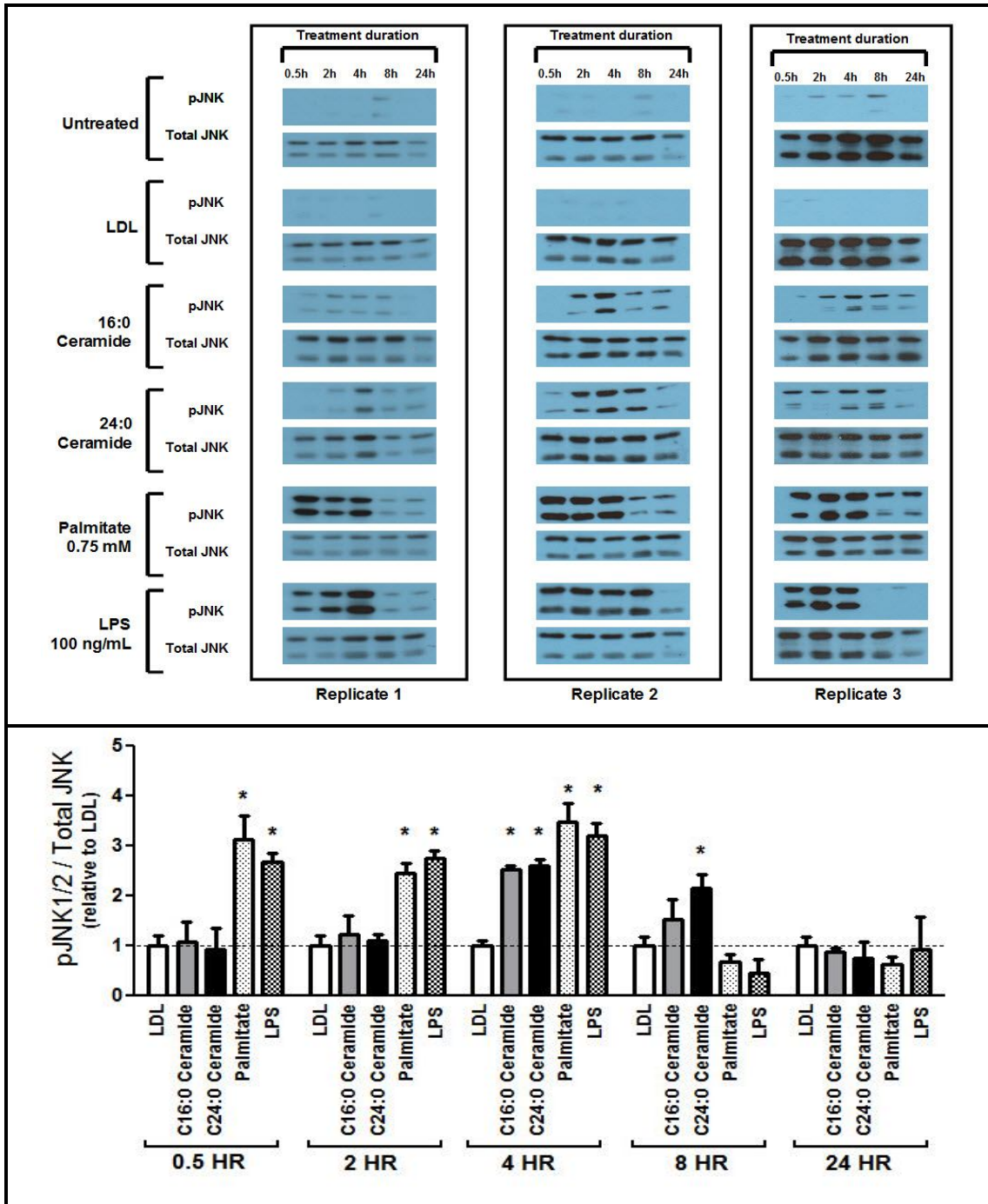
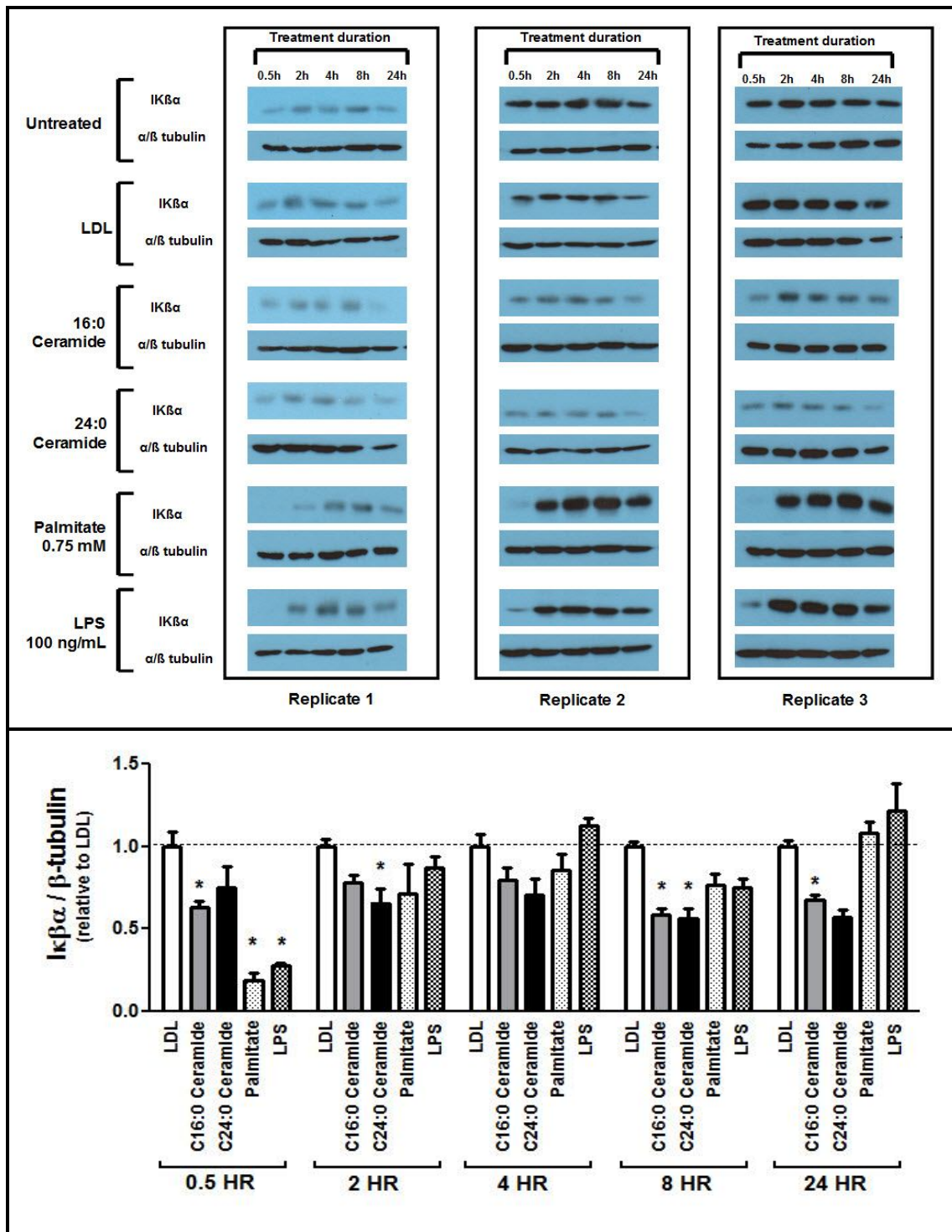


Fig 5-4. LDL-ceramide induces JNK activation in RAW 264.7 macrophage in a time dependent manner. Representative immunoblots above, Densitometry analysis below. ($n=3$ per group, $*P<0.05$ vs. LDL by Student's t -test). Figures depict mean \pm S.E.M.

5.4.5 LDL-ceramide reduces IκBα levels in RAW 264.7 macrophage in a sustained manner.

Given the difficulties with antibodies in detecting NF-κB activation directly via Western blotting, IκBα protein levels were used as an alternative method to measure NF-κB activation. When IκBα is bound to NF-κB it blocks nuclear localization, rendering it inactive in cytoplasm and unable to translocate to the nucleus²⁶³. Reduced IκBα protein levels detected in Western blotting would indicate more active NF-κB, since the repressor of NF-κB had been diminished.

The same series of experiments described in section 5.4.4 was repeated but IκBα was probed instead. There was a sharp and acute decrease in IκBα at 0.5 h when RAW 264.7 macrophages were treated with palmitate and LPS treatment. While there was a decrease in IκBα at 0.5 h with LDL-ceramide treatment, the effect was not as acute as that evoked by palmitate or LPS. The reduced levels of IκBα following LDL-ceramide treatment was sustained even up to 24 h, which when compared with palmitate and LPS, had returned to levels similar to LDL controls at a faster pace (Fig 5-5).



*Fig 5-5. LDL-ceramide reduces IκBα levels in RAW 264.7 macrophage in a sustained but less acute manner compared to palmitate and LPS treatment. Representative immunoblots above, Densitometry analysis below. (n=3 per group, *P<0.05 vs. LDL by Student's t-test). Figures depicts mean ± S.E.M.*

5.4.6. LDL-ceramide treatment induces intracellular ceramide accrual in RAW

264.7 macrophages

To examine whether LDL-ceramide is taken up by macrophage to exert its pro-inflammatory effects, RAW 264.7 macrophages were incubated with LDL-C16:0 ceramide or LDL-C24:0 ceramide for 24 h, after which the cells were lysed and intracellular ceramide species content analysed via mass-spectrometry. RAW 264.7 macrophages incubated with LDL-ceramide showed an increase in intracellular content of only the ceramide species that was used for treatment. Treatment with LDL-C16:0 ceramide resulted in intracellular C16:0 ceramide increase and LDL-C24:0 ceramide treated cells increased intracellular C24:0 ceramide content (Fig 5-6). There were no other increases in other ceramide species.

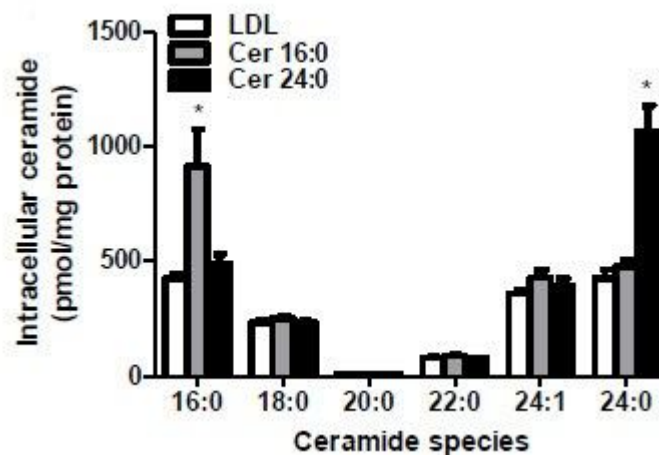


Fig 5-6. RAW 264.7 macrophage treated for 24 h with LDL-ceramide leads to increase in intracellular ceramide of the corresponding ceramide sub-species. Mass spectrometry analysis of intracellular ceramide content in lysates of treated cells. ($n=6$ per group, $*P<0.05$ vs. LDL by Student's t -test) Figures depicts mean \pm S.E.M.

5.4.7 LDL-ceramide induces JNK activation in a time dependent manner in macrophages deficient in MyD88 (*MyD88*^{-/-}) and TRIF (*Ticam*^{-/-})

To examine whether TLR signalling mediated the ceramide-induced inflammatory responses, macrophages deficient in MyD88 (*MyD88*^{-/-}) and TRIF (*Ticam*^{-/-}) which prevents propagation of all TLR signalling were used.

The same series of experiments described in section 5.4.4 was repeated but Myd88/TRIF DKO macrophages were used instead. pJNK could not be detected when Myd88/TRIF DKO macrophages were treated with LPS, which was expected, as LPS induced pJNK activation is dependent on TLR. This contrasted with LDL-ceramide treated cells which were able to robustly activate JNK after 2 h and continued to build up pJNK levels for 24 h (Fig 5-7). Since, JNK phosphorylation was increased by LDL-ceramide and not LPS, the result suggests that TLR signalling is not required but possibly the uptake/metabolism process of ceramide is used to activate JNK signaling instead.

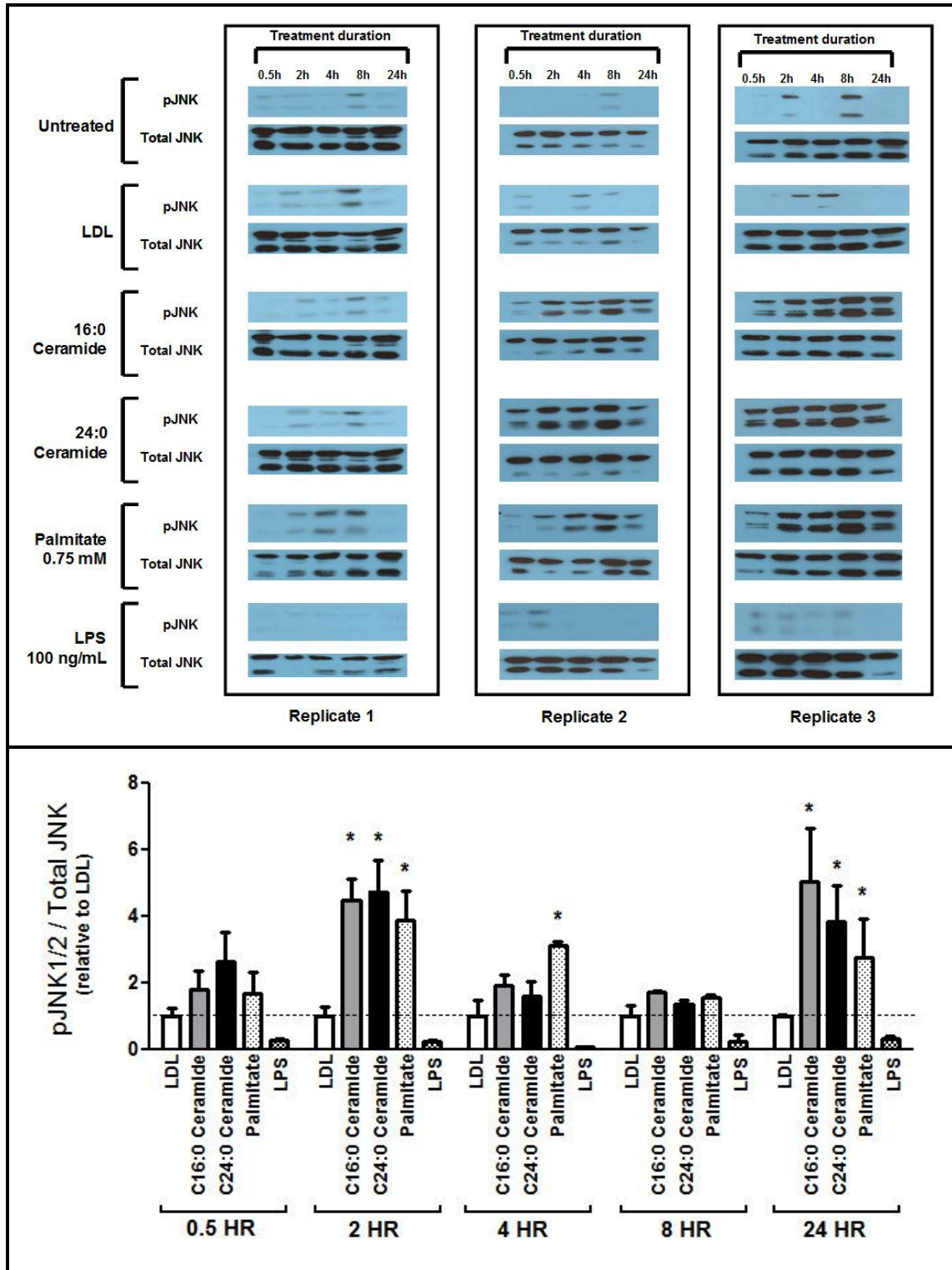


Fig 5-7. LDL-ceramide is able to activate JNK in MYD88/TRIF double knockout macrophages. Representative immunoblots above, densitometry analysis below. ($n=3$ per group, $*P<0.05$ vs. LDL by Student's t -test). Figures depict mean \pm S.E.M.

5.4.8 *LDL-ceramide does not reduce IκBα in macrophages deficient in MyD88 (MyD88^{-/-}) and TRIF (Ticam^{-/-})*

The same series of experiments described in section 5.4.4 was repeated but Myd88/TRIF DKO macrophages were used and IκBα probed. IκBα levels were not reduced in Myd88/TRIF DKO macrophages treated with LDL-ceramide at any of the time points tested. In addition, there was also no effect by palmitate or LPS in reducing IκBα (Fig. 5-8). In contrast RAW 264.7 macrophages which have an intact TLR signalling apparatus, showed a reduction in IκBα levels when treated with LDL-ceramide, palmitate or LPS (Fig. 5-5). Since IκBα degradation was not affected by LPS or LDL-ceramide in these Myd88/TRIF DKO macrophages, it suggests a dependency of TLR signaling for LDL-ceramide effects on NF-κB signaling.

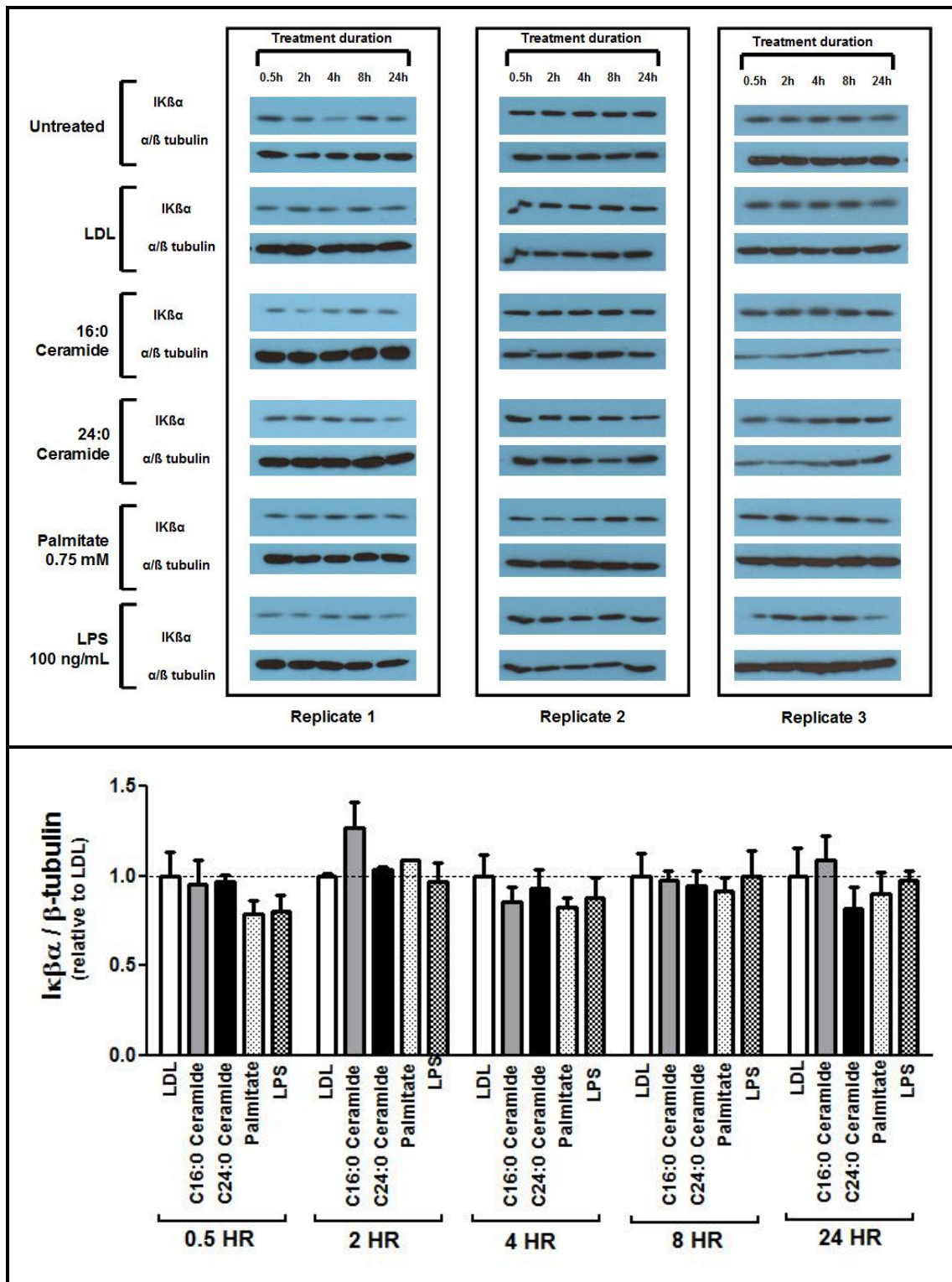


Fig 5-8. LDL-ceramide does not reduce $I\kappa\beta\alpha$ levels in MYD88/TRIF double knockout macrophages. Representative immunoblots above, densitometry analysis below. ($n=3$ per group, $*P<0.05$ vs. LDL by Student's t -test). Figures depict mean \pm S.E.M.

5.4.9 *LDL-ceramide activated RAW 264.7 macrophage conditioned medium reduce insulin stimulated glucose uptake in L6 Glut4-myc myotubes.*

Having established that LDL-ceramide causes macrophages to adopt a pro-inflammatory secretory profile, medium conditioned by LDL-ceramide activated RAW 264.7 macrophage was examined for the potential to desensitize the effects of insulin action in L6 Glut4-myc myotubes.

RAW 264.7 macrophages were treated for 24 h with LDL-ceramide, following which LDL-ceramide medium was removed and cells rinsed thoroughly with PBS before ceramide-free medium was added to the cells. After 24 h this medium (conditioned medium) was collected and filtered to remove residual cells and used to treat L6 glut4-myc myotubes and insulin responsiveness was evaluated by insulin stimulated glucose uptake assay. 1:2 dilution of the conditioned medium and 6 h treatment was chosen as the parameters to treat L6 Glut4-myc myotubes, as using undiluted condition medium for 6 h or 1:2 diluted conditioned medium for 24 h was toxic to the myotubes and resulted in cell death as evident by severe shrivelling and peeling of myotubes from culture plates. LDL-ceramide activated macrophage condition medium was able to reduce insulin stimulated glucose uptake in the myotubes (Fig 5-9). This indicates that LDL-ceramide can also induce insulin resistance in skeletal muscle indirectly by activating macrophages.

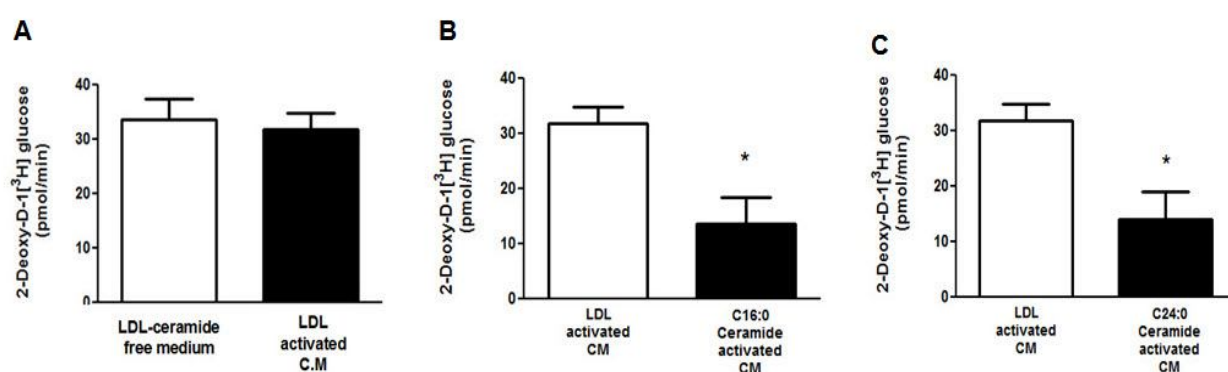


Fig 5.9. *Conditioned medium from LDL-ceramide activated RAW 264.7 cells reduces insulin stimulated glucose uptake in L6 Glut4-myc myotubes.*(A) *LDL activated RAW 264.7 condition medium, (B) LDL-C16:0 ceramide activated RAW 264.7 condition medium, (C) LDL-C24:0 ceramide activated RAW 264.7 condition medium. (n=6 per group, *P<0.05 vs. LDL by Student's t-test). Figure depicts mean ± S.E.M.*

5.5 Discussion

It is widely accepted that macrophage secrete inflammatory cytokines²⁶⁴ that activate serine/threonine kinases such as IKK β , JNK1/2 and ERK1/2 that antagonize insulin signalling transduction via the PI3K-AKT axis^{254, 265, 266}.

Several lines of evidence for a role of activated macrophages in the development of inflammation-induced insulin resistance exist. Among these include; depletion of CD11c⁺ activated macrophages reduces adipose tissue inflammation and improves insulin action in mice²⁶⁷, mice without CC-chemokine receptor 2 (CCR2) which is required for infiltration of inflammatory macrophages into tissues, are protected against obesity-induced inflammation and insulin resistance²⁶⁸, inflammation and insulin resistance worsens with the lack of GPR120, a G protein-coupled receptor which mediates the anti-inflammatory effects of omega 3 unsaturated fatty acids²⁶⁹, reduction of pro-inflammatory IKK β in myeloid cells²⁷⁰ and grafting of JNK-deficient bone marrow into mice, reduces inflammation mediated by myeloid cells and preserves insulin sensitivity²⁷¹.

Macrophage infiltration has been reported in pancreatic islets²⁷² and livers^{273, 274} of insulin resistant subjects, as well as in adipose tissue^{257, 275, 276} and skeletal muscle^{277, 278} of obese humans and animals. However, the extent of the contribution by individual tissue with regards to whole body insulin resistance during an inflammatory state is relatively unknown. While it is convenient to associate infiltrating macrophages as the main source of inflammation induced insulin resistance in skeletal muscle^{252, 279, 280}, one should also entertain the possibility that circulating lipids may activate macrophages located at distal sites to trigger the release of inflammatory cytokines into plasma, which are subsequently transported in the systemic circulation to elicit an effect.

Indeed, there are studies to support this possibility. Free fatty acids (FFA) themselves can induce an inflammatory response in macrophages located in adipose tissue via interaction with TLR2 and TLR4, which otherwise are more commonly known for their role in innate immune responses^{278, 281-283}. Additionally, *in vitro* studies involving RAW 264.7 macrophages and bone marrow-derived macrophages show

that fatty acids can result in the release of inflammatory cytokines²⁷⁸. There are also studies demonstrating that conditioned medium from fatty acid activated bone marrow macrophages reduced insulin stimulated glucose uptake in skeletal muscle cells^{252, 279}. It is highly suggestive from these reports that circulating lipids may interact with macrophages to invoke secretion of factors that induce insulin resistance. One possible candidate is ceramide.

Ceramides and inflammation are inextricably linked. On the one hand, ceramide is a molecular intermediate for conveying various inflammatory events. For example: A). Intracellular ceramide is increased by TNF- α via *de novo* synthesis or sphingomyelin hydrolysis and IL-1 is a potent inducer of ceramide²⁵². B) Activation of the innate immune receptor, TLR4, increases SPT transcription and activity, ceramide synthesis and plasma lipoprotein ceramide levels^{145, 147}. C) Many of the cytokines produced by TLR4 also promote ceramide synthesis (e.g. TNF- α), thereby invoking multiple ceramide producing stimuli.

On the other hand, ceramides themselves induce the production of inflammatory factors. In particular, the I κ B β -NF- κ B inflammatory axis is a known mediator of this interaction. Ceramide has been documented to cause NF- κ B activation^{284, 285}. TNF α , IL-6, IL-1 β and MCP-1 are also controlled by NF- κ B and blocking ceramide synthesis or inhibiting NF- κ B reduces TNF α and IL-6 production^{286, 287}, although others suggest that ceramide does not induce cytokine synthesis⁷.

TNF- α and IL-6 plasma levels have been correlated with insulin resistance^{288, 289} and one study which showed a strong correlation between serum IL-6 levels and plasma ceramide, also had a borderline significant correlation ($r=0.33$, $p=0.066$) between plasma ceramide and HOMA-IR²⁹⁰. In addition, ceramide concentrations also explained 35% of the variance of circulating IL-6 levels in that same study. There are also reports that provide evidence correlating plasma TNF- α concentration and circulating ceramide sub-species in adults with T2DM³⁰.

Given the evidence supporting an association between circulating ceramides, plasma pro-inflammatory cytokines and insulin resistance, it is logical to investigate whether circulating ceramides have a role in eliciting a pro-inflammatory response in

macrophages that causes insulin resistance. In this chapter, using the LDL-ceramide preparation from Chapter 3, LDL-ceramide was investigated whether it invokes a pro-inflammation in macrophages.

LDL-ceramide treatment was found to upregulate pro-inflammatory cytokine and chemokine gene expression such as TNF- α , MCP-1, IL-6 and down-regulate expression of the anti-inflammatory cytokine IL-10 in RAW 264.7 macrophages. MCP-1 (also known as CCL2) is a T-cell chemo-attractant that is required for macrophage cell infiltration²⁹¹⁻²⁹³, while IL-10 is an anti-inflammatory cytokine that is able to down regulate pro-inflammatory cytokine production²⁹⁴⁻²⁹⁶.

In addition to upregulation of inflammatory genes, by treating RAW 264.7 macrophages with LDL-ceramide, also resulted in accelerated secretion of pro-inflammatory TNF- α & IL-6 into culture medium. TNF- α inhibits insulin signalling transduction via JNK activation, which increases phosphorylation of serine 307 residues on IRS-1 and results in a suppressive effect on insulin signal propagation^{118, 254, 297, 298}. However, the mechanism behind IL-6 induced insulin resistance appears to be different from TNF- α ²⁹⁹. It has been suggested that one of the mechanisms behind IL-6 induced insulin resistance is the induction of SOCS-3, which reduces IRS-1 phosphorylation and, as a result, down regulation of PI-3K activation³⁰⁰. There is also some evidence that this mechanism increases ubiquitination and degradation of IRS molecules which are required for insulin signal transduction³⁰¹.

There appears to be conflicting reports regarding the inflammatory effects caused by ceramides. Some groups report ceramide being able to activate JNK and ERK^{302, 303}, while others showed that ceramides do not activate MAP kinases in macrophages or play a role in activating the inflammatory NF- κ B pathway given that ceramide did not affect I κ B α degradation³⁰⁴. One commonality of these studies is the use of short-chain water soluble ceramides.

Using pJNK levels as an indicator for MAPK activity and I κ B α for NF- κ B activation, it was found that LDL-ceramide increases JNK and NF- κ B signaling in a time dependent manner. These *in vitro* observations are consistent with increased cytokine production in mice infused with LDL-ceramide in chapter 4. Thus, increases in LDL-

ceramide can induce pro-inflammatory actions in macrophages and may contribute to a low-grade inflammation state.

Macrophages were analysed by mass-spectrometry after LDL-ceramide treatment to examine whether LDL-ceramides are taken up by the RAW 264.7 macrophages. Intracellular content of only the ceramide species that was used for treatment increased with no change in other ceramide species, indicating that the macrophages take up LDL-ceramides from the medium.

To examine whether TLR signalling is behind the mechanism of LDL-ceramide induced inflammation in macrophages, the double knockout (DKO) Myd88/TRIF macrophages cell line was used. Myd88 and TRIF encompass all possible combination of downstream TLR activation. Hence, the absence of these two TLR adaptor proteins would render TLR signal transduction inoperable. Myd88/TRIF DKO macrophages remained responsive to LDL-ceramide and continued to activate JNK. However, NF- κ B activation by LDL-ceramide in these macrophages was affected. This indicates that LDL-ceramide appears to mediate the pro-inflammatory response by different mechanisms: first, by activation of NF- κ B signaling that is dependent upon TLR signaling and second, activation of JNK signaling, which appears to be TLR-independent, is probably caused by the uptake and accumulation of ceramide as suggested by its time course effects. However, a limitation of the interpretability of the data was the appropriate wild type (WT) macrophage cells were not used alongside the Myd88/TRIF DKO macrophage as controls due to a variety of technical reasons.

Having established that LDL-ceramide is pro-inflammatory in macrophages as evident by upregulation of inflammatory genes, increased secretion of inflammatory cytokines in medium and activation of JNK and NF- κ B signaling, culture medium conditioned by LDL-ceramide activated macrophage was examined whether it reduces insulin stimulated glucose uptake in skeletal muscle cells. L6 Glut4-myc myotubes treated with LDL-ceramide activated macrophage conditioned medium reduced insulin stimulated glucose uptake. This provides proof of principal that LDL-ceramide can elicit insulin resistance via an indirect effect through activation of

macrophages which take on a secretory profile that causes insulin desensitization in skeletal myotubes.

In summary, this chapter showed that LDL-ceramides cause inflammation in macrophages and elicits a secretory profile that is insulin desensitizing in skeletal myotubes. LDL-ceramide upregulated inflammation associated genes (TNF- α , MCP-1, IL-6) and down-regulated an anti-inflammatory gene (IL-10), pro-inflammatory cytokine secretion (TNF- α and IL-6) is accelerated and JNK and NF- κ B signaling pathways are activated. In addition the mechanism behind LDL-ceramide induced inflammation was investigated using MyD88/TRIF DKO macrophage which revealed that LDL-ceramide appears to mediate inflammatory responses via different mechanism: First, a TLR dependent activation of NF- κ B signaling and second, by a TLR independent activation of JNK, possibly due to the uptake and accumulation of LDL-ceramide. Finally, as proof of principal that LDL-ceramide can indirectly cause insulin resistance in skeletal muscle by causing macrophages to adopt a secretory profile which is insulin desensitizing, it was shown that conditioned medium from LDL-ceramide activated macrophages decreased insulin stimulated glucose uptake in L6 Glut4-myc myotubes.

CHAPTER 6

General discussion

6. General discussion

Type 2 diabetes mellitus is characterized by deficient pancreatic beta islet cell function and insulin resistance due to impaired insulin sensitivity³⁰⁵. Both contribute to a diminished ability of the body to achieve euglycemia. Chronic exposure to high glucose levels beyond the normal physiological range causes damage at both the macro and micro vascular levels and leads to accelerated atherogenesis and reduced tissue perfusion, which translates to a higher risk of developing cardiovascular disease. In fact, patients with T2DM are four times more likely to develop cardiovascular morbidity³⁰⁶. The number of people with T2DM has reached epidemic proportions and continues to grow yearly and this places enormous strain on the socio-economic front of health-care systems trying to manage this disease due to its multiple associated complications³⁰⁷⁻³⁰⁹.

While a constellation of factors such as age, ethnicity, genetic factors, and lifestyle habits, such as overeating and sedentary behaviour, give rise to the development of T2DM³¹⁰⁻³¹⁵, the prevalent theories that seek to explain the mechanism behind insulin resistance of this disease are those of lipotoxicity and inflammation.

In the lipotoxicity theory of insulin de-sensitization, the view is that certain lipids are antagonistic to insulin signal transduction and over-exposure to them results in diminished insulin sensitivity. On the other hand, proponents of the inflammation theory of insulin resistance believe that the inflammatory cytokines produced by a hyper-activated immune system are mainly responsible for interfering with insulin signal transduction.

Given the multiple studies showing that insulin resistance can be caused by both lipotoxicity^{44, 45, 51} and inflammation^{254, 265, 266}, it is naïve to believe that insulin resistance stems from a single input. It is more than likely to be that these two theories are linked and complement each other to evoke this pathological state. One such provocateur of insulin resistance, which best encapsulates both these two theories, is the sphingolipid ceramide.

Myriad studies have reported on the insulin de-sensitizing effects of ceramide. Intracellular accrual of ceramide leads to insulin resistance²⁻⁶ and ceramides invoke inflammatory cytokines production which antagonises insulin signal transduction¹⁰⁻²⁷. While such studies highlight the insulin de-sensitizing effects of ceramide, several critiques on the methodology should be pointed out. Most of these *in vivo* studies do not directly show ceramide's ability to induce insulin resistance, but rather adopt an indirect approach, often utilizing a hyperlipidemic animal model to upregulate *de novo* ceramide synthesis and using inhibitors to show that inhibition of intracellular ceramide accumulation improves insulin sensitivity^{7, 8, 62, 248}.

While *in vitro* cell culture studies directly test ceramide causality as an agent of insulin resistance^{3, 9}, the criticism is that those studies use short chain ceramide analogues which are not entirely reflective of natural ceramides. Short chain ceramides do not exist naturally and are water-soluble compared with natural ceramides which are long chain and extremely hydrophobic. In addition, the metabolic properties of short-chain ceramides may well be different from those of natural long chain water ceramides, since short chain C2-ceramide deacylate much slower than their long chain counterparts²⁴⁶ thus, possibly having more direct effects. However, testing the direct effects of long chain ceramides is hampered by the fact that long chain ceramides are difficult to utilise within aqueous systems.

While intracellular ceramide accumulation is often used as a paradigm to explain ceramide induced insulin resistance, there are reports citing how insulin resistance can be invoked in rodents independent of ceramide content in tissue^{184, 249}. On the other hand, there are studies that show that elevated plasma ceramide levels are associated to insulin resistance³⁰. These contrasting reports suggest that perhaps, in addition to intracellular ceramide accrual, circulating ceramide may cause insulin resistance. To date, the biological relevance of plasma ceramides remain unknown. Are they directly implicated in the pathogenesis of insulin resistance or do they, via interactions with immune cells, trigger an inflammatory response to cause insulin desensitization? Therein, the purpose of the present studies was to establish the role of circulating ceramide in the development of insulin resistance and inflammation. A multi-level approach was used to address the aims of this study.

The initial component of this study (chapter 2 of this thesis) involved a human study examining plasma ceramide levels in insulin resistant T2DM patients and elucidation of the nature of water insoluble ceramide transport in plasma. Initially, little was known about plasma ceramide levels in human T2DM patients, however, while these studies were in progress, a report was published which showed elevated plasma ceramides levels in T2DM³⁰. Our work confirms these findings, however, this thesis addressed a question which was left unanswered by the published study, which was showing for the first time the lipoprotein-ceramide profile in human patients with T2DM.

The results in chapter 2 showed that ceramide levels are elevated in insulin resistant T2DM patients and is independent of BMI, plasma cholesterol, triacylglycerol and HDL levels. However, the link between plasma ceramides and insulin resistance remained associative, as the data did not explain whether plasma ceramides are a cause or an effect of the insulin resistant state.

To address whether LDL-ceramide is a cause of insulin resistance, a system of altering LDL-ceramide levels, independent of other factors, was required. Procuring a constant and reliable supply of native LDL-ceramide from patients is not feasible because of changes in other lipoprotein components (e.g. lipids, oxidised state) between individuals. Thus, to circumvent the logistical issues of LDL-ceramide procurement, the design and construction of a reconstituted LDL-ceramide preparation was conceptualized as a strategy to mimic the natural ceramide-lipoprotein system (chapter 3 of the thesis). While the protocol had several drawbacks, such as being laborious to execute and wasteful in terms of reagent usage, the procedure allows a controllable amount of long chain water insoluble ceramide to be reliably associated to LDL without structural disruption or interfering with the oxidation status of LDL and thus, providing a means of obtaining a limitless supply of LDL-ceramide.

Having successfully created a LDL-ceramide model; this biological tool was used as the backbone for the subsequent mechanistic studies in this thesis. The major aim of the thesis was to test the role of LDL-ceramide in the development of insulin

resistance and inflammation *in vitro*, using cell culture systems. Peripheral insulin resistance involves a defect of skeletal muscle glucose transport, as such, the main focus in chapter 4 was to examine the effect of LDL-ceramide on insulin sensitivity in skeletal muscle cells.

Ceramide inhibits insulin signaling by several independent mechanisms: by increasing PP2A activity³¹⁶ which decreases Akt phosphorylation and activity³¹⁷; by blocking the recruitment of Akt to the plasma membrane⁶³, which is required for activation by the upstream kinases PDK1 (at Akt Thr³⁰⁸) and TORC2 (at Akt Ser⁴⁷³); and by ceramide accumulating in caveolin enriched domains, binding and activating PKC ζ , which in turn sequesters Akt in a repressed state within these membrane domains and prevents insulin signaling⁹⁴. L6 Glut4-myc myotubes, upon LDL-ceramide treatment showed decreased insulin stimulated glucose uptake accompanied by a corresponding decrease in AKT activation. The precise signalling underpinning the reduced AKT phosphorylation requires further examination.

Aside from effects on signaling pathways, ceramide inhibits Rac-dependent remodelling of filamentous actin and Glut4 translocation, thereby decreasing insulin-mediated glucose uptake³¹⁸. In addition, ceramide forms microdomains in both fluid and gel state phosphatidylcholine membranes³¹⁹, and altering plasma membrane fluidity may attenuate Glut4 fusion to the plasma membrane³²⁰. The decrease in Glut4 translocation with LDL-ceramide treatment in L6 Glut4-myc myotubes is consistent with either of these possibilities.

Although evidence was provided in this study to directly implicate LDL-ceramide as a cause of insulin resistance *in vitro*, the “gold-standard” of showing causality is to replicate the pathological condition *in vivo* in an animal model. The reduction in insulin-stimulated glucose uptake in whole body and in skeletal muscle with LDL-ceramide administration *in vivo* was accompanied by ceramide accrual in the plasma membrane and reduced Akt phosphorylation.

While some scepticism persists, there is good evidence linking intracellular ceramide accumulation to insulin resistance, particularly in skeletal muscle²⁵². The controversy relating to the role of ceramide effects on insulin action may relate to the relatively

small changes in muscle ceramide in insulin resistant states²⁵², such as obesity and T2DM, and the likelihood that ceramide is enriched in specific cell regions, which would influence cell signalling with unappreciated specificity⁹⁴. For example, *Sptlc2* haplo insufficient mice have increased liver ceramide content, yet plasma membrane ceramides are reduced with concomitant improvements in hepatic insulin signaling³²¹.

In this study, no change in total muscle ceramide but enrichment of ceramide in the plasma membrane of skeletal muscle was detected. LDL can be transported into cells by receptor-mediated and receptor-independent processes; however, skeletal muscle takes up virtually no LDL by receptor-mediated processes¹⁷¹. In addition, receptor binding is not required for lipid soluble LDL associated products to be transferred to muscle cells (e.g. α -tocopherol)³²², suggestive of lipid-soluble exchange of products between the LDL and the muscle plasma membrane lipids. The study that shows that ceramide accumulates in myotubes with LDL-ceramide in the presence of a LDL receptor-neutralizing antibody supports this notion. Ceramide has limited transbilayer movement and stays tightly bound to the membrane³²³, so if ceramide is produced/obtained from the exoplasmic side (as is the case with LDL-ceramide), then ceramide would be more likely to act as a structural component of the PM rather than as second messenger/signaling molecule.

In addition to the direct effects of LDL-ceramide in inducing insulin resistance in skeletal muscle cells, the possibility that LDL-ceramide further exacerbates the insulin insensitive state via an indirect effect was examined from the angle of inflammation. Chapter 5 of this thesis investigated this by showing how LDL-ceramide, through interplay of inflammatory macrophage derived factors can induce insulin resistance. Depending on the nature of the stimulant, activated macrophages can secrete factors that may have a positive or negative influence on insulin sensitization in muscle cells³²⁴. Among the plethora of cytokines secreted by macrophages known to affect insulin regulated glucose homeostasis, TNF- α and IL-6, are two of the most prominent pro-inflammatory cytokines reported to induce insulin resistance and have been known to cause insulin de-sensitization in muscle, hepatic and adipose cells³²⁴⁻³²⁶. However, conflicting reports also exists which show that IL-6 can be protective against insulin de-sensitization³²⁷⁻³²⁹. Not all cytokines secreted by macrophages induce insulin resistance. IL-10 is one such cytokine secreted by

macrophage that exhibits anti-inflammatory properties, as it negates the insulin de-sensitizing effects of TNF- α ³²⁶.

LDL-ceramide stimulated upregulation of pro-inflammatory genes expression and accelerated inflammatory cytokine secretion in macrophages. In addition, JNK and NF- κ B signaling was increased in a time dependent manner. The observation that JNK and NF- κ B signaling activation by LDL-ceramide was less acute compared to LPS, prompted the question as to whether toll-like receptor (TLR) signalling which is the canonical sensing mechanism of macrophages, plays a role in LDL-ceramide induced inflammation.

To address this, a double knockout (DKO) Myd88/TRIF macrophage cell line was employed. Myd88 and TRIF are TLR adaptor proteins that are required to facilitate TLR signalling; thus, the deletion of these two TLR adaptor proteins disables all TLR signal transduction. It was found that TLR signaling in LDL-ceramide activated macrophages was not relevant to JNK activation, however, NF- κ B activation by LDL-ceramide via I κ B α required TLR signal propagation. These data supports the idea that multiple ligands, in addition to classical TLR ligands (i.e LPS) do exist which can elicit an immune response and that LDL-ceramide may be one such lipid that facilitates immune cell signalling by activating specific inflammatory pathways. The broader implications of this would be alternative therapeutic strategies can now be focused on limiting the inflammatory pathways triggered by LDL-ceramide and in doing so, improve insulin action.

Having established the pro-inflammatory effects of LDL-ceramide in macrophages, conditioned medium from LDL-ceramide activated macrophages was used to investigate whether LDL-ceramide could cause insulin resistance in skeletal muscle cells. Indeed, conditioned medium from LDL-ceramide activated macrophages dramatically reduced insulin stimulated glucose uptake in skeletal muscle cells. This result was similar to studies utilizing conditioned medium from fatty acid activated bone marrow macrophages which reduced insulin stimulated glucose uptake in skeletal muscle cells^{252, 279}. These observations show that circulating lipids can indirectly cause insulin resistance by triggering macrophages to adopt a secretory profile which is insulin de-sensitizing. In the case of LDL-ceramide activated

macrophage, a pro-inflammatory response is elicited which caused insulin resistance.

One area, which was not covered in this study, is the effect of LDL-ceramide on endothelial cells. Insulin has been documented to act through the PI3K-AKT/endothelial nitric oxide synthase pathway to cause dilation of arterioles to increase blood flow³³⁰⁻³³². This is physiologically important, as increasing capillary perfusion allows increased delivery of nutrients. In addition, there is enhanced recruitment of the so-called nutritive vascular beds within skeletal muscle and this enhances endothelial exchange surface area³³³⁻³³⁶. These vascular endothelial cells have been shown to be affected by insulin resistance³³⁷⁻³³⁹ and, since arterioles serve as the highways in which substances in plasma are transported, it would be interesting to investigate how endothelial cells are affected, given that they represent the “first point of contact” of circulating ceramides.

While this study shows that plasma ceramides are involved in insulin resistance, to use plasma ceramides as a clinical biomarker to predict T2DM is hampered on several fronts. An effective diagnostic tool must be cost-effective and the methodology quick to perform to allow up-scaling in clinical settings. The current method of determining plasma ceramide concentration is expensive, time consuming and requires considerable technical knowledge making it unsuitable for large scale clinical diagnostics. While this may be the case, the investigation of circulating ceramide is not without value.

Insulin resistance can be triggered by a multitude of molecular insults and to pin every novel agent as the first cause of the disorder is a simplistic way of examining its pathophysiology. However, that said, a continual effort is needed to build a robust catalogue of knowledge to understand the molecular mechanisms of the disease so as to enable future development of improved pharmacological concepts and better management of the disease, through risk stratification or identifying individuals who are pre-disposed to the disorder.

A major focus of the thesis is “how does insulin resistance occur in obesity?” This thesis, which shows that LDL-ceramides have the ability to invoke both the two major theories of lipotoxicity and inflammation, is a step forward in contributing to this field.

This work also fits and extends upon the theme that non LPS stimuli can also cause inflammation and supports the broad concept of multiple ligands acting on a classic immune responsive receptor to deliver an immune response. LDL-ceramides which comes from the liver also reinforces the idea that the liver may be an important driver of insulin resistance by releasing insulin de-sensitizing lipid-protein products. What this thesis achieved is to serve as a prospectus that clarifies the poorly investigated role of circulating ceramide in the development of insulin resistance and inflammation and show that circulating ceramides are part of the constellation of provocateurs that contribute to the pathophysiological of the disorder (Fig 6-1).

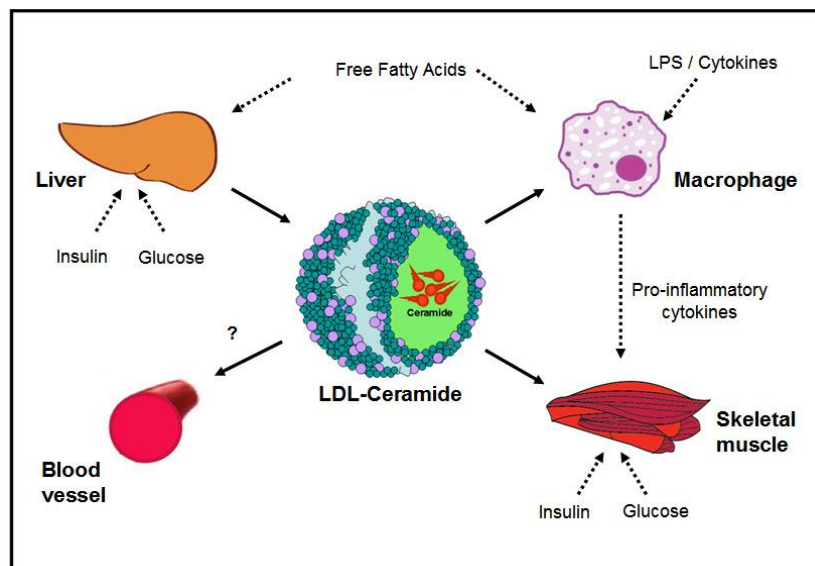


Fig. 6-1. General schematic of LDL-ceramide interaction with tissue. LDL-ceramide is produced in the liver and can elicit an inflammatory response in macrophage and induce insulin resistance in skeletal muscle. The effect of LDL-ceramide on blood vessels has yet to be elucidated.

REFERENCES

1. Hotamisligil GS. Inflammation and metabolic disorders. *Nature*. 2006; **444**(7121): 860-7.
2. Goodpaster BH, Kelley DE. Skeletal muscle triglyceride: marker or mediator of obesity-induced insulin resistance in type 2 diabetes mellitus? *Curr Diab Rep*. 2002; **2**(3): 216-22.
3. Hajdуч E, Balendran A, Batty IH, Litherland GJ, Blair AS, Downes CP, et al. Ceramide impairs the insulin-dependent membrane recruitment of protein kinase B leading to a loss in downstream signalling in L6 skeletal muscle cells. *Diabetologia*. 2001; **44**(2): 173-83.
4. Itani SI, Ruderman NB, Schmieder F, Boden G. Lipid-induced insulin resistance in human muscle is associated with changes in diacylglycerol, protein kinase C, and I κ B- α . *Diabetes*. 2002; **51**(7): 2005-11.
5. Virkamaki A, Korshennikova E, Seppala-Lindroos A, Vehkavaara S, Goto T, Halavaara J, et al. Intramyocellular lipid is associated with resistance to in vivo insulin actions on glucose uptake, antilipolysis, and early insulin signaling pathways in human skeletal muscle. *Diabetes*. 2001; **50**(10): 2337-43.
6. Watson ML, Coghlan M, Hundal HS. Modulating serine palmitoyl transferase (SPT) expression and activity unveils a crucial role in lipid-induced insulin resistance in rat skeletal muscle cells. *Biochem J*. 2009; **417**(3): 791-801.
7. Holland WL, Bikman BT, Wang LP, Yuguang G, Sargent KM, Bulchand S, et al. Lipid-induced insulin resistance mediated by the proinflammatory receptor TLR4 requires saturated fatty acid-induced ceramide biosynthesis in mice. *J Clin Invest*. 2011; **121**(5): 1858-70.
8. Holland WL, Brozinick JT, Wang LP, Hawkins ED, Sargent KM, Liu Y, et al. Inhibition of ceramide synthesis ameliorates glucocorticoid-, saturated-fat-, and obesity-induced insulin resistance. *Cell Metab*. 2007; **5**(3): 167-79.
9. Schmitz-Peiffer C, Craig DL, Biden TJ. Ceramide generation is sufficient to account for the inhibition of the insulin-stimulated PKB pathway in C2C12 skeletal muscle cells pretreated with palmitate. *J Biol Chem*. 1999; **274**(34): 24202-10.
10. Baldwin AS, Jr. The NF- κ B and I κ B proteins: new discoveries and insights. *Annu Rev Immunol*. 1996; **14**: 649-83.
11. Beg AA, Baldwin AS, Jr. The I κ B proteins: multifunctional regulators of Rel/NF- κ B transcription factors. *Genes Dev*. 1993; **7**(11): 2064-70.
12. Cho YH, Lee CH, Kim SG. Potentiation of lipopolysaccharide-inducible cyclooxygenase 2 expression by C2-ceramide via c-Jun N-terminal kinase-mediated activation of CCAAT/enhancer binding protein beta in macrophages. *Mol Pharmacol*. 2003; **63**(3): 512-23.
13. Giltiay NV, Karakashian AA, Alimov AP, Lighthle S, Nikolova-Karakashian MN. Ceramide- and ERK-dependent pathway for the activation of CCAAT/enhancer binding protein by interleukin-1beta in hepatocytes. *J Lipid Res*. 2005; **46**(11): 2497-505.
14. Machleidt T, Wiegmann K, Henkel T, Schutze S, Baeuerle P, Kronke M. Sphingomyelinase activates proteolytic I κ B- α degradation in a cell-free system. *J Biol Chem*. 1994; **269**(19): 13760-5.
15. Opal SM, DePalo VA. Anti-inflammatory cytokines. *Chest*. 2000; **117**(4): 1162-72.

16. Poli V. The role of C/EBP isoforms in the control of inflammatory and native immunity functions. *J Biol Chem.* 1998; **273**(45): 29279-82.
17. Thomas B, Berenbaum F, Humbert L, Bian H, Bereziat G, Crofford L, et al. Critical role of C/EBPdelta and C/EBPbeta factors in the stimulation of the cyclooxygenase-2 gene transcription by interleukin-1beta in articular chondrocytes. *Eur J Biochem.* 2000; **267**(23): 6798-809.
18. Wadleigh DJ, Reddy ST, Kopp E, Ghosh S, Herschman HR. Transcriptional activation of the cyclooxygenase-2 gene in endotoxin-treated RAW 264.7 macrophages. *J Biol Chem.* 2000; **275**(9): 6259-66.
19. Wiegmann K, Schutze S, Machleidt T, Witte D, Kronke M. Functional dichotomy of neutral and acidic sphingomyelinases in tumor necrosis factor signaling. *Cell.* 1994; **78**(6): 1005-15.
20. Wong MM, Fish EN. Chemokines: attractive mediators of the immune response. *Semin Immunol.* 2003; **15**(1): 5-14.
21. Feng GJ, Goodridge HS, Harnett MM, Wei XQ, Nikolaev AV, Higson AP, et al. Extracellular signal-related kinase (ERK) and p38 mitogen-activated protein (MAP) kinases differentially regulate the lipopolysaccharide-mediated induction of inducible nitric oxide synthase and IL-12 in macrophages: Leishmania phosphoglycans subvert macrophage IL-12 production by targeting ERK MAP kinase. *J Immunol.* 1999; **163**(12): 6403-12.
22. Kaminska B. MAPK signalling pathways as molecular targets for anti-inflammatory therapy--from molecular mechanisms to therapeutic benefits. *Biochim Biophys Acta.* 2005; **1754**(1-2): 253-62.
23. Lee JC, Laydon JT, McDonnell PC, Gallagher TF, Kumar S, Green D, et al. A protein kinase involved in the regulation of inflammatory cytokine biosynthesis. *Nature.* 1994; **372**(6508): 739-46.
24. Pearson G, Robinson F, Beers Gibson T, Xu BE, Karandikar M, Berman K, et al. Mitogen-activated protein (MAP) kinase pathways: regulation and physiological functions. *Endocr Rev.* 2001; **22**(2): 153-83.
25. Raingeaud J, Whitmarsh AJ, Barrett T, Derijard B, Davis RJ. MKK3- and MKK6-regulated gene expression is mediated by the p38 mitogen-activated protein kinase signal transduction pathway. *Mol Cell Biol.* 1996; **16**(3): 1247-55.
26. Westra J, Doornbos-van der Meer B, de Boer P, van Leeuwen MA, van Rijswijk MH, Limburg PC. Strong inhibition of TNF-alpha production and inhibition of IL-8 and COX-2 mRNA expression in monocyte-derived macrophages by RWJ 67657, a p38 mitogen-activated protein kinase (MAPK) inhibitor. *Arthritis Res Ther.* 2004; **6**(4): R384-92.
27. Widmann C, Gibson S, Jarpe MB, Johnson GL. Mitogen-activated protein kinase: conservation of a three-kinase module from yeast to human. *Physiol Rev.* 1999; **79**(1): 143-80.
28. Scherer M, Bottcher A, Schmitz G, Liebisch G. Sphingolipid profiling of human plasma and FPLC-separated lipoprotein fractions by hydrophilic interaction chromatography tandem mass spectrometry. *Biochim Biophys Acta.* 2011; **1811**(2): 68-75.
29. Wiesner P, Leidl K, Boettcher A, Schmitz G, Liebisch G. Lipid profiling of FPLC-separated lipoprotein fractions by electrospray ionization tandem mass spectrometry. *J Lipid Res.* 2009; **50**(3): 574-85.
30. Haus JM, Kashyap SR, Kasumov T, Zhang R, Kelly KR, Defronzo RA, et al. Plasma ceramides are elevated in obese subjects with type 2 diabetes and correlate with the severity of insulin resistance. *Diabetes.* 2009; **58**(2): 337-43.

31. Kumar VF, Nelson; Abbas, Abul K.; Cotran, Ramzi S. ; Robbins, Stanley L. . Robbins and Cotran Pathologic Basis of Disease (7th ed.). Philadelphia, Pa: Saunders; (2005).
32. National Heart Lung and Blood Institute. Clinical guidelines on the identification, evaluation, and treatment of overweight and obesity in adults. The evidence report. Obesity Research. 1998; **6 [Suppl 2]**: 51S–209S.
33. Chan JM, Rimm EB, Colditz GA, Stampfer MJ, Willett WC. Obesity, fat distribution, and weight gain as risk factors for clinical diabetes in men. Diabetes Care. 1994; **17**(9): 961-9.
34. Colditz GA, Willett WC, Rotnitzky A, Manson JE. Weight gain as a risk factor for clinical diabetes mellitus in women. Ann Intern Med. 1995; **122**(7): 481-6.
35. Hu FB, Manson JE, Stampfer MJ, Colditz G, Liu S, Solomon CG, et al. Diet, lifestyle, and the risk of type 2 diabetes mellitus in women. N Engl J Med. 2001; **345**(11): 790-7.
36. Must A, Spadano J, Coakley EH, Field AE, Colditz G, Dietz WH. The disease burden associated with overweight and obesity. JAMA. 1999; **282**(16): 1523-9.
37. Grill V. A comparison of brain glucose metabolism in diabetes as measured by positron emission tomography or by arteriovenous techniques. Ann Med. 1990; **22**(3): 171-6.
38. DeFronzo RA. Pathogenesis of type 2 diabetes mellitus. Med Clin North Am. 2004; **88**(4): 787-835, ix.
39. Baron AD, Brechtel G, Wallace P, Edelman SV. Rates and tissue sites of non-insulin- and insulin-mediated glucose uptake in humans. Am J Physiol. 1988; **255**(6 Pt 1): E769-74.
40. Smith U. Impaired ('diabetic') insulin signaling and action occur in fat cells long before glucose intolerance--is insulin resistance initiated in the adipose tissue? Int J Obes Relat Metab Disord. 2002; **26**(7): 897-904.
41. Hajdуч E, Litherland GJ, Hundal HS. Protein kinase B (PKB/Akt)--a key regulator of glucose transport? FEBS Lett. 2001; **492**(3): 199-203.
42. Whiteman EL, Cho H, Birnbaum MJ. Role of Akt/protein kinase B in metabolism. Trends Endocrinol Metab. 2002; **13**(10): 444-51.
43. Vanhaesebroeck B, Alessi DR. The PI3K-PDK1 connection: more than just a road to PKB. Biochem J. 2000; **346 Pt 3**: 561-76.
44. Milburn CC, Deak M, Kelly SM, Price NC, Alessi DR, Van Aalten DM. Binding of phosphatidylinositol 3,4,5-trisphosphate to the pleckstrin homology domain of protein kinase B induces a conformational change. Biochem J. 2003; **375**(Pt 3): 531-8.
45. Liao Y, Hung MC. Physiological regulation of Akt activity and stability. Am J Transl Res. 2010; **2**(1): 19-42.
46. Roden M, Krssak M, Stingl H, Gruber S, Hofer A, Fornsinn C, et al. Rapid impairment of skeletal muscle glucose transport/phosphorylation by free fatty acids in humans. Diabetes. 1999; **48**(2): 358-64.
47. Roden M, Price TB, Perseghin G, Petersen KF, Rothman DL, Cline GW, et al. Mechanism of free fatty acid-induced insulin resistance in humans. J Clin Invest. 1996; **97**(12): 2859-65.
48. Chavez JA, Knotts TA, Wang LP, Li G, Dobrowsky RT, Florant GL, et al. A role for ceramide, but not diacylglycerol, in the antagonism of insulin signal transduction by saturated fatty acids. J Biol Chem. 2003; **278**(12): 10297-303.
49. Boden G, Chen X. Effects of fat on glucose uptake and utilization in patients with non-insulin-dependent diabetes. J Clin Invest. 1995; **96**(3): 1261-8.

50. Boden G, Lebed B, Schatz M, Homko C, Lemieux S. Effects of acute changes of plasma free fatty acids on intramyocellular fat content and insulin resistance in healthy subjects. *Diabetes*. 2001; **50**(7): 1612-7.
51. Summers SA. Ceramides in insulin resistance and lipotoxicity. *Prog Lipid Res*. 2006; **45**(1): 42-72.
52. Gordon EE, Craigie A. Effect of intravenous glucose on splanchnic and peripheral metabolism of endogenous pyruvate and citrate in patients with cirrhosis and in subjects without liver disease. *J Lab Clin Med*. 1960; **55**: 841-8.
53. Reaven GM, Hollenbeck C, Jeng CY, Wu MS, Chen YD. Measurement of plasma glucose, free fatty acid, lactate, and insulin for 24 h in patients with NIDDM. *Diabetes*. 1988; **37**(8): 1020-4.
54. Boden G. Role of fatty acids in the pathogenesis of insulin resistance and NIDDM. *Diabetes*. 1997; **46**(1): 3-10.
55. Boden G, Jadali F. Effects of lipid on basal carbohydrate metabolism in normal men. *Diabetes*. 1991; **40**(6): 686-92.
56. Boden G, Jadali F, White J, Liang Y, Mozzoli M, Chen X, et al. Effects of fat on insulin-stimulated carbohydrate metabolism in normal men. *J Clin Invest*. 1991; **88**(3): 960-6.
57. Santomauro AT, Boden G, Silva ME, Rocha DM, Santos RF, Ursich MJ, et al. Overnight lowering of free fatty acids with Acipimox improves insulin resistance and glucose tolerance in obese diabetic and nondiabetic subjects. *Diabetes*. 1999; **48**(9): 1836-41.
58. Parton RG, Joggerst B, Simons K. Regulated internalization of caveolae. *J Cell Biol*. 1994; **127**(5): 1199-215.
59. Colombini M. Ceramide channels and their role in mitochondria-mediated apoptosis. *Biochim Biophys Acta*. 2010; **1797**(6-7): 1239-44.
60. Kolesnick RN, Kronke M. Regulation of ceramide production and apoptosis. *Annu Rev Physiol*. 1998; **60**: 643-65.
61. Stancevic B, Kolesnick R. Ceramide-rich platforms in transmembrane signaling. *FEBS Lett*. 2010; **584**(9): 1728-40.
62. Yang G, Badeanlou L, Bielawski J, Roberts AJ, Hannun YA, Samad F. Central role of ceramide biosynthesis in body weight regulation, energy metabolism, and the metabolic syndrome. *Am J Physiol Endocrinol Metab*. 2009; **297**(1): E211-24.
63. Stratford S, Hoehn KL, Liu F, Summers SA. Regulation of insulin action by ceramide: dual mechanisms linking ceramide accumulation to the inhibition of Akt/protein kinase B. *J Biol Chem*. 2004; **279**(35): 36608-15.
64. Marchesini N, Hannun YA. Acid and neutral sphingomyelinases: roles and mechanisms of regulation. *Biochem Cell Biol*. 2004; **82**(1): 27-44.
65. Brenner B, Ferlinz K, Grassme H, Weller M, Koppenhoefer U, Dichgans J, et al. Fas/CD95/Apo-I activates the acidic sphingomyelinase via caspases. *Cell Death Differ*. 1998; **5**(1): 29-37.
66. Garzotto M, White-Jones M, Jiang Y, Ehleiter D, Liao WC, Haimovitz-Friedman A, et al. 12-O-tetradecanoylphorbol-13-acetate-induced apoptosis in LNCaP cells is mediated through ceramide synthase. *Cancer Res*. 1998; **58**(10): 2260-4.
67. Goldkorn T, Balaban N, Shannon M, Chea V, Matsukuma K, Gilchrist D, et al. H₂O₂ acts on cellular membranes to generate ceramide signaling and initiate apoptosis in tracheobronchial epithelial cells. *J Cell Sci*. 1998; **111** (Pt 21): 3209-20.

68. Haimovitz-Friedman A, Kan CC, Ehleiter D, Persaud RS, McLoughlin M, Fuks Z, et al. Ionizing radiation acts on cellular membranes to generate ceramide and initiate apoptosis. *J Exp Med*. 1994; **180**(2): 525-35.
69. Jenkins GM, Cowart LA, Signorelli P, Pettus BJ, Chalfant CE, Hannun YA. Acute activation of de novo sphingolipid biosynthesis upon heat shock causes an accumulation of ceramide and subsequent dephosphorylation of SR proteins. *J Biol Chem*. 2002; **277**(45): 42572-8.
70. Schutze S, Potthoff K, Machleidt T, Berkovic D, Wiegmann K, Kronke M. TNF activates NF-kappa B by phosphatidylcholine-specific phospholipase C-induced "acidic" sphingomyelin breakdown. *Cell*. 1992; **71**(5): 765-76.
71. Won JS, Im YB, Khan M, Singh AK, Singh I. The role of neutral sphingomyelinase produced ceramide in lipopolysaccharide-mediated expression of inducible nitric oxide synthase. *J Neurochem*. 2004; **88**(3): 583-93.
72. Mandon EC, Ehses I, Rother J, van Echten G, Sandhoff K. Subcellular localization and membrane topology of serine palmitoyltransferase, 3-dehydrosphinganine reductase, and sphinganine N-acyltransferase in mouse liver. *J Biol Chem*. 1992; **267**(16): 11144-8.
73. Merrill AH, Jr. De novo sphingolipid biosynthesis: a necessary, but dangerous, pathway. *J Biol Chem*. 2002; **277**(29): 25843-6.
74. Lahiri S, Futerman AH. LASS5 is a bona fide dihydroceramide synthase that selectively utilizes palmitoyl-CoA as acyl donor. *J Biol Chem*. 2005; **280**(40): 33735-8.
75. Mizutani Y, Kihara A, Igarashi Y. Mammalian Lass6 and its related family members regulate synthesis of specific ceramides. *Biochem J*. 2005; **390**(Pt 1): 263-71.
76. Bose R, Verheij M, Haimovitz-Friedman A, Scotto K, Fuks Z, Kolesnick R. Ceramide synthase mediates daunorubicin-induced apoptosis: an alternative mechanism for generating death signals. *Cell*. 1995; **82**(3): 405-14.
77. Liao WC, Haimovitz-Friedman A, Persaud RS, McLoughlin M, Ehleiter D, Zhang N, et al. Ataxia telangiectasia-mutated gene product inhibits DNA damage-induced apoptosis via ceramide synthase. *J Biol Chem*. 1999; **274**(25): 17908-17.
78. Gomez del Pulgar T, Velasco G, Sanchez C, Haro A, Guzman M. De novo-synthesized ceramide is involved in cannabinoid-induced apoptosis. *Biochem J*. 2002; **363**(Pt 1): 183-8.
79. Kitatani K, Nemoto M, Akiba S, Sato T. Stimulation by de novo-synthesized ceramide of phospholipase A(2)-dependent cholesterol esterification promoted by the uptake of oxidized low-density lipoprotein in macrophages. *Cell Signal*. 2002; **14**(8): 695-701.
80. Chatelut M, Leruth M, Harzer K, Dagan A, Marchesini S, Gatt S, et al. Natural ceramide is unable to escape the lysosome, in contrast to a fluorescent analogue. *FEBS Lett*. 1998; **426**(1): 102-6.
81. Baumruker T, Bornancin F, Billich A. The role of sphingosine and ceramide kinases in inflammatory responses. *Immunol Lett*. 2005; **96**(2): 175-85.
82. Taha TA, Hannun YA, Obeid LM. Sphingosine kinase: biochemical and cellular regulation and role in disease. *J Biochem Mol Biol*. 2006; **39**(2): 113-31.
83. Chigorno V, Giannotta C, Ottico E, Sciannamblo M, Mikulak J, Prinetti A, et al. Sphingolipid uptake by cultured cells: complex aggregates of cell sphingolipids with serum proteins and lipoproteins are rapidly catabolized. *J Biol Chem*. 2005; **280**(4): 2668-75.

84. Kitatani K, Idkowiak-Baldys J, Hannun YA. The sphingolipid salvage pathway in ceramide metabolism and signaling. *Cell Signal*. 2008; **20**(6): 1010-8.
85. Gillard BK, Clement RG, Marcus DM. Variations among cell lines in the synthesis of sphingolipids in de novo and recycling pathways. *Glycobiology*. 1998; **8**(9): 885-90.
86. Tettamanti G, Bassi R, Viani P, Riboni L. Salvage pathways in glycosphingolipid metabolism. *Biochimie*. 2003; **85**(3-4): 423-37.
87. Mizutani Y, Kihara A, Igarashi Y. LASS3 (longevity assurance homologue 3) is a mainly testis-specific (dihydro)ceramide synthase with relatively broad substrate specificity. *Biochem J*. 2006; **398**(3): 531-8.
88. Pewzner-Jung Y, Ben-Dor S, Futerman AH. When do Lasses (longevity assurance genes) become CerS (ceramide synthases)? Insights into the regulation of ceramide synthesis. *J Biol Chem*. 2006; **281**(35): 25001-5.
89. Riebeling C, Allegood JC, Wang E, Merrill AH, Jr., Futerman AH. Two mammalian longevity assurance gene (LAG1) family members, trh1 and trh4, regulate dihydroceramide synthesis using different fatty acyl-CoA donors. *J Biol Chem*. 2003; **278**(44): 43452-9.
90. Pickersgill L, Litherland GJ, Greenberg AS, Walker M, Yeaman SJ. Key role for ceramides in mediating insulin resistance in human muscle cells. *J Biol Chem*. 2007; **282**(17): 12583-9.
91. Bruce CR, Kriketos AD, Cooney GJ, Hawley JA. Disassociation of muscle triglyceride content and insulin sensitivity after exercise training in patients with Type 2 diabetes. *Diabetologia*. 2004; **47**(1): 23-30.
92. Dube JJ, Amati F, Stefanovic-Racic M, Toledo FG, Sauers SE, Goodpaster BH. Exercise-induced alterations in intramyocellular lipids and insulin resistance: the athlete's paradox revisited. *Am J Physiol Endocrinol Metab*. 2008; **294**(5): E882-8.
93. Stratford S, DeWald DB, Summers SA. Ceramide dissociates 3'-phosphoinositide production from pleckstrin homology domain translocation. *Biochem J*. 2001; **354**(Pt 2): 359-68.
94. Blouin CM, Prado C, Takane KK, Lasnier F, Garcia-Ocana A, Ferre P, et al. Plasma membrane subdomain compartmentalization contributes to distinct mechanisms of ceramide action on insulin signaling. *Diabetes*. 2010; **59**(3): 600-10.
95. Chalfant CE, Kishikawa K, Mumby MC, Kamibayashi C, Bielawska A, Hannun YA. Long chain ceramides activate protein phosphatase-1 and protein phosphatase-2A. Activation is stereospecific and regulated by phosphatidic acid. *J Biol Chem*. 1999; **274**(29): 20313-7.
96. Cazzolli R, Carpenter L, Biden TJ, Schmitz-Peiffer C. A role for protein phosphatase 2A-like activity, but not atypical protein kinase Czeta, in the inhibition of protein kinase B/Akt and glycogen synthesis by palmitate. *Diabetes*. 2001; **50**(10): 2210-8.
97. Teruel T, Hernandez R, Lorenzo M. Ceramide mediates insulin resistance by tumor necrosis factor-alpha in brown adipocytes by maintaining Akt in an inactive dephosphorylated state. *Diabetes*. 2001; **50**(11): 2563-71.
98. Summers SA, Garza LA, Zhou H, Birnbaum MJ. Regulation of insulin-stimulated glucose transporter GLUT4 translocation and Akt kinase activity by ceramide. *Mol Cell Biol*. 1998; **18**(9): 5457-64.
99. Cortright RN, Azevedo JL, Jr., Zhou Q, Sinha M, Pories WJ, Itani SI, et al. Protein kinase C modulates insulin action in human skeletal muscle. *Am J Physiol Endocrinol Metab*. 2000; **278**(3): E553-62.

100. Bourbon NA, Sandirasegarane L, Kester M. Ceramide-induced inhibition of Akt is mediated through protein kinase C ζ : implications for growth arrest. *J Biol Chem*. 2002; **277**(5): 3286-92.
101. Powell DJ, Hajduch E, Kular G, Hundal HS. Ceramide disables 3-phosphoinositide binding to the pleckstrin homology domain of protein kinase B (PKB)/Akt by a PKC ζ -dependent mechanism. *Mol Cell Biol*. 2003; **23**(21): 7794-808.
102. Stretton C, Evans A, Hundal HS. Cellular depletion of atypical PKC $\{\lambda\}$ is associated with enhanced insulin sensitivity and glucose uptake in L6 rat skeletal muscle cells. *Am J Physiol Endocrinol Metab*. 2010; **299**(3): E402-12.
103. Hajduch E, Turban S, Le Liepvre X, Le Lay S, Lipina C, Dimopoulos N, et al. Targeting of PKC ζ and PKB to caveolin-enriched microdomains represents a crucial step underpinning the disruption in PKB-directed signalling by ceramide. *Biochem J*. 2008; **410**(2): 369-79.
104. Liu J, Schnitzer JE. Analysis of lipids in caveolae. *Methods Mol Biol*. 1999; **116**: 61-72.
105. Chidlow JH, Jr., Sessa WC. Caveolae, caveolins, and cavins: complex control of cellular signalling and inflammation. *Cardiovasc Res*. 2010; **86**(2): 219-25.
106. Pilch PF, Souto RP, Liu L, Jedrychowski MP, Berg EA, Costello CE, et al. Cellular spelunking: exploring adipocyte caveolae. *J Lipid Res*. 2007; **48**(10): 2103-11.
107. Oka N, Yamamoto M, Schwencke C, Kawabe J, Ebina T, Ohno S, et al. Caveolin interaction with protein kinase C. Isoenzyme-dependent regulation of kinase activity by the caveolin scaffolding domain peptide. *J Biol Chem*. 1997; **272**(52): 33416-21.
108. Li L, Ren CH, Tahir SA, Ren C, Thompson TC. Caveolin-1 maintains activated Akt in prostate cancer cells through scaffolding domain binding site interactions with and inhibition of serine/threonine protein phosphatases PP1 and PP2A. *Mol Cell Biol*. 2003; **23**(24): 9389-404.
109. Weickert MO, Pfeiffer AF. Signalling mechanisms linking hepatic glucose and lipid metabolism. *Diabetologia*. 2006; **49**(8): 1732-41.
110. Beutler B, Greenwald D, Hulmes JD, Chang M, Pan YC, Mathison J, et al. Identity of tumour necrosis factor and the macrophage-secreted factor cachectin. *Nature*. 1985; **316**(6028): 552-4.
111. Carswell EA, Old LJ, Kassel RL, Green S, Fiore N, Williamson B. An endotoxin-induced serum factor that causes necrosis of tumors. *Proc Natl Acad Sci U S A*. 1975; **72**(9): 3666-70.
112. Kolb WP, Granger GA. Lymphocyte in vitro cytotoxicity: characterization of human lymphotoxin. *Proc Natl Acad Sci U S A*. 1968; **61**(4): 1250-5.
113. Tracey KJ, Beutler B, Lowry SF, Merryweather J, Wolpe S, Milsark IW, et al. Shock and tissue injury induced by recombinant human cachectin. *Science*. 1986; **234**(4775): 470-4.
114. Kim MY, Linares C, Obeid L, Hannun Y. Identification of sphingomyelin turnover as an effector mechanism for the action of tumor necrosis factor alpha and gamma-interferon. Specific role in cell differentiation. *J Biol Chem*. 1991; **266**(1): 484-9.
115. Mathias S, Dressler KA, Kolesnick RN. Characterization of a ceramide-activated protein kinase: stimulation by tumor necrosis factor alpha. *Proc Natl Acad Sci U S A*. 1991; **88**(22): 10009-13.

116. Uysal KT, Wiesbrock SM, Marino MW, Hotamisligil GS. Protection from obesity-induced insulin resistance in mice lacking TNF-alpha function. *Nature*. 1997; **389**(6651): 610-4.
117. Xiao C, Ghosh S. NF-kappaB, an evolutionarily conserved mediator of immune and inflammatory responses. *Adv Exp Med Biol*. 2005; **560**: 41-5.
118. Hirosumi J, Tuncman G, Chang L, Gorgun CZ, Uysal KT, Maeda K, et al. A central role for JNK in obesity and insulin resistance. *Nature*. 2002; **420**(6913): 333-6.
119. Ruvolo PP. Intracellular signal transduction pathways activated by ceramide and its metabolites. *Pharmacol Res*. 2003; **47**(5): 383-92.
120. Sathyanarayana P, Barthwal MK, Kundu CN, Lane ME, Bergmann A, Tzivion G, et al. Activation of the Drosophila MLK by ceramide reveals TNF-alpha and ceramide as agonists of mammalian MLK3. *Mol Cell*. 2002; **10**(6): 1527-33.
121. Xu Z, Maroney AC, Dobrzanski P, Kukekov NV, Greene LA. The MLK family mediates c-Jun N-terminal kinase activation in neuronal apoptosis. *Mol Cell Biol*. 2001; **21**(14): 4713-24.
122. Subbaramaiah K, Chung WJ, Dannenberg AJ. Ceramide regulates the transcription of cyclooxygenase-2. Evidence for involvement of extracellular signal-regulated kinase/c-Jun N-terminal kinase and p38 mitogen-activated protein kinase pathways. *J Biol Chem*. 1998; **273**(49): 32943-9.
123. Newton R, Hart L, Chung KF, Barnes PJ. Ceramide induction of COX-2 and PGE(2) in pulmonary A549 cells does not involve activation of NF-kappaB. *Biochem Biophys Res Commun*. 2000; **277**(3): 675-9.
124. Goodridge HS, Harnett W, Liew FY, Harnett MM. Differential regulation of interleukin-12 p40 and p35 induction via Erk mitogen-activated protein kinase-dependent and -independent mechanisms and the implications for bioactive IL-12 and IL-23 responses. *Immunology*. 2003; **109**(3): 415-25.
125. Nishina H, Bachmann M, Oliveira-dos-Santos AJ, Kozieradzki I, Fischer KD, Odermatt B, et al. Impaired CD28-mediated interleukin 2 production and proliferation in stress kinase SAPK/ERK1 kinase (SEK1)/mitogen-activated protein kinase kinase 4 (MKK4)-deficient T lymphocytes. *J Exp Med*. 1997; **186**(6): 941-53.
126. Reimold AM, Grusby MJ, Kosaras B, Fries JW, Mori R, Maniwa S, et al. Chondrodysplasia and neurological abnormalities in ATF-2-deficient mice. *Nature*. 1996; **379**(6562): 262-5.
127. Subramaniam M, Saffaripour S, Van De Water L, Frenette PS, Mayadas TN, Hynes RO, et al. Role of endothelial selectins in wound repair. *Am J Pathol*. 1997; **150**(5): 1701-9.
128. Whitmarsh AJ, Yang SH, Su MS, Sharrocks AD, Davis RJ. Role of p38 and JNK mitogen-activated protein kinases in the activation of ternary complex factors. *Mol Cell Biol*. 1997; **17**(5): 2360-71.
129. Joseph CK, Byun HS, Bittman R, Kolesnick RN. Substrate recognition by ceramide-activated protein kinase. Evidence that kinase activity is proline-directed. *J Biol Chem*. 1993; **268**(27): 20002-6.
130. Liu J, Mathias S, Yang Z, Kolesnick RN. Renaturation and tumor necrosis factor-alpha stimulation of a 97-kDa ceramide-activated protein kinase. *J Biol Chem*. 1994; **269**(4): 3047-52.
131. Yao B, Zhang Y, Delikat S, Mathias S, Basu S, Kolesnick R. Phosphorylation of Raf by ceramide-activated protein kinase. *Nature*. 1995; **378**(6554): 307-10.
132. Adam D, Wiegmann K, Adam-Klages S, Ruff A, Kronke M. A novel cytoplasmic domain of the p55 tumor necrosis factor receptor initiates the neutral sphingomyelinase pathway. *J Biol Chem*. 1996; **271**(24): 14617-22.

133. Brigitte M, Schilte C, Plonquet A, Baba-Amer Y, Henri A, Charlier C, et al. Muscle resident macrophages control the immune cell reaction in a mouse model of notexin-induced myoinjury. *Arthritis Rheum.* 2010; **62**(1): 268-79.
134. Drosos AA, Dalakas MC. Identification of macrophages in the muscle biopsy preparations: a comparative study using specific monoclonal antimacrophage antibodies and acid phosphatase reaction. *Muscle Nerve.* 1995; **18**(2): 242-4.
135. McLennan IS. Degenerating and regenerating skeletal muscles contain several subpopulations of macrophages with distinct spatial and temporal distributions. *J Anat.* 1996; **188** (Pt 1): 17-28.
136. Pimorady-Esfahani A, Grounds MD, McMenemy PG. Macrophages and dendritic cells in normal and regenerating murine skeletal muscle. *Muscle Nerve.* 1997; **20**(2): 158-66.
137. Tidball JG, Villalta SA. Regulatory interactions between muscle and the immune system during muscle regeneration. *Am J Physiol Regul Integr Comp Physiol.* 2010; **298**(5): R1173-87.
138. Wehling M, Spencer MJ, Tidball JG. A nitric oxide synthase transgene ameliorates muscular dystrophy in mdx mice. *J Cell Biol.* 2001; **155**(1): 123-31.
139. Reyna SM, Ghosh S, Tantiwong P, Meka CS, Eagan P, Jenkinson CP, et al. Elevated toll-like receptor 4 expression and signaling in muscle from insulin-resistant subjects. *Diabetes.* 2008; **57**(10): 2595-602.
140. Shi H, Kokoeva MV, Inouye K, Tzameli I, Yin H, Flier JS. TLR4 links innate immunity and fatty acid-induced insulin resistance. *J Clin Invest.* 2006; **116**(11): 3015-25.
141. Saberi M, Woods NB, de Luca C, Schenk S, Lu JC, Bandyopadhyay G, et al. Hematopoietic cell-specific deletion of toll-like receptor 4 ameliorates hepatic and adipose tissue insulin resistance in high-fat-fed mice. *Cell Metab.* 2009; **10**(5): 419-29.
142. Lee JY, Ye J, Gao Z, Youn HS, Lee WH, Zhao L, et al. Reciprocal modulation of Toll-like receptor-4 signaling pathways involving MyD88 and phosphatidylinositol 3-kinase/AKT by saturated and polyunsaturated fatty acids. *J Biol Chem.* 2003; **278**(39): 37041-51.
143. Lee JY, Sohn KH, Rhee SH, Hwang D. Saturated fatty acids, but not unsaturated fatty acids, induce the expression of cyclooxygenase-2 mediated through Toll-like receptor 4. *J Biol Chem.* 2001; **276**(20): 16683-9.
144. Lee JY, Plakidas A, Lee WH, Heikkinen A, Chanmugam P, Bray G, et al. Differential modulation of Toll-like receptors by fatty acids: preferential inhibition by n-3 polyunsaturated fatty acids. *J Lipid Res.* 2003; **44**(3): 479-86.
145. Memon RA, Holleran WM, Moser AH, Seki T, Uchida Y, Fuller J, et al. Endotoxin and cytokines increase hepatic sphingolipid biosynthesis and produce lipoproteins enriched in ceramides and sphingomyelin. *Arterioscler Thromb Vasc Biol.* 1998; **18**(8): 1257-65.
146. Memon RA, Holleran WM, Uchida Y, Moser AH, Grunfeld C, Feingold KR. Regulation of sphingolipid and glycosphingolipid metabolism in extrahepatic tissues by endotoxin. *J Lipid Res.* 2001; **42**(3): 452-9.
147. Sims K, Haynes CA, Kelly S, Allegood JC, Wang E, Momin A, et al. Kdo2-lipid A, a TLR4-specific agonist, induces de novo sphingolipid biosynthesis in RAW264.7 macrophages, which is essential for induction of autophagy. *J Biol Chem.* 2010; **285**(49): 38568-79.
148. Cuschieri J, Bulger E, Billgrin J, Garcia I, Maier RV. Acid sphingomyelinase is required for lipid Raft TLR4 complex formation. *Surg Infect (Larchmt).* 2007; **8**(1): 91-106.

149. Chavez JA, Summers SA. Characterizing the effects of saturated fatty acids on insulin signaling and ceramide and diacylglycerol accumulation in 3T3-L1 adipocytes and C2C12 myotubes. *Arch Biochem Biophys*. 2003; **419**(2): 101-9.
150. Jiang XC, Paultre F, Pearson TA, Reed RG, Francis CK, Lin M, et al. Plasma sphingomyelin level as a risk factor for coronary artery disease. *Arterioscler Thromb Vasc Biol*. 2000; **20**(12): 2614-8.
151. Nelson JC, Jiang XC, Tabas I, Tall A, Shea S. Plasma sphingomyelin and subclinical atherosclerosis: findings from the multi-ethnic study of atherosclerosis. *Am J Epidemiol*. 2006; **163**(10): 903-12.
152. Drobnik W, Liebisch G, Audebert FX, Frohlich D, Gluck T, Vogel P, et al. Plasma ceramide and lysophosphatidylcholine inversely correlate with mortality in sepsis patients. *J Lipid Res*. 2003; **44**(4): 754-61.
153. Ichi I, Nakahara K, Miyashita Y, Hidaka A, Kutsukake S, Inoue K, et al. Association of ceramides in human plasma with risk factors of atherosclerosis. *Lipids*. 2006; **41**(9): 859-63.
154. Ichi I, Takashima Y, Adachi N, Nakahara K, Kamikawa C, Harada-Shiba M, et al. Effects of dietary cholesterol on tissue ceramides and oxidation products of apolipoprotein B-100 in ApoE-deficient mice. *Lipids*. 2007; **42**(10): 893-900.
155. Ichi I, Nakahara K, Miyashita Y, Hidaka A, Kutsukake S, Inoue K, et al. Association of ceramides in human plasma with risk factors of atherosclerosis. *Lipids*. 2006; **41**(9): 859-63.
156. Kasumov T, Huang H, Chung YM, Zhang R, McCullough AJ, Kirwan JP. Quantification of ceramide species in biological samples by liquid chromatography electrospray ionization tandem mass spectrometry. *Anal Biochem*. 2010; **401**(1): 154-61.
157. Tserng KY, Griffin R. Quantitation and molecular species determination of diacylglycerols, phosphatidylcholines, ceramides, and sphingomyelins with gas chromatography. *Anal Biochem*. 2003; **323**(1): 84-93.
158. Yano M, Kishida E, Muneyuki Y, Masuzawa Y. Quantitative analysis of ceramide molecular species by high performance liquid chromatography. *J Lipid Res*. 1998; **39**(10): 2091-8.
159. Gu M, Kerwin JL, Watts JD, Aebersold R. Ceramide profiling of complex lipid mixtures by electrospray ionization mass spectrometry. *Anal Biochem*. 1997; **244**(2): 347-56.
160. Ichi I, Nakahara K, Fujii K, Iida C, Miyashita Y, Kojo S. Increase of ceramide in the liver and plasma after carbon tetrachloride intoxication in the rat. *J Nutr Sci Vitaminol (Tokyo)*. 2007; **53**(1): 53-6.
161. Mano N, Oda Y, Yamada K, Asakawa N, Katayama K. Simultaneous quantitative determination method for sphingolipid metabolites by liquid chromatography/ion spray ionization tandem mass spectrometry. *Anal Biochem*. 1997; **244**(2): 291-300.
162. Groener JE, Poorthuis BJ, Kuiper S, Hollak CE, Aerts JM. Plasma glucosylceramide and ceramide in type 1 Gaucher disease patients: correlations with disease severity and response to therapeutic intervention. *Biochim Biophys Acta*. 2008; **1781**(1-2): 72-8.
163. Merrill AH, Jr., Lingrell S, Wang E, Nikolova-Karakashian M, Vales TR, Vance DE. Sphingolipid biosynthesis de novo by rat hepatocytes in culture. Ceramide and sphingomyelin are associated with, but not required for, very low density lipoprotein secretion. *J Biol Chem*. 1995; **270**(23): 13834-41.

164. Havel RJ, Eder HA, Bragdon JH. The distribution and chemical composition of ultracentrifugally separated lipoproteins in human serum. *J Clin Invest.* 1955; **34**(9): 1345-53.
165. DiPiro JTT, R.L.; Yee, G.C ; Matzke, G.R ; Wells, B.G ; Posey, L.M. *Pharmacotherapy: A Pathophysiologic Approach* (7th ed.). New York: McGraw-Hill; 2008.
166. Bishop MLS, L.E; Fody, E.P. *Clinical Chemistry: Principles, Procedures, Correlations* (5th edition). Baltimore (MD): Lippincott Williams & Wilkins; 2004.
167. Sigma-Aldrich. Lipoprotein Function. [cited 2011 August 8]; Available from: <http://www.sigmaaldrich.com/life-science/metabolomics/enzyme-explorer/learning-center/plasma-blood-protein/lipoprotein-function.html>
168. Lewis B. The lipoproteins: predictors, protectors, and pathogens. *Br Med J (Clin Res Ed).* 1983; **287**(6400): 1161-4.
169. Brown MS, Faust JR, Goldstein JL. Role of the low density lipoprotein receptor in regulating the content of free and esterified cholesterol in human fibroblasts. *J Clin Invest.* 1975; **55**(4): 783-93.
170. Brown MS, Goldstein JL. Multivalent feedback regulation of HMG CoA reductase, a control mechanism coordinating isoprenoid synthesis and cell growth. *J Lipid Res.* 1980; **21**(5): 505-17.
171. Spady DK, Bilheimer DW, Dietschy JM. Rates of receptor-dependent and -independent low density lipoprotein uptake in the hamster. *Proc Natl Acad Sci U S A.* 1983; **80**(11): 3499-503.
172. Goldstein JL, Brown MS. Atherosclerosis: the low-density lipoprotein receptor hypothesis. *Metabolism.* 1977; **26**(11): 1257-75.
173. Goldstein JL, Brown MS. Progress in understanding the LDL receptor and HMG-CoA reductase, two membrane proteins that regulate the plasma cholesterol. *J Lipid Res.* 1984; **25**(13): 1450-61.
174. Shepherd J, Bicker S, Lorimer AR, Packard CJ. Receptor-mediated low density lipoprotein catabolism in man. *J Lipid Res.* 1979; **20**(8): 999-1006.
175. Brown MS, Goldstein JL. Lipoprotein metabolism in the macrophage: implications for cholesterol deposition in atherosclerosis. *Annu Rev Biochem.* 1983; **52**: 223-61.
176. Brown MS, Ho YK, Goldstein JL. The cholesteryl ester cycle in macrophage foam cells. Continual hydrolysis and re-esterification of cytoplasmic cholesteryl esters. *J Biol Chem.* 1980; **255**(19): 9344-52.
177. Steinberg D, Parthasarathy S, Carew TE, Khoo JC, Witztum JL. Beyond cholesterol. Modifications of low-density lipoprotein that increase its atherogenicity. *N Engl J Med.* 1989; **320**(14): 915-24.
178. Shoji T, Nishizawa Y, Fukumoto M, Shimamura K, Kimura J, Kanda H, et al. Inverse relationship between circulating oxidized low density lipoprotein (oxLDL) and anti-oxLDL antibody levels in healthy subjects. *Atherosclerosis.* 2000; **148**(1): 171-7.
179. Holvoet P, Vanhaecke J, Janssens S, Van de Werf F, Collen D. Oxidized LDL and malondialdehyde-modified LDL in patients with acute coronary syndromes and stable coronary artery disease. *Circulation.* 1998; **98**(15): 1487-94.
180. Van Berkel TJ, De Rijke YB, Kruijt JK. Different fate in vivo of oxidatively modified low density lipoprotein and acetylated low density lipoprotein in rats. Recognition by various scavenger receptors on Kupffer and endothelial liver cells. *J Biol Chem.* 1991; **266**(4): 2282-9.

181. Basu A, Basu R, Shah P, Vella A, Rizza RA, Jensen MD. Systemic and regional free fatty acid metabolism in type 2 diabetes. *Am J Physiol Endocrinol Metab.* 2001; **280**(6): E1000-6.
182. Groop LC, Saloranta C, Shank M, Bonadonna RC, Ferrannini E, DeFronzo RA. The role of free fatty acid metabolism in the pathogenesis of insulin resistance in obesity and noninsulin-dependent diabetes mellitus. *J Clin Endocrinol Metab.* 1991; **72**(1): 96-107.
183. Bickerton AS, Roberts R, Fielding BA, Tornqvist H, Blaak EE, Wagenmakers AJ, et al. Adipose tissue fatty acid metabolism in insulin-resistant men. *Diabetologia.* 2008; **51**(8): 1466-74.
184. Serlie MJ, Meijer AJ, Groener JE, Duran M, Endert E, Fliers E, et al. Short-term manipulation of plasma free fatty acids does not change skeletal muscle concentrations of ceramide and glucosylceramide in lean and overweight subjects. *J Clin Endocrinol Metab.* 2007; **92**(4): 1524-9.
185. Wilson PW, Meigs JB, Sullivan L, Fox CS, Nathan DM, D'Agostino RB, Sr. Prediction of incident diabetes mellitus in middle-aged adults: the Framingham Offspring Study. *Arch Intern Med.* 2007; **167**(10): 1068-74.
186. Samad F, Hester KD, Yang G, Hannun YA, Bielawski J. Altered adipose and plasma sphingolipid metabolism in obesity: a potential mechanism for cardiovascular and metabolic risk. *Diabetes.* 2006; **55**(9): 2579-87.
187. Ichi I, Nakahara K, Kiso K, Kojo S. Effect of dietary cholesterol and high fat on ceramide concentration in rat tissues. *Nutrition.* 2007; **23**(7-8): 570-4.
188. Matthews DR, Hosker JP, Rudenski AS, Naylor BA, Treacher DF, Turner RC. Homeostasis model assessment: insulin resistance and beta-cell function from fasting plasma glucose and insulin concentrations in man. *Diabetologia.* 1985; **28**(7): 412-9.
189. Preiss J, Loomis CR, Bishop WR, Stein R, Niedel JE, Bell RM. Quantitative measurement of sn-1,2-diacylglycerols present in platelets, hepatocytes, and ras- and sis-transformed normal rat kidney cells. *J Biol Chem.* 1986; **261**(19): 8597-600.
190. Watt MJ, Hevener A, Lancaster GI, Febbraio MA. Ciliary neurotrophic factor prevents acute lipid-induced insulin resistance by attenuating ceramide accumulation and phosphorylation of c-Jun N-terminal kinase in peripheral tissues. *Endocrinology.* 2006; **147**(5): 2077-85.
191. Hojjati MR, Li Z, Jiang XC. Serine palmitoyl-CoA transferase (SPT) deficiency and sphingolipid levels in mice. *Biochim Biophys Acta.* 2005; **1737**(1): 44-51.
192. Adams JM, 2nd, Pratipanawat T, Berria R, Wang E, DeFronzo RA, Sullards MC, et al. Ceramide content is increased in skeletal muscle from obese insulin-resistant humans. *Diabetes.* 2004; **53**(1): 25-31.
193. Kolak M, Westerbacka J, Velagapudi VR, Wagsater D, Yetukuri L, Makkonen J, et al. Adipose tissue inflammation and increased ceramide content characterize subjects with high liver fat content independent of obesity. *Diabetes.* 2007; **56**(8): 1960-8.
194. Straczkowski M, Kowalska I, Nikolajuk A, Dzienis-Straczkowska S, Kinalska I, Baranowski M, et al. Relationship between insulin sensitivity and sphingomyelin signaling pathway in human skeletal muscle. *Diabetes.* 2004; **53**(5): 1215-21.
195. Fischer H, Ellstrom P, Ekstrom K, Gustafsson L, Gustafsson M, Svanborg C. Ceramide as a TLR4 agonist; a putative signalling intermediate between sphingolipid receptors for microbial ligands and TLR4. *Cell Microbiol.* 2007; **9**(5): 1239-51.
196. Goni FM, Alonso A. Sphingomyelinases: enzymology and membrane activity. *FEBS Lett.* 2002; **531**(1): 38-46.

197. Turinsky J, O'Sullivan DM, Bayly BP. 1,2-Diacylglycerol and ceramide levels in insulin-resistant tissues of the rat in vivo. *J Biol Chem.* 1990; **265**(28): 16880-5.
198. Boyanovsky B, Karakashian A, King K, Giltaiy N, Nikolova-Karakashian M. Uptake and metabolism of low density lipoproteins with elevated ceramide content by human microvascular endothelial cells: implications for the regulation of apoptosis. *J Biol Chem.* 2003; **278**(29): 26992-9.
199. Blair A, Shaul PW, Yuhanna IS, Conrad PA, Smart EJ. Oxidized low density lipoprotein displaces endothelial nitric-oxide synthase (eNOS) from plasmalemmal caveolae and impairs eNOS activation. *J Biol Chem.* 1999; **274**(45): 32512-9.
200. Basu SK, Goldstein JL, Anderson GW, Brown MS. Degradation of cationized low density lipoprotein and regulation of cholesterol metabolism in homozygous familial hypercholesterolemia fibroblasts. *Proc Natl Acad Sci U S A.* 1976; **73**(9): 3178-82.
201. Goldstein JL, Dana SE, Brown MS. Esterification of low density lipoprotein cholesterol in human fibroblasts and its absence in homozygous familial hypercholesterolemia. *Proc Natl Acad Sci U S A.* 1974; **71**(11): 4288-92.
202. Mahley RW, Innerarity TL. Interaction of canine and swine lipoproteins with the low density lipoprotein receptor of fibroblasts as correlated with heparin/manganese precipitability. *J Biol Chem.* 1977; **252**(11): 3980-6.
203. Gustafson A, Alaupovic P, Furman RH. Studies of the Composition and Structure of Serum Lipoproteins: Isolation, Purification, and Characterization of Very Low Density Lipoproteins of Human Serum. *Biochemistry.* 1965; **4**: 596-605.
204. Krieger M, Brown MS, Faust JR, Goldstein JL. Replacement of endogenous cholesteryl esters of low density lipoprotein with exogenous cholesteryl linoleate. Reconstitution of a biologically active lipoprotein particle. *J Biol Chem.* 1978; **253**(12): 4093-101.
205. Walsh MT, Atkinson D. Calorimetric and spectroscopic investigation of the unfolding of human apolipoprotein B. *J Lipid Res.* 1990; **31**(6): 1051-62.
206. Barak LS, Webb WW. Fluorescent low density lipoprotein for observation of dynamics of individual receptor complexes on cultured human fibroblasts. *J Cell Biol.* 1981; **90**(3): 595-604.
207. Borkman M, Storlien LH, Pan DA, Jenkins AB, Chisholm DJ, Campbell LV. The relation between insulin sensitivity and the fatty-acid composition of skeletal-muscle phospholipids. *N Engl J Med.* 1993; **328**(4): 238-44.
208. Bloomgarden ZT. Insulin resistance: current concepts. *Clin Ther.* 1998; **20**(2): 216-31; discussion 5.
209. Summers SA. Sphingolipids and insulin resistance: the five Ws. *Curr Opin Lipidol.* 2010; **21**(2): 128-35.
210. Mitumoto Y, Burdett E, Grant A, Klip A. Differential expression of the GLUT1 and GLUT4 glucose transporters during differentiation of L6 muscle cells. *Biochem Biophys Res Commun.* 1991; **175**(2): 652-9.
211. Mitumoto Y, Klip A. Development regulation of the subcellular distribution and glycosylation of GLUT1 and GLUT4 glucose transporters during myogenesis of L6 muscle cells. *J Biol Chem.* 1992; **267**(7): 4957-62.
212. Yaffe D. Retention of differentiation potentialities during prolonged cultivation of myogenic cells. *Proc Natl Acad Sci U S A.* 1968; **61**(2): 477-83.
213. Niu W, Huang C, Nawaz Z, Levy M, Somwar R, Li D, et al. Maturation of the regulation of GLUT4 activity by p38 MAPK during L6 cell myogenesis. *J Biol Chem.* 2003; **278**(20): 17953-62.

214. Seglen PO. Hepatocyte suspensions and cultures as tools in experimental carcinogenesis. *J Toxicol Environ Health*. 1979; **5**(2-3): 551-60.
215. Aden DP, Fogel A, Plotkin S, Damjanov I, Knowles BB. Controlled synthesis of HBsAg in a differentiated human liver carcinoma-derived cell line. *Nature*. 1979; **282**(5739): 615-6.
216. Weinstein IB, Orenstein JM, Gebert R, Kaighn ME, Stadler UC. Growth and structural properties of epithelial cell cultures established from normal rat liver and chemically induced hepatomas. *Cancer Res*. 1975; **35**(1): 253-63.
217. Green H, Meuth M. An established pre-adipose cell line and its differentiation in culture. *Cell*. 1974; **3**(2): 127-33.
218. Alnemri ES, Livingston DJ, Nicholson DW, Salvesen G, Thornberry NA, Wong WW, et al. Human ICE/CED-3 protease nomenclature. *Cell*. 1996; **87**(2): 171.
219. Nahmias Y, Casali M, Barbe L, Berthiaume F, Yarmush ML. Liver endothelial cells promote LDL-R expression and the uptake of HCV-like particles in primary rat and human hepatocytes. *Hepatology*. 2006; **43**(2): 257-65.
220. Charron MJ, Brosius FC, 3rd, Alper SL, Lodish HF. A glucose transport protein expressed predominately in insulin-responsive tissues. *Proc Natl Acad Sci U S A*. 1989; **86**(8): 2535-9.
221. Douen AG, Ramlal T, Rastogi S, Bilan PJ, Cartee GD, Vranic M, et al. Exercise induces recruitment of the "insulin-responsive glucose transporter". Evidence for distinct intracellular insulin- and exercise-recruitable transporter pools in skeletal muscle. *J Biol Chem*. 1990; **265**(23): 13427-30.
222. Fukumoto H, Kayano T, Buse JB, Edwards Y, Pilch PF, Bell GI, et al. Cloning and characterization of the major insulin-responsive glucose transporter expressed in human skeletal muscle and other insulin-responsive tissues. *J Biol Chem*. 1989; **264**(14): 7776-9.
223. James DE, Strube M, Mueckler M. Molecular cloning and characterization of an insulin-regulatable glucose transporter. *Nature*. 1989; **338**(6210): 83-7.
224. Lund S, Flyvbjerg A, Holman GD, Larsen FS, Pedersen O, Schmitz O. Comparative effects of IGF-I and insulin on the glucose transporter system in rat muscle. *Am J Physiol*. 1994; **267**(3 Pt 1): E461-6.
225. Niu W, Bilan PJ, Ishikura S, Schertzer JD, Contreras-Ferrat A, Fu Z, et al. Contraction-related stimuli regulate GLUT4 traffic in C2C12-GLUT4myc skeletal muscle cells. *Am J Physiol Endocrinol Metab*. 2010; **298**(5): E1058-71.
226. Fujita H, Nedachi T, Kanzaki M. Accelerated de novo sarcomere assembly by electric pulse stimulation in C2C12 myotubes. *Exp Cell Res*. 2007; **313**(9): 1853-65.
227. McMahon DK, Anderson PA, Nassar R, Bunting JB, Saba Z, Oakeley AE, et al. C2C12 cells: biophysical, biochemical, and immunocytochemical properties. *Am J Physiol*. 1994; **266**(6 Pt 1): C1795-802.
228. Nedachi T, Fujita H, Kanzaki M. Contractile C2C12 myotube model for studying exercise-inducible responses in skeletal muscle. *Am J Physiol Endocrinol Metab*. 2008; **295**(5): E1191-204.
229. Kotliar N, Pilch PF. Expression of the glucose transporter isoform GLUT 4 is insufficient to confer insulin-regulatable hexose uptake to cultured muscle cells. *Mol Endocrinol*. 1992; **6**(3): 337-45.
230. Straczkowski M, Kowalska I. The role of skeletal muscle sphingolipids in the development of insulin resistance. *Rev Diabet Stud*. 2008; **5**(1): 13-24.
231. Kim YB, Nikoulina SE, Ciaraldi TP, Henry RR, Kahn BB. Normal insulin-dependent activation of Akt/protein kinase B, with diminished activation of

- phosphoinositide 3-kinase, in muscle in type 2 diabetes. *J Clin Invest*. 1999; **104**(6): 733-41.
232. Nadler ST, Stoehr JP, Rabaglia ME, Schueler KL, Birnbaum MJ, Attie AD. Normal Akt/PKB with reduced PI3K activation in insulin-resistant mice. *Am J Physiol Endocrinol Metab*. 2001; **281**(6): E1249-54.
233. Whitehead JP, Molero JC, Clark S, Martin S, Meneilly G, James DE. The role of Ca²⁺ in insulin-stimulated glucose transport in 3T3-L1 cells. *J Biol Chem*. 2001; **276**(30): 27816-24.
234. Hoehn KL, Hohnen-Behrens C, Cederberg A, Wu LE, Turner N, Yuasa T, et al. IRS1-independent defects define major nodes of insulin resistance. *Cell Metab*. 2008; **7**(5): 421-33.
235. Clark AE, Holman GD, Kozka IJ. Determination of the rates of appearance and loss of glucose transporters at the cell surface of rat adipose cells. *Biochem J*. 1991; **278** (Pt 1): 235-41.
236. Hausdorff SF, Fingar DC, Morioka K, Garza LA, Whiteman EL, Summers SA, et al. Identification of wortmannin-sensitive targets in 3T3-L1 adipocytes. Dissociation of insulin-stimulated glucose uptake and GLUT4 translocation. *J Biol Chem*. 1999; **274**(35): 24677-84.
237. Somwar R, Kim DY, Sweeney G, Huang C, Niu W, Lador C, et al. GLUT4 translocation precedes the stimulation of glucose uptake by insulin in muscle cells: potential activation of GLUT4 via p38 mitogen-activated protein kinase. *Biochem J*. 2001; **359**(Pt 3): 639-49.
238. Somwar R, Niu W, Kim DY, Sweeney G, Randhawa VK, Huang C, et al. Differential effects of phosphatidylinositol 3-kinase inhibition on intracellular signals regulating GLUT4 translocation and glucose transport. *J Biol Chem*. 2001; **276**(49): 46079-87.
239. Zierler K. Does insulin-induced increase in the amount of plasma membrane GLUTs quantitatively account for insulin-induced increase in glucose uptake? *Diabetologia*. 1998; **41**(6): 724-30.
240. Miyake Y, Kozutsumi Y, Nakamura S, Fujita T, Kawasaki T. Serine palmitoyltransferase is the primary target of a sphingosine-like immunosuppressant, ISP-1/myriocin. *Biochem Biophys Res Commun*. 1995; **211**(2): 396-403.
241. Turpin SM, Lancaster GI, Darby I, Febbraio MA, Watt MJ. Apoptosis in skeletal muscle myotubes is induced by ceramides and is positively related to insulin resistance. *Am J Physiol Endocrinol Metab*. 2006; **291**(6): E1341-50.
242. Minehira K, Young SG, Villanueva CJ, Yetukuri L, Oresic M, Hellerstein MK, et al. Blocking VLDL secretion causes hepatic steatosis but does not affect peripheral lipid stores or insulin sensitivity in mice. *J Lipid Res*. 2008; **49**(9): 2038-44.
243. Monetti M, Levin MC, Watt MJ, Sajan MP, Marmor S, Hubbard BK, et al. Dissociation of hepatic steatosis and insulin resistance in mice overexpressing DGAT in the liver. *Cell Metab*. 2007; **6**(1): 69-78.
244. Brown MS, Goldstein JL. Selective versus total insulin resistance: a pathogenic paradox. *Cell Metab*. 2008; **7**(2): 95-6.
245. Mei J, Wang CN, O'Brien L, Brindley DN. Cell-permeable ceramides increase basal glucose incorporation into triacylglycerols but decrease the stimulation by insulin in 3T3-L1 adipocytes. *Int J Obes Relat Metab Disord*. 2003; **27**(1): 31-9.
246. Hanna AN, Chan EY, Xu J, Stone JC, Brindley DN. A novel pathway for tumor necrosis factor-alpha and ceramide signaling involving sequential activation of tyrosine kinase, p21(ras), and phosphatidylinositol 3-kinase. *J Biol Chem*. 1999; **274**(18): 12722-9.

247. Hanna AN, Berthiaume LG, Kikuchi Y, Begg D, Bourgoin S, Brindley DN. Tumor necrosis factor-alpha induces stress fiber formation through ceramide production: role of sphingosine kinase. *Mol Biol Cell*. 2001; **12**(11): 3618-30.
248. Ussher JR, Koves TR, Cadete VJ, Zhang L, Jaswal JS, Swyrd SJ, et al. Inhibition of de novo ceramide synthesis reverses diet-induced insulin resistance and enhances whole-body oxygen consumption. *Diabetes*. 2010; **59**(10): 2453-64.
249. Yu C, Chen Y, Cline GW, Zhang D, Zong H, Wang Y, et al. Mechanism by which fatty acids inhibit insulin activation of insulin receptor substrate-1 (IRS-1)-associated phosphatidylinositol 3-kinase activity in muscle. *J Biol Chem*. 2002; **277**(52): 50230-6.
250. Pont F, Duvillard L, Florentin E, Gambert P, Verges B. Early kinetic abnormalities of apoB-containing lipoproteins in insulin-resistant women with abdominal obesity. *Arterioscler Thromb Vasc Biol*. 2002; **22**(10): 1726-32.
251. Bell M, Wang H, Chen H, McLenithan JC, Gong DW, Yang RZ, et al. Consequences of lipid droplet coat protein downregulation in liver cells: abnormal lipid droplet metabolism and induction of insulin resistance. *Diabetes*. 2008; **57**(8): 2037-45.
252. Holland WL, Summers SA. Sphingolipids, insulin resistance, and metabolic disease: new insights from in vivo manipulation of sphingolipid metabolism. *Endocr Rev*. 2008; **29**(4): 381-402.
253. Engelman JA, Berg AH, Lewis RY, Lisanti MP, Scherer PE. Tumor necrosis factor alpha-mediated insulin resistance, but not dedifferentiation, is abrogated by MEK1/2 inhibitors in 3T3-L1 adipocytes. *Mol Endocrinol*. 2000; **14**(10): 1557-69.
254. Aguirre V, Uchida T, Yenush L, Davis R, White MF. The c-Jun NH(2)-terminal kinase promotes insulin resistance during association with insulin receptor substrate-1 and phosphorylation of Ser(307). *J Biol Chem*. 2000; **275**(12): 9047-54.
255. Fujishiro M, Gotoh Y, Katagiri H, Sakoda H, Ogihara T, Anai M, et al. Three mitogen-activated protein kinases inhibit insulin signaling by different mechanisms in 3T3-L1 adipocytes. *Mol Endocrinol*. 2003; **17**(3): 487-97.
256. Rocha VZ, Folco EJ, Sukhova G, Shimizu K, Gotsman I, Vernon AH, et al. Interferon-gamma, a Th1 cytokine, regulates fat inflammation: a role for adaptive immunity in obesity. *Circ Res*. 2008; **103**(5): 467-76.
257. Weisberg SP, McCann D, Desai M, Rosenbaum M, Leibel RL, Ferrante AW, Jr. Obesity is associated with macrophage accumulation in adipose tissue. *J Clin Invest*. 2003; **112**(12): 1796-808.
258. Wu H, Ghosh S, Perrard XD, Feng L, Garcia GE, Perrard JL, et al. T-cell accumulation and regulated on activation, normal T cell expressed and secreted upregulation in adipose tissue in obesity. *Circulation*. 2007; **115**(8): 1029-38.
259. Wellen KE, Hotamisligil GS. Inflammation, stress, and diabetes. *J Clin Invest*. 2005; **115**(5): 1111-9.
260. Raschke WC, Baird S, Ralph P, Nakoinz I. Functional macrophage cell lines transformed by Abelson leukemia virus. *Cell*. 1978; **15**(1): 261-7.
261. Watanabe N, Nakada K, Kobayashi Y. Processing and release of tumor necrosis factor alpha. *Eur J Biochem*. 1998; **253**(3): 576-82.
262. Abbasi F, Brown BW, Jr., Lamendola C, McLaughlin T, Reaven GM. Relationship between obesity, insulin resistance, and coronary heart disease risk. *J Am Coll Cardiol*. 2002; **40**(5): 937-43.
263. Jacobs MD, Harrison SC. Structure of an IkappaBalpha/NF-kappaB complex. *Cell*. 1998; **95**(6): 749-58.

264. Nathan CF. Secretory products of macrophages. *J Clin Invest.* 1987; **79**(2): 319-26.
265. De Fea K, Roth RA. Modulation of insulin receptor substrate-1 tyrosine phosphorylation and function by mitogen-activated protein kinase. *J Biol Chem.* 1997; **272**(50): 31400-6.
266. Ozcan U, Cao Q, Yilmaz E, Lee AH, Iwakoshi NN, Ozdelen E, et al. Endoplasmic reticulum stress links obesity, insulin action, and type 2 diabetes. *Science.* 2004; **306**(5695): 457-61.
267. Patsouris D, Li PP, Thapar D, Chapman J, Olefsky JM, Neels JG. Ablation of CD11c-positive cells normalizes insulin sensitivity in obese insulin resistant animals. *Cell Metab.* 2008; **8**(4): 301-9.
268. Weisberg SP, Hunter D, Huber R, Lemieux J, Slaymaker S, Vaddi K, et al. CCR2 modulates inflammatory and metabolic effects of high-fat feeding. *J Clin Invest.* 2006; **116**(1): 115-24.
269. Oh DY, Talukdar S, Bae EJ, Imamura T, Morinaga H, Fan W, et al. GPR120 is an omega-3 fatty acid receptor mediating potent anti-inflammatory and insulin-sensitizing effects. *Cell.* 2010; **142**(5): 687-98.
270. Arkan MC, Hevener AL, Greten FR, Maeda S, Li ZW, Long JM, et al. IKK-beta links inflammation to obesity-induced insulin resistance. *Nat Med.* 2005; **11**(2): 191-8.
271. Solinas G, Vilcu C, Neels JG, Bandyopadhyay GK, Luo JL, Naugler W, et al. JNK1 in hematopoietically derived cells contributes to diet-induced inflammation and insulin resistance without affecting obesity. *Cell Metab.* 2007; **6**(5): 386-97.
272. Ehses JA, Perren A, Eppler E, Ribaux P, Pospisilik JA, Maor-Cahn R, et al. Increased number of islet-associated macrophages in type 2 diabetes. *Diabetes.* 2007; **56**(9): 2356-70.
273. Li Z, Diehl AM. Innate immunity in the liver. *Curr Opin Gastroenterol.* 2003; **19**(6): 565-71.
274. Odegaard JI, Ricardo-Gonzalez RR, Red Eagle A, Vats D, Morel CR, Goforth MH, et al. Alternative M2 activation of Kupffer cells by PPARdelta ameliorates obesity-induced insulin resistance. *Cell Metab.* 2008; **7**(6): 496-507.
275. Di Gregorio GB, Yao-Borengasser A, Rasouli N, Varma V, Lu T, Miles LM, et al. Expression of CD68 and macrophage chemoattractant protein-1 genes in human adipose and muscle tissues: association with cytokine expression, insulin resistance, and reduction by pioglitazone. *Diabetes.* 2005; **54**(8): 2305-13.
276. Xu H, Barnes GT, Yang Q, Tan G, Yang D, Chou CJ, et al. Chronic inflammation in fat plays a crucial role in the development of obesity-related insulin resistance. *J Clin Invest.* 2003; **112**(12): 1821-30.
277. Varma V, Yao-Borengasser A, Rasouli N, Nolen GT, Phanavanh B, Starks T, et al. Muscle inflammatory response and insulin resistance: synergistic interaction between macrophages and fatty acids leads to impaired insulin action. *Am J Physiol Endocrinol Metab.* 2009; **296**(6): E1300-10.
278. Nguyen MT, Favelyukis S, Nguyen AK, Reichart D, Scott PA, Jenn A, et al. A subpopulation of macrophages infiltrates hypertrophic adipose tissue and is activated by free fatty acids via Toll-like receptors 2 and 4 and JNK-dependent pathways. *J Biol Chem.* 2007; **282**(48): 35279-92.
279. Hevener AL, Olefsky JM, Reichart D, Nguyen MT, Bandyopadhyay G, Leung HY, et al. Macrophage PPAR gamma is required for normal skeletal muscle and hepatic insulin sensitivity and full antidiabetic effects of thiazolidinediones. *J Clin Invest.* 2007; **117**(6): 1658-69.

280. Samokhvalov V, Bilan PJ, Schertzer JD, Antonescu CN, Klip A. Palmitate- and lipopolysaccharide-activated macrophages evoke contrasting insulin responses in muscle cells. *Am J Physiol Endocrinol Metab.* 2009; **296**(1): E37-46.
281. Kamei N, Tobe K, Suzuki R, Ohsugi M, Watanabe T, Kubota N, et al. Overexpression of monocyte chemoattractant protein-1 in adipose tissues causes macrophage recruitment and insulin resistance. *J Biol Chem.* 2006; **281**(36): 26602-14.
282. Senn JJ. Toll-like receptor-2 is essential for the development of palmitate-induced insulin resistance in myotubes. *J Biol Chem.* 2006; **281**(37): 26865-75.
283. Song MJ, Kim KH, Yoon JM, Kim JB. Activation of Toll-like receptor 4 is associated with insulin resistance in adipocytes. *Biochem Biophys Res Commun.* 2006; **346**(3): 739-45.
284. Boland MP, O'Neill LA. Ceramide activates NFkappaB by inducing the processing of p105. *J Biol Chem.* 1998; **273**(25): 15494-500.
285. Kitajima I, Soejima Y, Takasaki I, Beppu H, Tokioka T, Maruyama I. Ceramide-induced nuclear translocation of NF-kappa B is a potential mediator of the apoptotic response to TNF-alpha in murine clonal osteoblasts. *Bone.* 1996; **19**(3): 263-70.
286. Wu D, Ren Z, Pae M, Guo W, Cui X, Merrill AH, et al. Aging up-regulates expression of inflammatory mediators in mouse adipose tissue. *J Immunol.* 2007; **179**(7): 4829-39.
287. Schwartz EA, Zhang WY, Karnik SK, Borwege S, Anand VR, Laine PS, et al. Nutrient modification of the innate immune response: a novel mechanism by which saturated fatty acids greatly amplify monocyte inflammation. *Arterioscler Thromb Vasc Biol.* 2010; **30**(4): 802-8.
288. Bluher M, Fasshauer M, Tonjes A, Kratzsch J, Schon MR, Paschke R. Association of interleukin-6, C-reactive protein, interleukin-10 and adiponectin plasma concentrations with measures of obesity, insulin sensitivity and glucose metabolism. *Exp Clin Endocrinol Diabetes.* 2005; **113**(9): 534-7.
289. Hotamisligil GS, Shargill NS, Spiegelman BM. Adipose expression of tumor necrosis factor-alpha: direct role in obesity-linked insulin resistance. *Science.* 1993; **259**(5091): 87-91.
290. de Mello VD, Lankinen M, Schwab U, Kolehmainen M, Lehto S, Seppanen-Laakso T, et al. Link between plasma ceramides, inflammation and insulin resistance: association with serum IL-6 concentration in patients with coronary heart disease. *Diabetologia.* 2009; **52**(12): 2612-5.
291. Carr MW, Roth SJ, Luther E, Rose SS, Springer TA. Monocyte chemoattractant protein 1 acts as a T-lymphocyte chemoattractant. *Proc Natl Acad Sci U S A.* 1994; **91**(9): 3652-6.
292. Xia M, Sui Z. Recent developments in CCR2 antagonists. *Expert Opin Ther Pat.* 2009; **19**(3): 295-303.
293. Xu LL, Warren MK, Rose WL, Gong W, Wang JM. Human recombinant monocyte chemotactic protein and other C-C chemokines bind and induce directional migration of dendritic cells in vitro. *J Leukoc Biol.* 1996; **60**(3): 365-71.
294. Berlato C, Cassatella MA, Kinjyo I, Gatto L, Yoshimura A, Bazzoni F. Involvement of suppressor of cytokine signaling-3 as a mediator of the inhibitory effects of IL-10 on lipopolysaccharide-induced macrophage activation. *J Immunol.* 2002; **168**(12): 6404-11.

295. O'Farrell AM, Liu Y, Moore KW, Mui AL. IL-10 inhibits macrophage activation and proliferation by distinct signaling mechanisms: evidence for Stat3-dependent and -independent pathways. *EMBO J*. 1998; **17**(4): 1006-18.
296. Riley JK, Takeda K, Akira S, Schreiber RD. Interleukin-10 receptor signaling through the JAK-STAT pathway. Requirement for two distinct receptor-derived signals for anti-inflammatory action. *J Biol Chem*. 1999; **274**(23): 16513-21.
297. Lee YH, Giraud J, Davis RJ, White MF. c-Jun N-terminal kinase (JNK) mediates feedback inhibition of the insulin signaling cascade. *J Biol Chem*. 2003; **278**(5): 2896-902.
298. Rui L, Aguirre V, Kim JK, Shulman GI, Lee A, Corbould A, et al. Insulin/IGF-1 and TNF-alpha stimulate phosphorylation of IRS-1 at inhibitory Ser307 via distinct pathways. *J Clin Invest*. 2001; **107**(2): 181-9.
299. Rotter V, Nagaev I, Smith U. Interleukin-6 (IL-6) induces insulin resistance in 3T3-L1 adipocytes and is, like IL-8 and tumor necrosis factor-alpha, overexpressed in human fat cells from insulin-resistant subjects. *J Biol Chem*. 2003; **278**(46): 45777-84.
300. Senn JJ, Klover PJ, Nowak IA, Zimmers TA, Koniaris LG, Furlanetto RW, et al. Suppressor of cytokine signaling-3 (SOCS-3), a potential mediator of interleukin-6-dependent insulin resistance in hepatocytes. *J Biol Chem*. 2003; **278**(16): 13740-6.
301. Rui L, Yuan M, Frantz D, Shoelson S, White MF. SOCS-1 and SOCS-3 block insulin signaling by ubiquitin-mediated degradation of IRS1 and IRS2. *J Biol Chem*. 2002; **277**(44): 42394-8.
302. Hsu YW, Chi KH, Huang WC, Lin WW. Ceramide inhibits lipopolysaccharide-mediated nitric oxide synthase and cyclooxygenase-2 induction in macrophages: effects on protein kinases and transcription factors. *J Immunol*. 2001; **166**(9): 5388-97.
303. Medvedev AE, Blanco JC, Qureshi N, Vogel SN. Limited role of ceramide in lipopolysaccharide-mediated mitogen-activated protein kinase activation, transcription factor induction, and cytokine release. *J Biol Chem*. 1999; **274**(14): 9342-50.
304. Chiba N, Masuda A, Yoshikai Y, Matsuguchi T. Ceramide inhibits LPS-induced production of IL-5, IL-10, and IL-13 from mast cells. *J Cell Physiol*. 2007; **213**(1): 126-36.
305. Stumvoll M, Goldstein BJ, van Haefen TW. Type 2 diabetes: principles of pathogenesis and therapy. *Lancet*. 2005; **365**(9467): 1333-46.
306. Zimmet P, Alberti KG, Shaw J. Global and societal implications of the diabetes epidemic. *Nature*. 2001; **414**(6865): 782-7.
307. UK Prospective Diabetes Study Group. Intensive blood-glucose control with sulphonylureas or insulin compared with conventional treatment and risk of complications in patients with type 2 diabetes. *Lancet*; 1998. p. 837-53.
308. UK Prospective Diabetes Study Group. Effect of intensive blood-glucose control with metformin on complications in overweight patients with type 2 diabetes. *Lancet*. 1998; **352**: 854-65.
309. Wei M, Gaskill SP, Haffner SM, Stern MP. Effects of diabetes and level of glycemia on all-cause and cardiovascular mortality. The San Antonio Heart Study. *Diabetes Care*. 1998; **21**(7): 1167-72.
310. Bonadonna RC, Stumvoll M, Fritsche A, Muggeo M, Haring H, Bonora E, et al. Altered homeostatic adaptation of first- and second-phase beta-cell secretion in the offspring of patients with type 2 diabetes: studies with a minimal model to assess beta-cell function. *Diabetes*. 2003; **52**(2): 470-80.

311. Gerich JE. The genetic basis of type 2 diabetes mellitus: impaired insulin secretion versus impaired insulin sensitivity. *Endocr Rev.* 1998; **19**(4): 491-503.
312. Kaprio J, Tuomilehto J, Koskenvuo M, Romanov K, Reunanen A, Eriksson J, et al. Concordance for type 1 (insulin-dependent) and type 2 (non-insulin-dependent) diabetes mellitus in a population-based cohort of twins in Finland. *Diabetologia.* 1992; **35**(11): 1060-7.
313. Newman B, Selby JV, King MC, Slemenda C, Fabsitz R, Friedman GD. Concordance for type 2 (non-insulin-dependent) diabetes mellitus in male twins. *Diabetologia.* 1987; **30**(10): 763-8.
314. Pierce M, Keen H, Bradley C. Risk of diabetes in offspring of parents with non-insulin-dependent diabetes. *Diabet Med.* 1995; **12**(1): 6-13.
315. Tattersal RB, Fajans SS. Prevalence of diabetes and glucose intolerance in 199 offspring of thirty-seven conjugal diabetic parents. *Diabetes.* 1975; **24**(5): 452-62.
316. Dobrowsky RT, Kamibayashi C, Mumby MC, Hannun YA. Ceramide activates heterotrimeric protein phosphatase 2A. *J Biol Chem.* 1993; **268**(21): 15523-30.
317. Resjo S, Goransson O, Harndahl L, Zolnierowicz S, Manganiello V, Degerman E. Protein phosphatase 2A is the main phosphatase involved in the regulation of protein kinase B in rat adipocytes. *Cell Signal.* 2002; **14**(3): 231-8.
318. JeBailey L, Wanono O, Niu W, Roessler J, Rudich A, Klip A. Ceramide- and oxidant-induced insulin resistance involve loss of insulin-dependent Rac-activation and actin remodeling in muscle cells. *Diabetes.* 2007; **56**(2): 394-403.
319. Holopainen JM, Medina OP, Metso AJ, Kinnunen PK. Sphingomyelinase activity associated with human plasma low density lipoprotein. *J Biol Chem.* 2000; **275**(22): 16484-9.
320. Hoffman NJ, Elmendorf JS. Signaling, cytoskeletal and membrane mechanisms regulating GLUT4 exocytosis. *Trends Endocrinol Metab.* 2011; **22**(3): 110-6.
321. Li Z, Zhang H, Liu J, Liang CP, Li Y, Teitelman G, et al. Reducing plasma membrane sphingomyelin increases insulin sensitivity. *Mol Cell Biol.* 2011; **31**(20): 4205-18.
322. Gurusingham A, de Niese M, Renaud JF, Austin L. The binding of lipoproteins to human muscle cells: binding and uptake of LDL, HDL, and alpha-tocopherol. *Muscle Nerve.* 1988; **11**(12): 1231-9.
323. van Blitterswijk WJ, van der Luit AH, Veldman RJ, Verheij M, Borst J. Ceramide: second messenger or modulator of membrane structure and dynamics? *Biochem J.* 2003; **369**(Pt 2): 199-211.
324. Zhou L, Sell H, Eckardt K, Yang Z, Eckel J. Conditioned medium obtained from in vitro differentiated adipocytes and resistin induce insulin resistance in human hepatocytes. *FEBS Lett.* 2007; **581**(22): 4303-8.
325. Hotamisligil GS, Spiegelman BM. Tumor necrosis factor alpha: a key component of the obesity-diabetes link. *Diabetes.* 1994; **43**(11): 1271-8.
326. Kim HJ, Higashimori T, Park SY, Choi H, Dong J, Kim YJ, et al. Differential effects of interleukin-6 and -10 on skeletal muscle and liver insulin action in vivo. *Diabetes.* 2004; **53**(4): 1060-7.
327. Matthews VB, Allen TL, Risis S, Chan MH, Henstridge DC, Watson N, et al. Interleukin-6-deficient mice develop hepatic inflammation and systemic insulin resistance. *Diabetologia.* 2010; **53**(11): 2431-41.

328. Pedersen BK, Steensberg A, Fischer C, Keller C, Keller P, Plomgaard P, et al. Searching for the exercise factor: is IL-6 a candidate? *J Muscle Res Cell Motil.* 2003; **24**(2-3): 113-9.
329. Starkie R, Ostrowski SR, Jauffred S, Febbraio M, Pedersen BK. Exercise and IL-6 infusion inhibit endotoxin-induced TNF- α production in humans. *FASEB J.* 2003; **17**(8): 884-6.
330. Baron AD, Steinberg H, Brechtel G, Johnson A. Skeletal muscle blood flow independently modulates insulin-mediated glucose uptake. *Am J Physiol.* 1994; **266**(2 Pt 1): E248-53.
331. Segal SS. Regulation of blood flow in the microcirculation. *Microcirc.* 2005; **12**(1): 33-45.
332. Yki-Jarvinen H, Utriainen T. Insulin-induced vasodilatation: physiology or pharmacology? *Diabetologia.* 1998; **41**(4): 369-79.
333. Clerk LH, Rattigan S, Clark MG. Lipid infusion impairs physiologic insulin-mediated capillary recruitment and muscle glucose uptake in vivo. *Diabetes.* 2002; **51**(4): 1138-45.
334. Rattigan S, Clark MG, Barrett EJ. Hemodynamic actions of insulin in rat skeletal muscle: evidence for capillary recruitment. *Diabetes.* 1997; **46**(9): 1381-8.
335. Vincent MA, Barrett EJ, Lindner JR, Clark MG, Rattigan S. Inhibiting NOS blocks microvascular recruitment and blunts muscle glucose uptake in response to insulin. *Am J Physiol Endocrinol Metab.* 2003; **285**(1): E123-9.
336. Vincent MA, Clerk LH, Lindner JR, Klibanov AL, Clark MG, Rattigan S, et al. Microvascular recruitment is an early insulin effect that regulates skeletal muscle glucose uptake in vivo. *Diabetes.* 2004; **53**(6): 1418-23.
337. Kim JA, Koh KK, Quon MJ. The union of vascular and metabolic actions of insulin in sickness and in health. *Arterioscler Thromb Vasc Biol.* 2005; **25**(5): 889-91.
338. Kim JA, Montagnani M, Koh KK, Quon MJ. Reciprocal relationships between insulin resistance and endothelial dysfunction: molecular and pathophysiological mechanisms. *Circulation.* 2006; **113**(15): 1888-904.
339. Li G, Barrett EJ, Barrett MO, Cao W, Liu Z. Tumor necrosis factor- α induces insulin resistance in endothelial cells via a p38 mitogen-activated protein kinase-dependent pathway. *Endocrinology.* 2007; **148**(7): 3356-63.